

UNIVERSITÀ DEGLI STUDI DI PADOVA

DIPARTIMENTO DI INGEGNERIA INDUSTRIALE

CORSO DI LAUREA MAGISTRALE IN INGEGNERIA CHIMICA E DEI PROCESSI INDUSTRIALI

**Tesi di Laurea Magistrale in
Ingegneria Chimica e dei Processi Industriali**

Techno-economic evaluation of an on-board carbon capture plant for container ships

Relatore: Dr. Federico d'Amore

Correlatore: Prof. Fabrizio Bezzo

Laureando: MARCO VISONA'

ANNO ACCADEMICO 2022 – 2023

Abstract

This work presents a techno-economic analysis of a carbon capture system on board a large container ship, within the context of decarbonizing the maritime industry. The selected vessel, the Munich Maersk, is a 20,650 twenty foot equivalent unit (TEU) container vessel powered by two 32 MW dual-fuel engines (Heavy fuel oil (HFO) and liquefied natural gas (LNG)).

Carbon capture is carried out by using post-combustion technology based on chemical absorption with Monoethanolamine (MEA). Different case studies are proposed depending on the fuel used by the ship and the strategy to produce steam to supply the reboiler of the stripper. For each propulsion system (i.e., depending on the choice of using HFO or LNG to fuel the ship), a base case is examined in which the thermal energy required for the capture process is provided by a conventional boiler. Subsequently, the integration of an electrified heat pump system aimed at recovering heat from the engine exhaust gases is studied. Finally, a case based on a reduced rate of carbon captured is proposed. For each case, estimates of capital expenditures and operational costs are provided. The economics are discussed under three different scenarios, considering various hypothetical distributions of ports equipped for unloading carbon dioxide. Finally, a sensitivity analysis is conducted to evaluate the effect on economic results of the introduction of a carbon tax.

The results highlight that on-board carbon capture determines an increase in fuel consumption with respect to the conventional ship, that varies depending on the exhaust gas CO₂ content (hence, on the ship fuel) and temperature. The integration of the heat pump leads to significant decreases in fuel consumption. The overall carbon capture cost for on-board applications is found in the range of 64 to 95€/t of CO₂. In general, it can be observed that cases related to LNG-powered ships are more economically favorable compared to those using HFO. The study highlights that the introduction of a carbon tax would be beneficial to equalize the costs of on-board carbon capture, and that this tax should have a minimum value of €70/t of CO₂ (LNG) and €89/t (HFO), to make this technology economically attractive.

Riassunto

Questo lavoro presenta un'analisi tecnico-economica di un sistema di cattura della carbonio a bordo di una grande nave portacontainer, nel contesto della decarbonizzazione dell'industria marittima. La nave selezionata, la Munich Maersk, è una nave portacontainer da 20,650 unità equivalenti a venti piedi (TEU) alimentata da due motori a doppio combustibile da 32 MW (olio combustibile pesante (HFO) e gas naturale liquefatto (LNG)).

La cattura del carbonio viene effettuata utilizzando una tecnologia di post-combustione basata sull'assorbimento chimico con la Monoetanolamina (MEA). Sono proposti diversi casi di studio a seconda del carburante utilizzato dalla nave e della strategia per produrre vapore per alimentare il riportatore dello stripping. Per ciascun sistema di propulsione (cioè a seconda della scelta di utilizzare HFO o LNG per alimentare la nave), viene esaminato un caso in cui l'energia termica richiesta per il processo di cattura è fornita da una caldaia convenzionale. Successivamente, viene studiata l'integrazione di un sistema di pompa di calore elettrificato mirato al recupero del calore dai gas di scarico del motore. Infine, viene proposto un caso basato su un tasso ridotto di cattura del carbonio. Per ciascun caso, vengono fornite stime dei costi di investimento e dei costi operativi. L'economia è discussa in tre diversi scenari, considerando diverse distribuzioni ipotetiche di porti attrezzati per lo scarico dell'anidride carbonica. Infine, viene condotta un'analisi di sensibilità per valutare l'effetto sui risultati economici dell'introduzione di una tassa sul carbonio.

I risultati evidenziano che la cattura del carbonio a bordo comporta un aumento del consumo di carburante rispetto alla nave convenzionale, che varia a seconda del contenuto di CO₂ nei gas di scarico (quindi, del carburante della nave) e della temperatura. L'integrazione della pompa di calore porta a significative diminuzioni del consumo di carburante. Il costo complessivo della cattura del carbonio per le applicazioni a bordo è compreso nell'intervallo di 64 a 95€/t di CO₂. In generale, si può osservare che i casi relativi alle navi alimentate a LNG sono economicamente più favorevoli rispetto a quelli che utilizzano l'HFO. Lo studio mette in luce che l'introduzione di una tassa sul carbonio sarebbe vantaggiosa e che questa tassa dovrebbe avere un valore minimo di €70/t di CO₂ (LNG) e €89/t (HFO) per rendere questa tecnologia economicamente conveniente.

Index

Figure list.....	1
Table list	3
Introduction.....	5
Chapter 1.....	7
Scope and goals.....	7
1.1 Background	7
1.2. Energy efficiency	8
1.3 Fuel switching	9
1.2.1 LNG	9
1.2.2 Hydrogen	10
1.2.2 Ammonia	12
1.2.3 Methanol	12
1.3 Carbon capture on-board	13
1.4 Scope of this work.....	14
Chapter 2.....	15
Carbon capture.....	15
2.1 Carbon capture and storage	15
2.2 Carbon capture	15
2.2.1 Post-combustion.....	16
2.2.2 Pre-combustion	17
2.2.3 Oxy-combustion	18
2.3 Transportation	18
2.4. Storage.....	18
2.5. Carbon capture on-board ships	19
Chapter 3.....	27
Methodology	27

3.1 Reference ship and flue gas composition	27
3.2 Carbon capture unit	30
3.2.1 Solvent	30
3.2.2 Carbon capture flowsheet	31
3.2.3 Thermodynamic and kinetic model	32
3.2.4 Columns	34
3.2.5 Energy recovery and CCR	35
3.2.6 Heat pump	36
3.3 Purification, liquefaction and storage	40
3.4 Economic analysis	41
3.4.3 FOPEX	42
2.4.4 VOPEX	42
3.4.5 Transport and storage cost	43
3.4.6 Container loss	44
3.4.7 Fuel cost and freight rates	46
3.4.8 Carbon tax and freight rates increase	47
3.4.9 Other assumptions	47
Chapter 4	49
Case study	49
4.1 Voyage and scenario definition	49
4.2 Scenario effect	52
Chapter 5	53
Results	53
5.1 Technical discussion	53
5.1.1 LNG and HFO: Fuel boiler plants	54
5.1.2 Heat pump integration	55
5.1.3 Base case	57
5.1.4 Purification and liquefaction	58
5.2 Economic results	58
5.2.1 Baseline capacity	58
5.2.2 Carbon dioxide volume requirements	60
5.2.2 Container loss	62

5.2.3 Transport ad storage	67
5.2.4 CAPEX	69
5.2.5 Total annual costs.....	71
5.2.6 Freight rates increase	73
5.2.7 Carbon tax	73
Conclusion	77
Nomenclature	79
Bibliography	83

Figure list

Figure 2.1. Summary of main carbon capture routes. Note: in pre-combustion case is, combustion is not mandatory, fuel cell usage can also be employed.....	17
Figure 3.1. Block scheme of the process.....	29
Figure 3.2. General MEA based carbon capture plant. In blue the seawater for cooling, in dashed line red is presented the direct flue gas-reboiler heating.....	32
Figure 3.3. Generic heat pump scheme.....	37
Figure 3.4. Heat pump cycle integration (dark blue). The steam produced, and directed to the reboiler, is recirculated in a closed cycle not showed for graphic reasons.....	38
Figure 3.5. HPtot plant. All steam cycles are closed, not showed for graphic reasons.....	39
Figure 3.6. Purification and liquefaction section for LNG case.....	41
Figure 3.7. Purification and liquefaction section for HFO case with additional ammonia cycle.....	41
Figure 3.8. Example of possible capacity profile along a voyage.....	45
Figure 4.1. Route from Shanghai to Rotterdam and back.....	49
Figure 4.2. CCS project along there route sailed.....	51
Figure 5.1. Reboiler duty profile varying the carbon capture rate and heat disposable in the flue gas.....	57
Figure 5.2. Capacity profile for baseline LNG ship.....	59
Figure 5.3. Capacity profile for baseline HFO ship.....	60
Figure 5.4. LNG-FB carbon dioxide volume requirement on a leg basis.....	60
Figure 5.5. HFO-FB carbon dioxide volume requirement on a leg basis.....	61
Figure 5.6. LNG-FB container loss expressed in TEU along the voyage.....	63
Figure 5.7. HFO-FB container loss expressed in TEU along the voyage.....	63
Figure 5.8. LNG-Base container loss expressed in TEU along the voyage.....	64
Figure 5.9. Total container to destination percentage change respect to baseline.....	65
Figure 5.10. Total container carried percentage change respect to baseline.....	66
Figure 5.11. Container revenue percentage loss.....	67
Figure 5.12. Container revenue loss.....	67
Figure 5.13. Transport cost for scenario 1, (unload every port).....	68
Figure 5.14. Transport cost for scenario 2, (unload one every two ports).....	68
Figure 5.15. Transport cost for scenario 3, (unload only when possible).....	69

Figure 5.16. Capital expenditure in 2019 euro.....	70
Figure 5.17. Capital expenditure distribution between different sections of the plant, scenario1.....	70
Figure 5.18. Total operating expenses per year (left) and carbon capture cost expressed as €/ton (right)	71
Figure 5.19 Operating cost distribution for LNG-FB plant.....	72
Figure 5.20. Operating cost distribution for LNG-base plant.....	73
Figure 5.21. Carbon tax sensitivity and effect on annual expenses (LNG).....	74
Figure 5.22. Carbon tax impact on cost of captured carbon (CCC).....	75

Table list

Table 2.1 Summary of disadvantages and advantages of carbon capture processes.....	20
Table 2.2. Comparison of on-board carbon capture plants studied by other authors. (/) stands for value not provided.....	24
Table 3.1. Reference ship data, TEU (twenty foot equivalent unit) is the standard size of a container box. Deadweight is the difference between the displacement and the mass of empty vessel (lightweight) at any given draught, in other terms the maximal wight a ship can carry including cargo, fuel and other supplies.....	28
Table 3.2. Summary of flue gas characteristics.....	29
Table 3.3 Kinetic parameters.....	34
Table 3.4. Cases summary.....	36
Table 3.5. Distance from injection storage facility, transportation method chosen and relative cost according to IPCC. All values are converted in Euro considering EUR/USD exchange rate of 1.08 (2023).....	44
Table 4.1. Port calls and details on leg duration.....	50
Table 5.1 Summary of plants main performance parameters.....	53
Table 5.2. Key operating parameters for purification and liquefaction.....	58
Table 5.3. Max volume requirement for every proposed plant.....	61

Introduction

Decarbonizing the shipping industry is of paramount importance in the global fight against climate change. Shipping plays a vital role in international trade, handling over 80% of global cargo by volume. However, it is also a significant source of greenhouse gas (GHG) emissions, contributing approximately 2% of global emissions in 2022, a figure that is expected to rise substantially without intervention. In the context of the broader effort to combat global warming and achieve the objectives of the Paris Agreement, reducing emissions from the shipping sector is imperative. This is not only because of the substantial contribution of this sector to overall emissions, but also because the carbon footprint of shipping has largely remained unchanged in the last years, even as other industries have made progress in reducing emissions.

Decarbonizing shipping could involve mainly three strategies: the transitioning towards low-carbon and zero-emission fuels, improvements in energy efficiency, and the implementation of on-board carbon capture technologies. In this work the concept of carbon capture on-board ships is introduced as a possible emission mitigation technology. It involves capturing carbon dioxide emissions during ship operations, liquefying the CO₂, and storing it onboard for later unloading and storing it in integrated onshore carbon capture and storage (CCS) networks. As such, carbon capture on-board is seen as a complementary solution to reduce emissions intensity in existing fossil-fueled vessels, as it avoids the direct emissions to the atmosphere.

This work expands the knowledge on this technology by providing a techno-economic evaluation of on-board carbon capture plant for an ultra large container vessel.

Furthermore, the research aims to provide insights into the economic implications of on-board carbon capture and its potential contribution to achieving emissions reduction goals in the shipping industry.

This thesis is structured into five chapters. In the first chapter, the most relevant solution for shipping decarbonization are discussed, focusing on their potential and limitations. In the second chapter the carbon capture process will be reviewed from a technical and bibliographic standpoint, while the proposed design for on-board carbon capture will be analyzed in detail. The third chapter will depict the technical model and the economic one deployed in this study, focusing on the development of the plants. In the fourth one a case study based on a voyage sailed by the ship and its implications in the study will be discussed. In chapter five the main

results will be discussed both from a technical and economic standpoint followed by a final conclusion summarizing the main findings.

Chapter 1

Scope and goals

1.1 Background

Shipping is an artery of international commerce handling more than 80% of international trade by volume, and being currently fueled almost exclusively by fossil fuels. In 2022, the share of low-carbon fuels accounted for just 0.1% of the total energy according to IEA (2023). As such, this sector poses a significant burden to global greenhouse gases (GHG) emissions. In 2022, the shipping sector accounted for 706 Mt of CO₂ emitted in the atmosphere, which corresponds to about 2% of global emissions, rising from pre-covid levels (IEA, 2023). Furthermore, as the maritime trade is expected to increase over the medium term, at a 2.1% per year rate (UNCTAD, 2022), so does the expected emissions from the sector if no abatement measure is taken. The international maritime organization (IMO) depicted a concerning scenario of an increase in maritime emissions between 90 and 130% by 2050 against the 2008 level (IMO, 2020).

In April 2018 the international maritime organization (IMO) set the goal to peak GHG emissions from international shipping as soon as possible and to reduce them by at least 50% by 2050 with respect to the 2008 level. This should be done by adopting different measures such as:

- Increasing the efficiency of ships through the concept of Energy Efficiency Design Index (EEDI).
- Switching to zero (or near zero) emissions fuels.
- Carbon capture on-board.

There are though different plans set up by different organizations, such as the European Commission goal to achieve carbon-neutrality by 2050 through, in addition to IMO measures, the inclusion of the shipping sector in the EU's Emissions Trading System (EU ETS) starting from January 2024. All large ships entering EU ports, regardless of their flag, must purchase and use emission allowances for each ton of reported CO₂ emission as its already done for

onshore applications such as electricity generation, refineries and others since 2005 (European commission, n.d.). This is the first global initiative which see a direct financial burden on shipping liners to effectively reduce their emissions.

Apart from this European initiative, no international economical measure has been effectively taken up to now, due to disagreement between countries over mechanisms that could asymmetrically damage economies of shipping. Discussions are still ongoing, with member states adopting the 2023 IMO Strategy on Reduction of GHG Emissions from ships, outlining the date for approval and implementation of measures such as carbon pricing to 2026. As currently operating ships have a lifetime of up to 25 to 30 years and the construction of new ones takes several years, there is an urgent need to put into place policy and economic measures to reach the decarbonization goal set for the shipping sector by the 2050.

1.2. Energy efficiency

Regarding the increase in efficiency, IMO sets it as one of the actions needed to meet the 2050 GHG emissions goal, to be achieved through the implementation of the EEDI. First mentioned by the Marine Environment Protection Committee (MEPC) in 2009, the EEDI has become in 2011 necessary to any new ship (Barreiro et al., 2022).

The International Convention for the Prevention of Pollution from Ships (MARPOL) is concerned with preventing marine pollution from ships (IMO, 2013). The annex VI of this convention establishes ship energy efficiency regulations (Stec et al., 2021). The MARPOL treaty defined a baseline EEDI as a function of the ship size and type and also established a progressive reduction of the EEDI (increase in efficiency) pathway from each baseline level. The EEDI reduction is divided into three phases coming into force in 2015, 2020 and 2025 with corresponding EEDI reduction factors of 10%, 20% and 30%, respectively. Various solutions on the market are available to increase the energy efficiency of ships, such as:

- Speed reduction: slow-steaming, despite advantages like fuel consumption reduction and no required investment or modification, has drawbacks: slower speed means reduced fleet transport capacity, longer transport time; hence, an increase in the fleet of ships (Barreiro et al., 2022; Farkas et al., 2022).
- Modification of hull parameters: The process of optimization of the ship by reducing its hull resistance is based on an attempt to decrease the wetted surface for the vessels in

order to decrease the drag on the ship (Barreiro et al., 2022). It is possible to achieve this by increasing hull length and the beam of the ship (Lindstad et al., 2018).

- Propulsion system optimization: one of the main ways to reduce GHG emissions is by the optimization of the main propulsion engines of the ship (Barreiro et al., 2022).
- Route optimization: Voyage optimization is a procedure where an optimal route is selected based on weather forecast, seas, currents, and the ship performance, by determining the optimal sailing speeds under specific real-time updated environmental factors, which allows to save fuel while ensuring the engine performance (Lu et al., 2013).
- Trim optimization: Trim is the difference between the draughts forward and aft. For each draft and speed, there is a resistance optimum trim. Trim optimization is a relatively new concept, it requires no ship structural modification, and can be attained by ballast water management and load distribution (Islam and Soares, 2019).

While increases in ship efficiencies are desirable, these are not enough to meet the goal of net zero emissions. Accordingly, other measures need to be taken such as fuel switching and carbon capture on-board the ship.

1.3 Fuel switching

One solution which is common among organizations is the possibility of switching from fuels with high pollution levels (such as the heavy fuel oil) to fuels with lower or zero impact in terms of GHG emissions.

In particular, IMO (2023) indicated the goal regarding the uptake of zero or near-zero GHG emission technologies, fuels and/or energy sources to represent at least 5%, striving for 10%, of the energy used by international shipping by 2030. Though not being specified in the IMO (2023) report, the low-carbon alternative fuels which are currently being investigated are liquefied natural gas (LNG), hydrogen, methanol and ammonia.

1.2.1 LNG

When compared with heavy fuel oil (HFO), LNG involves lower carbon intensity and higher engines efficiency (McKinlay et al., 2021). For this reason, notwithstanding the higher capital costs, LNG is being rapidly adopted by liner as a short term solution to decrease direct carbon dioxide emissions and also to comply with MARPOL regulations concerning emissions (Deng

et al., 2021).

While from a tank to wake approach LNG is less harmful than HFO in terms of GHG emissions, LNG is affected by the methane slip which, if accounted in the calculation, would make GHG emission between 75 to 97 ton CO₂/TJ fuel, with the upper value being potentially higher than HFO (91 CO₂/TJ fuel) (Verbeek et al., 2015). Hence, the importance of limiting as much as possible methane slip. New ordered ships should employ new low slip engines with the potential to cut GHG emissions by up to 23% on a well-to-wake basis. LNG is the only scalable fuel available today for deep-sea shipping that addresses (at least in part) climate challenges with a sustainable cost (Lagemann et al., 2022). As of September 2020, there were 173 LNG-powered vessels (excluding LNG carriers) and 227 confirmed orders for new vessels, placing LNG as the first alternative fuel by orderbook.

On a net zero 2050 scenario, however, LNG should be a limited option in the fuel energy mix and coupled with CCS technologies due to its partial decarbonization capabilities.

1.2.2 Hydrogen

Hydrogen is one of the main candidates for long term substitution because of its high energy per unit of mass and because its use does not produce any carbon dioxide. It can be used in internal combustion engines (ICE) or as anode inlet to fuel cells. For instance, this latter option has been investigated by Ye et al. (2022) and McKinlay et al. (2021) via proton exchange membrane fuel cells (PEMFC) with efficiencies in the range 45-65%. Nevertheless, the system efficiency (including electrical energy and thermal energy) can reach 60%–80% if low-grade heat can be effectively recovered by energy recovery subsystem (Luo et al., 2021).

Some disadvantages limit or hinder the adoption of H₂ as fuel for the maritime sector, such as:

- Fuel cells lifetime: this system currently exhibits a shorter lifetime than conventional ICE engines, which would result in more frequent stack replacements (e.g., every 5 years using those available by Ballard, 2020). This, combined with the high capital costs, results in high total cost of ownership as discussed by Korberg et al. (2021).
- H₂ production: the current practice involves the production of grey H₂ through the steam reforming of methane (SMR), which leads to significant CO₂ emissions (in the order of 10-14 kg CO₂-eq/kg H₂) (IEA, 2023). A way to decrease the impact of grey H₂ would require the implementation of carbon capture downstream the SMR (i.e., blue H₂), which still results in a carbon intensity of about 0.8-6 kg CO₂-eq/kg H₂ (assuming a

carbon capture rate of 90% or above). The economic and environmental implications of adopting other options, such as green H₂ from renewables and electrolytic processes, currently pose strong challenges in their implementation at a significant scale as that required to fuel the shipping sector. In 2021, total global hydrogen production was 94 million tons with grey hydrogen route accounting for 62% of hydrogen production (IEA, 2022). Still according to IEA, low-emission hydrogen production was less than 1 Mt (0.7%) in 2021, almost all from fossil fuels with carbon dioxide capture & utilization or storage (CCUS), with only 35 kt H₂ from electricity via water electrolysis. Furthermore, if all the announced projects for hydrogen from water electrolysis or fossil fuels with CCUS currently under development were realized, the annual production of low-emission hydrogen would reach more than 24 Mt H₂ by 2030, which is still a very small value compared to the 120 Mt estimated demand by IEA in the same year. This difference between estimated demand and green and blue hydrogen supply translates in prohibitive costs in the medium term especially if green H₂ is considered (due to the high costs of electrolysis) (EMAS, 2020; Korberg et al., 2021).

- Bunkering: logistics also need to be considered, with the total lack of any bunkering facility for liquefied hydrogen being an additional barrier for adoption. Notwithstanding this, according to the report prepared by the IEA for the G20 held in Japan in 2019 much of the existing demand for pure hydrogen (e.g. refineries, steel plants) is already placed in coastal hubs, and thus there is the potential to integrate industry and transport applications leading to a fast developing of bunkering facilities.
- Tank volume: low energy density and thus high tanks volume are required, leading to problems such as cargo displacement. In fact, also in the case of liquefied storage (volume reduced by nearly 50% with respect to compressed gas storage at 700 bar, Hwang et al., 2014), the tank would be in a range between 3-5 times a HFO tank, which could limit the application on certain type of ships. The low energy density of H₂ impacts the ship also from an operating standpoint, as it determines more frequent refueling. For instance, Mao et al. (2020), considered a fleet of container ships fueled by hydrogen traveling from Shanghai to Los Angeles, showing that only 29% of the ships involved could make the entire voyage without cargo being displaced; the number increased to 100% with two intermediate port stops for refueling or alternatively with a 5% cargo displacement.

1.2.2 Ammonia

Ammonia is being considered a potential green fuel for ships (e.g., McKinlay et al., 2021; Korberg et al., 2021; Ye et al., 2022). It presents some advantages over H₂ such as the already present bunkering facilities in major commercial ports and a higher energy density. The latter would reduce the volume and complexity of storage tanks due to the less challenging conditions required by ammonia to be stored as liquid (-34°C vs -252°C at 1 bar). Like hydrogen, ammonia can be used both in ICE and as fuel for a solid oxide fuel cell (SOFC) or PEMFC (Ye et al., 2022). ICE engines, even if with lower efficiency (nearly 30%) compared with ammonia use in fuel cells, are considered the main option in the medium term, with the first ICE engine expected to be produced by MAN in 2024.

On the flip side, the production and utilization of ammonia as a fuel for the shipping sector poses some challenges:

- The production of ammonia requires hydrogen as feedstock which, as already seen in Section 1.2.1, is currently largely dependent on fossil fuels such as natural gas. Plus, it must be combined with nitrogen (e.g., Haber-Bosch process) via energy intensive processes involving high emissions (e.g., 2.4 ton CO₂ per ton of NH₃, IEA, 2021). According to IEA, in 2020 only 23% of Ammonia production capacity was integrated with CCU (all related to coal as raw material) (IEA, 2021).
- Ammonia also presents a competition problem because of its important use as an agricultural feedstock. Mass adoption of ammonia as a fuel could increase the price of food with relevant social implications.
- The hazardous nature of this compound must be taken into account when discussing its possible use, especially for non static applications, such as the naval sector. Tanks for ammonia storage are very similar to those for LPG, with additional safety systems given its high toxicity (Dujim et al., 2005).

1.2.3 Methanol

Methanol has recently attracted considerable attention as an alternative fuel for ships. The adoption of the IMO interim guidelines for ships using methyl or ethyl alcohol as a fuel has been an enabler for shifting shipowners interest towards methanol-fueled ships.

Although methanol could be in principle used both in fuel cells and ICE, the second option is seen as the preferred route due to lower costs, easier maintenance and presence of dual fuel

engines which make this fuel already suitable for adoption. Methanol has a GHG emission potential between 60 and 70 ton/TJ on a tank-to-wake approach, i.e. up to 30% lower than HFO (UMAS, 2020).

Currently, around 98 Mt of methanol are produced on a yearly basis, almost entirely derived from fossil fuels (either natural gas or coal) (IRENA, 2021). The so-called e-Methanol route (green H₂ and CO₂ from CCU) is still at an early stage of development. Aside electro-routes, methanol can be produced also by fermentation of biomass such as wood and agricultural wastes (i.e., bio-Methanol). These routes are more technologically mature than e-Methanol, but potentially more limited in capacity due to availability of feedstock and low agricultural yields (EMSA, 2022). According to IRENA (2021), only 0.2 Mt of renewable Methanol are currently produced worldwide, with an estimated scale up to 250 million Mt of e-Methanol and 135 Mt of bio-Methanol by 2050.

Methanol entails a strong advantage over other alternative low-carbon fuels in terms of logistics, as its physical properties would allow using current bunkering facilities with minimal modifications. In fact, according to DNV (2021), 122 commercial ports already have bunkering facilities for methanol. Methanol is currently available at prices sustainable for shippers and it does not impact too much the cargo capacity of the ships with a volume requirement nearly double the HFO baseline (McKinlay et al., 2021; Korberg et al., 2021; Methanol Institute, 2021). Also, as methanol is liquid at ambient temperature, this makes this fuel less difficult and safer to handle with respect to gaseous compounds like hydrogen and ammonia.

1.3 Carbon capture on-board

While it is difficult to infer from the discussion above which will be the most probable mix that will fuel the next generation of ships, it is plausible to infer that there will be a more diversified fleet with respect to the past; in this perspective, other solutions, such as carbon capture on-board, cannot be ruled out a priori.

In the short-to-medium term, it is important to investigate alternatives able to meet the IMO goals for 2050 without having the technical and economic burdens associated to fuel switching. As such, one possibility is to capture the carbon dioxide emissions on-board during the operation of the ship, liquify it in order to store it in tanks on the ships, and then unload it to suitable ports where it can be handled in broader onshore/offshore carbon capture and storage (CCS) networks. On-board carbon capture could be a complementary and additional tool for

shipbuilders to comply with IMO regulations and net zero targets. In general, on-board carbon capture could be a solution to reduce emission intensity of existing fossil-fueled vessels (bridging technology) with the first commercial applications expected for 2025, Mærsk McKinney Møller Center for Zero Carbon Shipping (2022).

1.4 Scope of this work

In the context of decarbonizing the shipping industry, this work proposes a techno-economic analysis of installing and operating an on-board carbon capture system for a large container ship. As such, the main objective is to investigate the techno-economic performance of installing and operating a carbon capture plant on-board a large commercial ship. The selected ship is representative of the size of vessels currently traveling the east Asia to North Europe. In particular, this study will take into account the container ship Munich Maersk, an ultra large container vessel (ULCV) with a capacity of 20650 twenty-foot equivalent unit (TEU) containers and a deadweight (DWT) of nearly 190000 tons, which is powered by two dual fuel engines (HFO or LNG), providing a combined 65 MW of propulsion power.

In this work, several case studies will be proposed depending on the type of ship fueling strategy, and on the design of the carbon capture plant. A total of seven cases will be proposed: three for the heavy fuel oil-fed ship and four for the LNG-fed one. A base case will be investigated for each fuel system, where the thermal energy necessary for the capture process is provided by a steam boiler fed with the same fuel used for propulsion. Then, an additional study will be given on the integration of an electrified heat pump system with heat recovery section from the engines flue gas. Two final case studies will be proposed to assess the effect on the techno-economic results of designing the carbon capture system for partial carbon capture rates (CCR).

For each of the above-mentioned case studies, an estimate of capital expenditures and of operating costs will be provided, and the results will be presented in terms of total cost of ownership (TCO) and of carbon capture cost (CCC). The economics of the ship will be discussed under three scenarios, by differentiating the distribution of ports allowed to handle the captured CO₂. A sensitivity analysis will analyze the effect on the economic results of the introduction of a global carbon tax.

Chapter 2

Carbon capture

2.1 Carbon capture and storage

Carbon capture and storage is a climate change mitigation technology first mentioned in 1977, in which CO₂ is captured from power plants and other industrial processes (e.g., refineries and cement plants), transported, and permanently stored in geological basins, preventing the CO₂ from reaching the atmosphere.

The International Energy Agency has claimed that in a sustained development scenario, CCS has the capability to reduce 13% of power generation-related global CO₂ emissions and up to 33.5% of heavy industry emissions by 2050, and as such, CCS must be part of the policy to mitigate the severe effects of global warming (IEA, 2020).

Notwithstanding the promising features of this technology, only 40 CCS commercial facilities are currently in operation. Martin-Roberts et al. (2021) state that the deployment has trailed behind expectations in the past due to a lack of regulation, financial incentives, and negative perceptions of technology. But momentum has grown substantially in recent years, with over 500 projects in various stages of development across the CCUS value chain (IEA, 2023). In 2022, project developers have announced new capture facilities to be operating by 2030, with a total capture capacity of 125 Mt CO₂ per year. Nevertheless, even at such a level, CCUS deployment would remain substantially below (around a third) the around 1.2 Gt CO₂ per year that is required in the Net Zero Emissions by 2050 (NZE) scenario.

2.2 Carbon capture

The capture of CO₂ can generally follow three alternative routes (Fig. 2.1):

- Pre-combustion
- Post-combustion
- Oxy-combustion

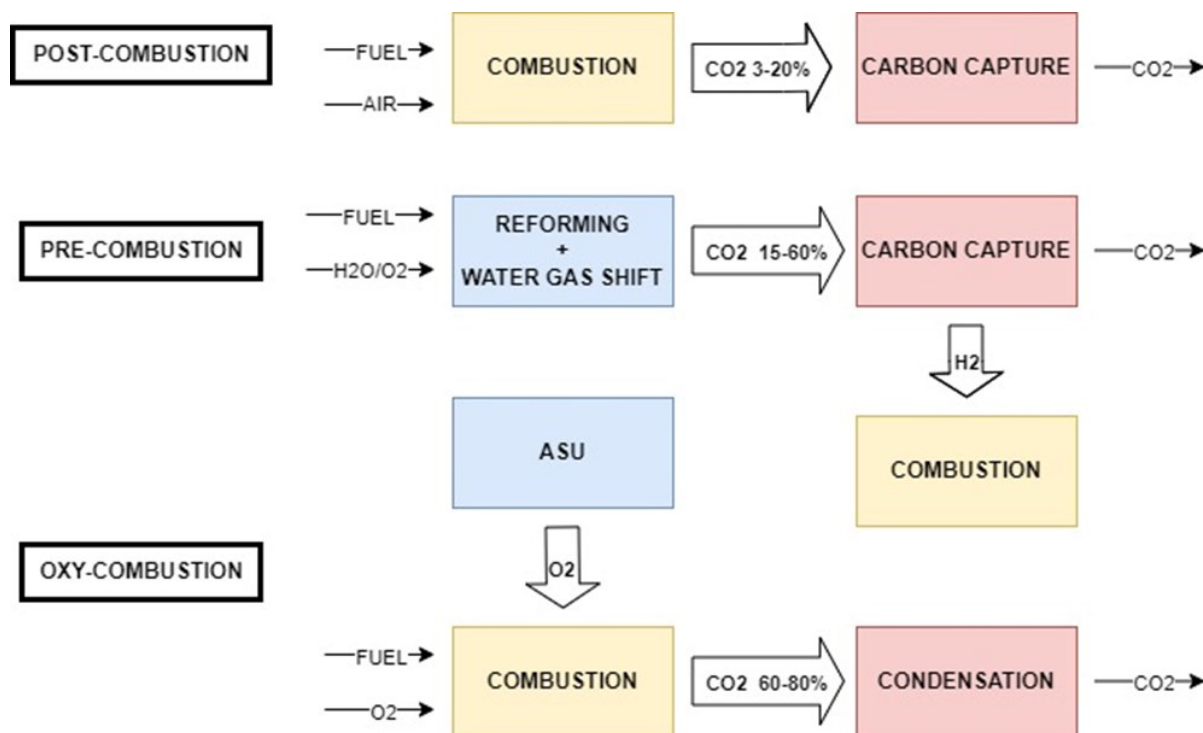


Figure 2.1. Summary of main carbon capture routes. Note: in pre-combustion case is, combustion is not mandatory, fuel cell usage can also be employed

2.2.1 Post-combustion

Post-combustion capture is the more developed and widely used technology to capture CO₂. In this process the carbon dioxide is separated after combustion in a process (e.g., chemical, membrane separation, cryogenic).

Post-combustion capture faces many challenges in design and industrial implementation, most notably the unfavorable condition of flue gas having a low concentration of CO₂ (3–20%), since the CO₂ is diluted in the flue gas by the presence of combustion air inert products (e.g., N₂). The resulting low partial pressure leads to a low driving force for CO₂ capture, which usually excludes the possibility of physical absorption. The process typically involves the usage of aqueous amine solutions (e.g., MEA, piperazine), compounds these with a high energy requirements for regeneration, factor this leading to high energy penalties compared to pre-combustion. Corrosion and solvent degradation are other significant problems in absorption processes. Amines are very corrosive to equipment such as the reboiler, heat exchangers, pipes, and the column (Chao et al., 2021).

Furthermore, the relatively low concentration of CO₂ imply the usage of large equipment due

to the large volume of gas handled (Godin et al., 2021).

Notwithstanding this, post-combustion is comparatively economical, has operational flexibility, a high level of technology readiness and has the advantage of being implemented downstream of a process without requiring significant modification to the original plant.

More advanced configurations (such as molten carbonate fuel cells) have been proposed in recent years besides solvent-based processes. This technology offers the advantage of exhibiting superior capture efficiencies in comparison to solvents. However, it entails elevated capital costs primarily attributed to the replacement of fuel cell stacks, which is currently estimated every (about) 5 years. Furthermore, this technology has not yet been validated at a significant scale (Campanari et al., 2009, 2013; d'Amore et al., 2023).

2.2.2 Pre-combustion

In pre-combustion, carbon dioxide is separated before the combustion process. Fossil fuel reacts with air or oxygen, with or without steam, and undergoes reforming to generate synthesis gas, a mix of (mainly) H₂ and CO. After removing the impurities, syngas passes through the water-gas shift reactor (WGS) where the carbon monoxide (CO) in the presence of water gets converted into CO₂ at a low temperature, involving the production of more hydrogen (Jansen et al., 2015).

After the reaction, concentrated CO₂ (15–60%) in the fuel gas is captured either by physical or chemical methods using adsorption, absorption (*e.g.*, Selexol, Rectisol processes), or membrane techniques at a pressure of 20–70 bar. The hydrogen can then be used as fuel in a fuel cell or combusted in a gas turbine for power generation. The absorption efficiency using this route is higher due to the higher CO₂ concentration in fuel gas, which also enables the usage of weak solvents with lower energy requirements for regeneration (Cebrecan et al., 2022). Furthermore, due to the high pressure of the gas coming from the reforming, the process requires smaller equipment (Pires et al., 2011), and less energy is also required for subsequent transportation (Zaman e Lee, 2013).

Disadvantageous for this technology is the high CAPEX connected to the components for the syngas generation. Also, major modifications are required to the plant process due to the high level of integration embedded with this capture mechanism. Thus, this capture route is difficult to implement for retrofitting applications and more suitable instead for new plant design. Currently, no full-scale plants for pre-combustion capture with power generation exist, despite several pilot projects (Godin et al., 2021).

2.2.3 Oxy-combustion

Oxy-combustion stands out due to the unique aspect that the fuel is burned with pure oxygen instead of air. This leads to the absence of nitrogen in the exhaust gas and high CO₂ concentrations (up to 70%), allowing thus CO₂ separation and capture by water condensation. This technology is currently at an early stage of implementation. Though being quite efficient and technically feasible, it consumes a large quantity of oxygen, which needs to be separated from the air by using an air separation unit (ASU). This technology involve high energy penalties depending on the scale of the plant but potentially being higher than those involved in post combustion capture (Leung et al., 2014; Vasudevan et al., 2016) with the ASU accounting for ~85% of the total energy needed in the plant (Dubey e Arora, 2022). Furthermore this unit is characterized by an elevated capital expenditure. These two factors combined make this capture option more suitable for high capacity projects.

2.3 Transportation

After being captured, the CO₂ must be transported to the final storage or utilization facility. Two modes can be typically deployed for large-scale CO₂ transport: networks of pressurized pipelines and ship transport. The efficacy of either of these two depends to a great extent on the quantity of CO₂ and the distance from its point of storage or utilization (Bui et al., 2018). The transportation of CO₂ through pipelines shares similarities with natural gas pipelines. However, CO₂ pipeline transportation presents some additional concerns. In fact, pipeline transportation is notably influenced by temperature, pressure, and impurities, often resulting in phase transformations during transit, (Liu et al., 2019). Also CO₂ pipelines are more susceptible to ductile fractures due to the challenges posed by low-temperature transport and pressure variations (Lu et al., 2020).

In cases where the scale of operations does not justify the use of pipelines in CCUS projects, alternative transportation methods like ships, become a viable options.

2.4. Storage

Geological storage of CO₂ (also known as geological sequestration) consists in injecting the CO₂ deep underground into stable underground basins.

The primary storage locations for CO₂ include saline aquifers and depleted oil and gas reservoirs. The significant storage capacity and the more wide distribution and greater regional coverage of saline aquifers makes them an important option even if they are not currently being adopted due to uncertainty over the actual capacity and operability .

CO₂ storage in depleted oil and gas reservoirs instead offers different several benefits. These reservoirs come with substantial existing surface and underground infrastructure, which can be repurposed for CO₂ storage with minimal adjustments (Cao et al., 2020) and also can be additionally used for enhanced oil recovery.

2.5. Carbon capture on-board ships

Besides onshore applications, carbon capture could be in principle deployed also on-board ships, to mitigate their emissions. The basic idea is to employ one of the technologies discussed in Section 1.1 and summarized in Table 2.1 to directly capture the carbon dioxide produced by the engines on board the ship. Given the greater complexity inherent with operating a plant offshore in a limited space environment and the intrinsic features of bridge technology that characterize this measure, the previously discussed options need to be evaluated in the context of this specific application to determine the most feasible and cost-effective choice.

Table 2.1. Summary of disadvantages and advantages of carbon capture processes

Technology	Advantages	Disadvantages
Pre-Combustion	<ul style="list-style-type: none"> - high CO₂ concentration in fuel gas. - Small equipment - Potential for physical absorption 	<ul style="list-style-type: none"> - high CAPEX for syngas generation. - no implementation on existing plants
Post-Combustion	<ul style="list-style-type: none"> - mature technology - economically feasible - minor plant modification required. 	<ul style="list-style-type: none"> - low CO₂ concentration in flue gas -high energy requirements for solvent regeneration.
Oxy-Combustion	<ul style="list-style-type: none"> - CO₂ capture through condensation. -small capture equipment 	<ul style="list-style-type: none"> - ASU capital and energy intensive -difficult retrofit

- Oxy-combustion CO₂ capture is not considered being a feasible option at this stage, with the main barrier being the absence of an engine able to operate with oxygen due to the excessively high temperature reached in the combustion. Also, the feasibility of storing an ASU unit on a ship has not been sufficiently investigated, but the large ASU equipment size and investment and the high specific energy consumption due to the small scale of the plant could be factors inhibiting this technology (Tesch et al., 2018).
- Pre-combustion, while more promising, is not chosen because of excessive capital costs and also because of its difficulty in being retrofitted to existing ships. Also, fuel reforming is currently not applicable to diesel-fueled ships; in fact, direct diesel steam reforming at high temperatures (~800°C) is still at a relatively early research and development stage. Typically, diesel SR catalysts become deactivated within a few hours due to coking, sulfur poisoning, and sintering of the catalyst (Martin et al., 2015).
- Post-combustion is here considered the most suitable process for maritime applications because of the maturity level of the technology, the higher level of retrofit ability compared to pre-combustion, and the possibility of installing the plant downstream of the propulsion system without major modification to the engine system. In considering the selection between the solvent process and the MFCF approach, it is essential to recognize that the latter is currently at an initial developmental phase with no on-scale projects being evaluated yet. Moreover, due to challenges associated with stack replacement and other associated expenses, it is deemed unsuitable for fulfilling the requirements of being a bridge technology for on-board carbon capture in a near-term perspective.

Once CO₂ is captured, it can be stored on-board the ship in either liquid or gaseous form, or as solid carbon. Liquid storage is the route chosen in this study because it allows storage at low pressure and at a lower volume compared to gaseous storage. The carbon dioxide is then unloaded in a port where facilities for handling are present and finally the carbon dioxide can enter the CCS network briefly described in Section 2.2 and Section 2.3.

One of the first systematic studies on solvent-based carbon capture for ships is attributable to Luo and Wang (2017), where the entire system, comprised of engine, afterburner, capture, and purification, was simulated on ASPEN Plus® for a HFO fueled cargo ship with a deadweight

of 12500 tons and powered by two diesel engines providing 17 MW of power. Their simulation was divided into two scenarios, one considering the fuel excess needed for running the plant and one without any fuel excess, and resulted in a carbon capture rate (CCR) of 90% and 73%, respectively. Their high-temperature flue gas, approximately 362 °C, allowed producing steam directly in a waste heat recovery system, explaining the high CCR in the case without fuel excess. Notwithstanding this, the fuel excess necessary for the 90% capture rate was estimated being nearly 21% of the propulsion fuel consumption, a value that brings in significant challenges to the economics of the ship. The tank volume necessary to store the liquefied carbon dioxide, was designed for a traveling time of only 2-3 days, which could be a strong limitation for longer journeys. Also, an economic estimation was done, which resulted in a cost of captured carbon (CCC) of 151 €/ton for the case with fuel excess and 72 €/ton in the case without. The computation shown as the annualized capital expenditure is the most relevant to the overall results, even if some operating costs, such as the revenue loss from space otherwise dedicated to cargo purposes (in this work referred as ‘container loss’) and the carbon dioxide unloading costs, were not estimated. The container loss arises from the difference in mass between the fuel burned and the carbon dioxide stored on-board, this increase in weight leads to a container loss which can impact the revenues. The unloading cost is instead the cost that the liner must sustain to discharge the captured CO₂ in a port and it is related to the transportation and storage cost downstream shipping.

Awoyomi et al., (2019) proposed to expand the study by introducing the process for a LNG-fueled ship and also introducing exhaust gas recirculation (EGR) with the aim of increasing the carbon dioxide concentration in the flue gas, a critical factor because of its impact on the reboiler-specific energy required. While in a stationary application the CO₂ concentration in the flue gas is usually 11-13%^{mol} in a ship application the range of concentration is much lower, around 4/5%^{mol} depending on air excess and thus on particular fuel and engine specifications. The EGR proved effective, increasing the concentration from 7 %m to 11%^m and decreasing the specific reboiler duty from 10.5 MJ/kg of CO₂ to 7.5 MJ/kg of CO₂ captured, still values well above specific heat requirements for carbon capture at stationary plants. The authors simulated the plant with NH₃ as a solvent instead of MEA, arguing that it presented some advantages such as lower energy consumption, fewer corrosion problems, and a higher loading capacity. However, they recognize some drawbacks of using NH₃ in place of MEA, such as its slow kinetics for absorption and volatility, which require larger capacity equipment and an abatement system. This could pose challenges due to the limited space available on-board ships.

Also in this case, an economic analysis was performed, which showed that for the ship under examination, a CO₂ carrier with 10 MW of propulsion power could achieve a design CCC of 108 euro per ton with EGR and 120 without. Furthermore, a sensitivity analysis on the engine load factor (portion of the rated engine power that is utilized) was performed, showing that partial loadings produce a decrease in the economic performance of the carbon capture plant.

Feenstra et al. (2019) developed an on-board carbon capture system for an LNG and diesel engine, using the flue gas to directly provide heat to the reboiler. In this manner, with flue gas available at 325°C for the diesel and 350°C for the LNG, it was possible to achieve 90% of the capture rate without providing excess energy considering a minimum temperature difference approach of 10°C for the heat recovery section. Their results showed that the LNG case is less costly than the diesel case, primarily because LNG is able to provide the cooling duty necessary to liquefy the captured CO₂, while in the diesel-fueled ship, a refrigeration cycle based on ammonia was needed. This leads to higher CAPEX and higher variable operating expenses (VOPEX) related to higher compressor electricity demand. Also, the scale and size of the ship was shown to greatly affect the results, with a 1.2 MW inland vessel having a CCC ranging from 185 to 231 €/ton, while for a 3 MW cargo vessel, costs decreased to 93–130 €/ton. Ship size is therefore of paramount importance for the economics of the capture, primarily due to economies of scale over capital expenditures.

Mærsk Mc-Kinney Møller Center for Zero Carbon Shipping (2022) conducted a study on the application of on-board carbon capture to different classes of ships and fuels. The results were quite different and more pessimistic with respect to Feenstra et al. (2019), showing excess energy consumption reaching peaks of 45% for 15000 TEU diesel-fueled ships and 18% for a LNG-fueled one. Even though a deeper analysis of the methodology deployed was not provided in this study, another report by the Oil and Gas Climate Initiative (2021) shows similar results in terms of excess energy. This was calculated by using only the available heat energy from the main propulsion engine, and only 8% of the carbon dioxide emissions could be captured. This relatively low figure hints at the lack of available waste heat energy that can be obtained from the efficient, slow-speed, two-stroke engine they deploy. As the capture rate increased, the amount of energy needed increased. This could only be supplied through excess fuel burned in the auxiliary engines and oil-fired boilers. Compared with the reference case, this amounted to 22% and 53% more fuel consumed. They also reported that low exhaust gas temperatures from the main propulsion engine primarily drive the need for additional fuel consumption in the

auxiliary engines and boiler. However, they also pointed out that these engines were designed and optimized to deliver high efficiency and not to support the implementation of a carbon capture system. Consequently, measures to recalibrate engine performance or optimize the waste heat recovery units to complement a carbon capture system have not been explored, so the figures shown here may be assumed to be a worst-case estimate.

The literature highlights how the energy required for carbon capture represents the main bottleneck for adoption; in fact, as demonstrated by achieving high capture rates, this requires more energy, and if this energy cannot be provided from the ship system, more fuel is needed, which starts a feedback loop requiring more fuel to run the process and reach the design carbon capture rate, impacting the economic performance of the process. A detailed energy analysis was mainly treated by Einbu et al. (2021), considering varying engine loads and fuel, capture rates, and equipment sizing. The results showed that, in general, a capture plant downstream a diesel engine is more energy efficient than downstream an LNG one, as typically the carbon dioxide concentration is significantly higher in the flue gas of a diesel engine rather than in those from an LNG ship. Also, they showed that increasing the absorber and stripping height favor the capture, even if in on-board applications, space constraints related to the type of ship must be taken into account, especially in retrofit problems. Differently from Luo e Wang (2017) and Feenstra et al. (2019), Einbu et al. (2021) find that an afterburner (which imply extra fuel to be burned) is necessary for 50% CCR.

While the waste heat recovery system methodology is not clearly discussed neither in this paper nor in the ones previously cited, it can be assessed in a preliminary way that a certain level of difference between works is explainable by the difference in flue gas temperature and thus engine characteristics.

From an economic perspective, the references mentioned, despite presenting varying economic outcomes as summarized in Table 2.2, concur in emphasizing that capital expenditure constitutes the most significant portion of overall expenses. This observation can be attributed to their shared emphasis on smaller to medium-sized vessels. It must be pointed out, though, that their calculation neglects some operative costs associated with the plant such as the CO₂ unloading cost and the revenue loss associated with the container loss. In detail the first is the fee the liner must pay to discharge in a port the captured carbon dioxide, while the second arise from the excessive tonnage resulting from the difference between the fuel burned and the pollutant stored in a liquefied form on-board. As such, these costs depend on the geographic characteristics of the actual journey of the ship. For instance, Negri et al. (2022) assumed a

distance from final geological storage sites of 200 km; notwithstanding this, the cited work, as well as the others already discussed, tested the plant on a medium-sized ship, a 8500 TEU container vessel, designed to operate only for short-distance voyages. Furthermore Negri et al. (2022), even though reporting a container capacity reduction related to the installed equipment mass, did not consider the operative loss due to the increase in mass during the navigation alongside CO₂ capture plant operation.

Table 2.1. Comparison of on-board carbon capture plants-related studies. (/) stands for value not provided

Author	fuel	DWT	CCR	Specific reboiler duty	solvent	Excess energy	CCC
		Tons	%	$\frac{MJ}{kg}$		%	$\frac{€}{ton}$
Luo et al.	HFO	12500	73	3.77	MEA	0	72
	HFO		90	3.85	MEA	21.4	151
Feenstra et al.	HFO	8000	90%	/	MEA	0	111-130
	LNG		90%	/	MEA	0	/
Awoyomi et al.	LNG	/	90%	3.30	NH ₃	12.5	120
			90%	1.21	NH ₃	12.5	108
Negri et al.	HFO	115000	94	5.9	MEA	/	85

This work combines different innovative components. Firstly, the integration of an electric heat pump marks a novelty from a thermal energy recovery-perspective to fulfill the capture plant (thermal) energy requirements. Heat pumps are an efficient way to extract energy from a moderate temperature stream and thus could be a viable option to extract more heat from the flue gas with the aim to produce (at least part of) the steam needed by the reboiler of the carbon capture section. Additionally, from an operational standpoint this study considers an entire voyage composed by multiple legs, trying in this way to provide a holistic understanding of the logistic and economic complexities involved in sizing an on-board carbon capture plant (comprehensive of on-board CO₂ storage vessel). Under the same assumptions (i.e., long-distance, multi-leg trip) also the container loss due to on-board carbon storage is included in the calculations, with the aim of evaluating the loss of revenue that shipping companies may need to sustain to capture the CO₂ during a ‘standard’ journey. Lastly, this study focuses on a ultra large container vessel of nearly 190000 tons, significantly of a greater scale in comparison

to the cited literature, with the aim to appreciate the effect of a substantial ship size (and consequently, with a significant level of CO₂ emissions) on the feasibility of this technology.

Chapter 3

Methodology

3.1 Reference ship and flue gas composition

The ship selected for this study is the Munich Maersk, an ultra-large container vessel (ULCV) of the Maersk company, currently operating on the route connecting east Asia with north Europe. This vessel was built in 2017, with a nominal capacity of 20568 TEU and a deadweight (DWT) of nearly 190000 tons, (Marine traffic, n.d.), powered by two MAN engines (Table 3.1). The chosen propulsion system is composed of two dual-fuel (i.e., it can operate either with LNG or with HFO) MAN 7G80ME-C10.5-GI-HPSCR gas Opt. of nearly 33 MW each, which are compatible with the vessel required engine power (in the order of 65 MW according to Maersk). Operating data such as the engine load, fuel consumption, flue gas flowrate, and temperature were retrieved from MAN's CEAS engine calculator application for both the LNG and HFO modes and are summarized in Table 3.2.

The flue gas composition resulting from combustion was calculated via the ASPEN Plus software by computing a stoichiometric combustion with imposed total fuel conversion and pre-set flue gas temperature. Fuel flow rates were retrieved from the engine datasheet by assuming a load factor of 80% of the nominal engine power (which is a reasonable value based on current practice for large container vessels). LNG composition was assumed to be 90%^{mol} of CH₄, 7.5%^{mol} of ethane, and the remaining propane. The composition of HFO was assumed to be 85.1%^w of C, 10.9%^w of H and the remaining 4%^w being sulfur. As a result, the two LNG engines produce flue gas at a rate of 114.2 kg/s, available at a temperature of 206 °C. This gas contains 3.06% CO₂ on a wet basis and 3.25% on a dry basis. In contrast, when operating at an 80% load factor, the HFO propulsion system generates flue gas at a rate of 122.4 kg/s. This gas has a higher CO₂ content, measuring 3.99% on a wet basis and 4.12% on a dry basis, and a temperature of 214 °C. This difference in CO₂ concentration is primarily attributed to the greater carbon-to-hydrogen (C/H) ratio in HFO compared to LNG. It is also important to note that, for the same power output, the flue gas flow rate is higher for HFO due to the lower energy

content of HFO compared to LNG. To give a perspective the ship under study, considering four voyages per year can emit more than 154195 tons of CO₂ if fueled with LNG or 212480 tons if fueled with HFO.

Table 3.1. Reference ship data, TEU (twenty foot equivalent unit) is the standard size of a container box. Deadweight is the difference between the displacement and the mass of empty vessel (lightweight) at any given draught, in other terms the maximal weight a ship.

Ship name	Munich Maersk
DWT	190300 tons
TEU	20568
Construction year	2017
Engine power	65940 kW
Engine	2X 7G80ME-C10.5-GI-HPSCR Gas Opt. (dual fuel)

HFO combustion leads to the production of other pollutants, such as SO_x. Notwithstanding this fact, these compounds were treated as inert in this system because ships powered by HFO employ desulfurization systems to comply with MARPOL regulations. In fact, to fulfill the obligations of Annex VI of the MARPOL Convention (IMO, 2013) related to sulfur emission and, simultaneously, to prevent excessive degradation of the amine solvent in the carbon capture system, the exhaust gas desulfurization system is required. Such desulfurization systems can be implemented upstream the carbon capture plant (Negri et al., 2022).

Differently, LNG does not produce SO_x during combustion; thus, the flue gas can directly bypass the desulfurization plant and be sent to the carbon capture plant.

Regarding NO_x, these form when nitrogen reacts with oxygen at high combustion temperatures. This occurs almost independently of the fuel type and depends on the peak engine flame temperature. An effective way to reduce emissions without impacting the downstream process could be the use of exhaust gas recirculation (EGR) technology, as stated by Deng et al. (2021). Recirculation of about 30% of the exhaust gas increases the heat capacity and lowers the oxygen content during combustion, which in turn reduces the flame peak temperature and thereby minimizes NO_x formation. Additionally, as demonstrated by Awoyomi et al. (2020), this measure could also be effective in increasing CO₂ concentration and favor its separation via carbon capture.

Since LNG NO_x formation is more than 80% lower with respect to other sources, no reduction

technology is needed (Deng et al., 2021).

The overall assumption that emerged from this discussion is that it is not necessary to simulate these desulfurization and denitrification units and also not to consider them in the flue gas composition. While this is an approximation, the error is considered acceptable considering that NO_x and SO_x combined concentrations in untreated flue gas are below 0.2% (Issa et al., 2019).

Table 3.2. Summary of flue gas characteristics. Remaining compounds are impurities, Ar, S.

		HFO	LNG
Flue gas	[kg/s]	122.4	114.2
Flue gas	[Kmol/s]	4.21	3.99
T	[°C]	214	206
CO ₂ conc.	[%m (dry)]	4.1	3.3
Mol fractions	[%]		
H ₂ O		3.05	5.84
CO ₂		4.00	3.06
O ₂		15.1	14.4
N ₂		76.8	75.7

The objective of this study is to abate the CO₂ emissions deriving from the fuel combustion in the main propulsion engines of the ship described above. As such, the proposed plant scheme is composed by (Figure 3.1):

- A carbon capture unit, which is needed to separate the CO₂ from the flue gases deriving from the combustion in the engines.
- A low-temperature purification and liquefaction unit to increase the carbon dioxide concentration for an effective liquefaction.
- A storage tank to keep the carbon dioxide in liquid state through the voyage.

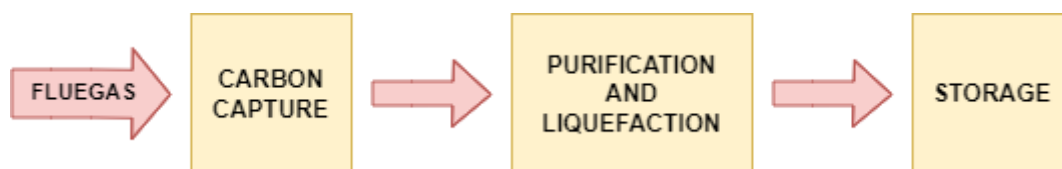


Figure 3.1. Block scheme of the process

3.2 Carbon capture unit

While amine-based carbon capture is a mature technology for onshore applications (e.g., post combustion CO₂ capture on flue gas streams for energy and industry sectors), major challenges need to be faced when applying this technology to offshore and not stationary application, such as a ship. In fact, several limitations need to be considered, as summarized by Luo et al., (2017), such as the space limitation, the need to provide thermal and electrical energy to the carbon capture unit, the increase in weight, and the space required for the carbon dioxide on-board storage in tanks depending on storage conditions. Water supply is not considered a limitation assuming the presence of an on-board desalinization plant.

3.2.1 Solvent

Chemical absorption is generally preferred over physical absorption for CO₂ post-combustion capture in flue gas because of their higher absorption capacity at a low partial pressure of CO₂. Several solvents are available for this purpose with the most employed according to Tan et al. (2012), being:

- Monoethanolamine (MEA): Fast absorption rate but limited CO₂ loading capacity. Prone to degradation and operational issues such as equipment corrosion.
- Diethanolamine (DEA): Quick absorption, relatively less stable carbamates than MEA, but still limited CO₂ capacity. Some corrosion risk.
- Methyldiethanolamine (MDEA): Higher CO₂ loading, lower energy for regeneration, less degradation, non-corrosive to carbon steel, but slow absorption kinetics. (Tan et al., 2012)
- 2-Amino-2-methyl-1-propanol (AMP): High CO₂ loading, low regeneration energy, less corrosion, better degradation resistance, but slower absorption.
- Piperazine (PZ): High CO₂ loading, fast reaction, resistant to thermal and oxidative degradation, used as a promoter in amine systems.
- Ammonia: High absorption capacity, low energy for regeneration, but highly volatile with potential ammonia slip.
- Potassium Carbonate (K₂CO₃): Lower absorption enthalpy, requires promoting amines and higher temperatures, corrosive to carbon steel.

These solvents offer various trade-offs in terms of reactivity, capacity, corrosion risk, and

operational considerations, depending on the specific application and requirements. The most employed solvent for this process is the MEA. The main advantage of MEA is the fast absorption reaction, factor this critical to keep the equipment height under control especially for low CO₂ concentration flue gases (Mota-Martinez et al., 2017). Given the constrained space available on a ship MEA has been therefore selected as the solvent for this work.

3.2.2 Carbon capture flowsheet

The capture plant was simulated through the ASPEN Plus process simulator. The engine flue is deployed to provide heat to the reboiler to cover part of the thermal energy required for the MEA solvent regeneration (Streams #1-#2 in Figure 3.2). Differently to Feenstra et al., (2019), a temperature difference between hot and cold streams of at least 30°C was ensured, giving a resulting flue gas outlet temperature of 150°C. The cooled flue gas is then directly contacted with seawater (#13), assumed to be disposable at 10°C, in order to partially condense H₂O, increase the CO₂ concentration, and reduce the temperature at the inlet of the absorber. This is done to increase the absorption capacity of MEA, considering the thermodynamics of the exothermic CO₂ absorption system that could cause reversible reactions when the temperature is too high. Furthermore, the increase in temperature could also increase the CO₂ vapor pressure over the solution, which leads to a decrease in the physical solubility of CO₂ in the solvent (Tan et al., 2012; Gul e Un, 2022). The cooled exhaust gas is then fed to the bottom of the absorber (#3), where it is contacted with an aqueous MEA solution coming in countercurrent from the top (#10). The MEA solution is able to chemically absorb the carbon dioxide, allowing the cleaned flue gas to be disposed of from the top of the column. The off-gases from the top (#11) of the absorber are then cooled down with seawater in order to recover the MEA solvent, which is then recirculated back to the column. After this step, the cleaned-up gas, containing only a minor fraction of solvent, is emitted to the atmosphere (#12).

The CO₂-rich stream exiting from the bottom of the absorber is heated up with the regenerated solvent coming from the stripper (#4-#5). Then, the heated stream (#5) is charged at the top of the column. In the stripper column, the inverse process of the absorber occurs in an endothermic reaction, and the carbon dioxide exits as a gas from the top (#6) while the regenerated solvent solution exits from the bottom (#8) and is recirculated back at the absorber. The CO₂-rich stream is then cooled with seawater (#6-#7) to recover the solvent and further increase the concentration of CO₂.

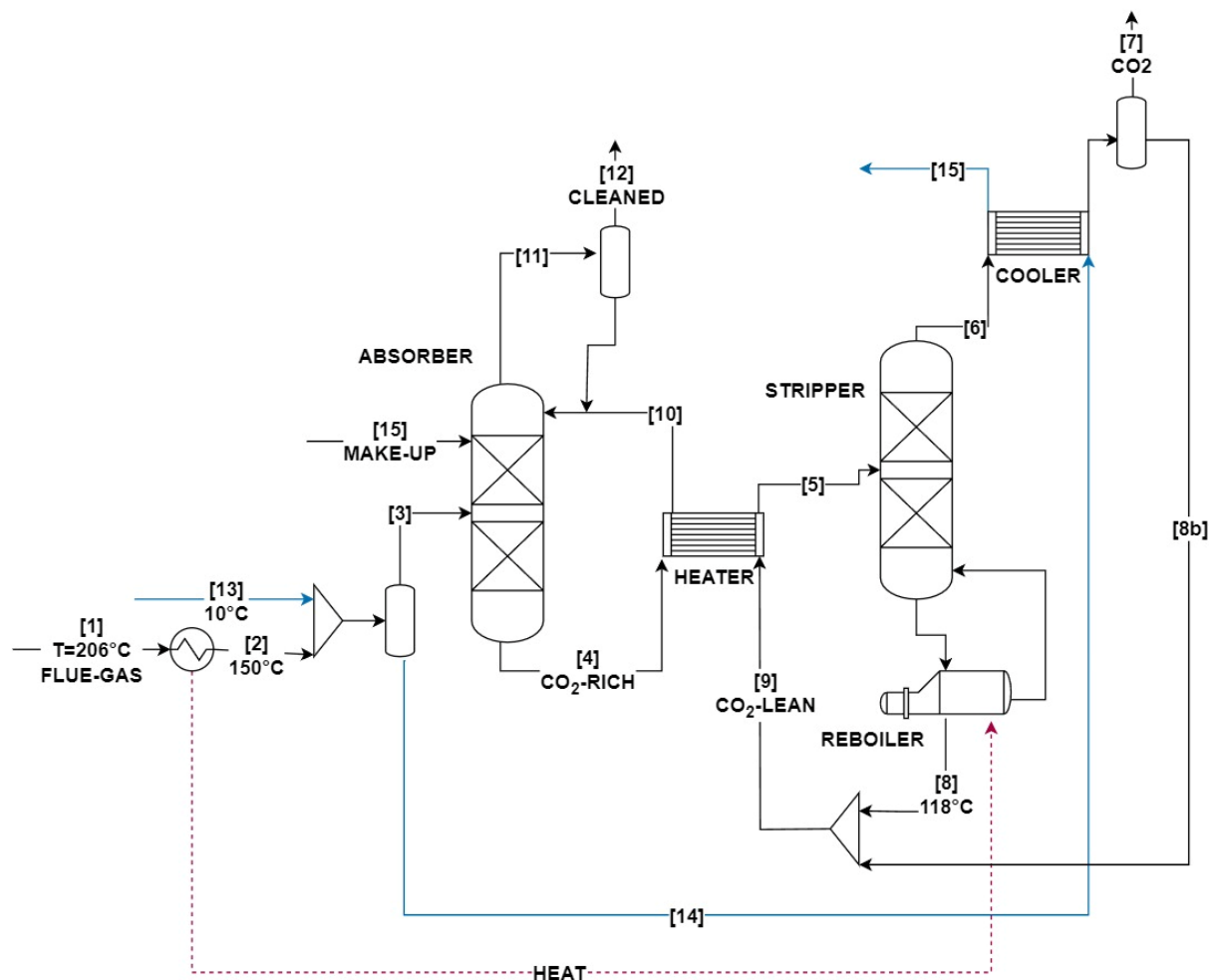


Figure 3.2. General MEA based carbon capture plant. In blue the seawater for cooling, in dashed line red is presented the direct flue gas-reboiler heating

3.2.3 Thermodynamic and kinetic model

The ternary system composed of CO_2 , H_2O , and MEA has been widely studied in the past few years following the increased demand for capturing carbon dioxide in exhaust gases. The thermodynamic model used in this system is the one proposed by Hilliard et al. (2008), an electrolyte non-random two-liquid (e-NRTL) activity coefficient model used for the absorber, stripper, and other equipment related to the carbon capture section, coupled with Henry's law and the Redlich-Kwong EoS to describe CO_2 solubility and vapor properties, respectively (Madeddu et al., 2017).

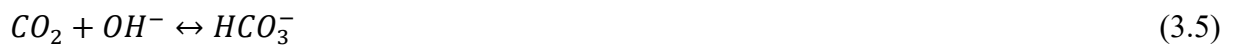
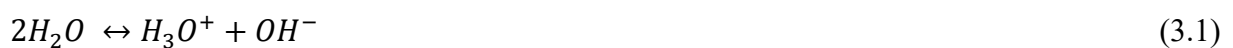
The absorber and the stripper column are modeled in Aspen Plus with the RadFrac™ model. Two different approaches can be employed to represent the reactive absorption system:

- Equilibrium stages model: assumes that the liquid and gaseous phases are in intimate contact for a time sufficient for the establishment of thermodynamic equilibrium between the streams exiting each stage.
- Rate-based mode: with this approach, it is possible to take into account the limitations to mass transfer due to the presence of chemical reactions. Rate-based multistage separation models assume that separation is caused by mass transfer between the contacting phases, equilibrium is achieved only at the vapor-liquid interface, and the Maxwell-Stefan theory is used to calculate mass transfer rates (Zhang et al., 2009).

In both cases, the column height is discretized into a certain number of parts, which are referred to as stages in Aspen Plus®, though in the case of the rate-based mode they should be referred to as segments.

In this work, the absorber and stripper were modeled with a rate-based model, widely considered in the literature to be the best way to model this equipment for this process. In fact, as reported by Øi (2007), the typical values of the Murphree efficiency for the reactive absorption of CO₂ are averagely 0.2%, indicating that the process is far from the phase equilibrium condition. For this reason, the most commonly used approach in the case of the reactive absorption-stripping of CO₂ with MEA is the so-called rate-based one.

As reported in numerous works on CO₂ post-combustion capture with MEA, both kinetic and equilibrium reactions are involved. In particular, a set including three ionic equilibrium reactions (Eqs. 3.1–3.3) and two kinetic reversible reactions involving CO₂ (Eqs. 3.4 and 3.5) were considered (Madeddu et al., 2019).



Equilibrium constant were calculated with the Aspen Plus method of the standard Gibbs free energy change as follow Eq. (3.6):

$$K_{eq} = \exp\left(-\frac{\Delta G^0}{RT^L}\right) \quad (3.6)$$

With ΔG^0 values used in Aspen and T^L being the temperature of the liquid phase.

Concerning instead the kinetic rates, the forward rate's and reverse rates parameters are provided for by Hikita et al., (1977) for reaction 3.4 and by Pinsent et al (1956) for reaction 3.5

and are summarized in Table 3.3. Kinetic constants are expressed in the Arrhenius form as in Eq. (3.7)

$$k = A \cdot \exp\left(-\frac{E_a}{RT}\right) \quad (3.7)$$

Table 3.3. Kinetic parameters

Reaction	Forward reaction		Reverse reaction	
	$\frac{\text{kmol}}{\text{m}^3 \cdot \text{s}}$	$\frac{\text{cal}}{\text{mol}}$	$\frac{\text{kmol}}{\text{m}^3 \cdot \text{s}}$	$\frac{\text{cal}}{\text{mol}}$
3.4	$9.77 \cdot 10^{10}$	9855.8	$3.23 \cdot 10^{19}$	15,655
3.5	$4.32 \cdot 10^{13}$	13,249	$2.38 \cdot 10^{17}$	29,451

Where A is the pre-exponential factor with units of $\frac{\text{kmol}}{\text{m}^3 \cdot \text{s}}$ and E_a is the activation energy with units of $\frac{\text{cal}}{\text{mol}}$.

3.2.4 Columns

Characteristics of columns, such as the height of the packing and the type of packing used, exert a significant influence on the performance of carbon dioxide (CO₂) capture processes. In fact, as suggested by previous research (Einbu et al., 2017), when the packing height of the absorber is increased, the specific reboiler duty, expressed in MJ/kg CO₂ captured, decreases, indicating an enhancement in the efficiency of the capture process. In a ship's environment, the height is constrained by the space available on board for the installation of machinery. For this reason, in this work, a total packed height of 20 m for the absorber and 9 m for the stripper is assumed, with the stripper height being lower for the faster kinetics compared to absorption.

The selection of column packing is of particular significance. It has been observed that the lowest reboiler duty is associated with structured packing that possesses a high surface area, resulting in the highest loading of rich CO₂. Additionally, the surface area of various packing materials exhibits an inverse relationship with temperature profiles along the column. Furthermore, packing materials with higher surface areas yield higher CO₂ loading profiles, and conversely, those with lower surface areas produce lower loading profiles, as reported by Rahmanian et al. (2017). The reason for the reduced reboiler duty with high contact surface area in structured packing is that it leads to a higher absorption of CO₂ in the absorber, necessitating less circulation of the solvent. As a result, the quantity of solvent processed in the stripper is reduced, leading to a decrease in the energy required to heat up the solvent.

In this work, a structured packing is chosen, in particular a Sulzer MELLAPAK 250Y, in accordance with Feenstra et al. (2019) and Agbonghae et al. (2014).

3.2.5 Energy recovery and CCR

In this work, different concept plants are provided that differ in function according to the fuel used by the ship and the energy system employed to provide the thermal energy to the reboiler. In particular, for the cases denominated LNG-FB and HFO-FB, the thermal energy is provided by steam produced in a boiler fueled by the same fuel used for propulsion. The boiler is assumed to have an efficiency of 95%, as stated by Vakkilainen et al. (2016).

The cases denominated LNG-Base and HFO-Base are instead two cases denominated in this way because no extra energy is provided to permit the CCR specification to be met, and thus the capture rate is limited by the heat provided to the reboiler by the flue gas.

The remaining three cases that are going to be discussed in this work, summarized in Table 3.4, see an energy recovery unit composed of heat pumps that will provide the steam used in the plant. In particular, the difference between HPpart and HPTot lies in the number of heat pumps employed. In the former, only one cycle is designed to be placed upstream of the absorber in order to recover the heat available in the flue gas, while in the latter, an additional cycle is placed after the reboiler in order to recover part of the heat before the cross-heat exchanger and produce additional steam.

The design specifications required a capture rate of 90%. In cases where it was not possible to achieve this 90% capture rate, the target was adjusted to the maximum permissible value based on heat energy and case constraints. This adjustment will be further discussed in the next chapter to provide a deeper understanding of the energy limitations of the process. It is important to note that the CCR is based on the carbon dioxide emitted by the propulsion engine without considering the additional carbon dioxide emitted for excess energy and the auxiliary engine consumption. Thus, in the discussion, an estimate of the effective CCR will be provided considering those emissions.

Table 3.4. cases summary

case	fuel	Excess thermal energy system
LNG-FB	LNG	BOILER
LNG-HPpart	LNG	HEAT PUMP
LNG-HPtot	LNG	HEAT PUMP
LNG-Base	LNG	NONE
HFO-FB	HFO	BOILER
HFO-HPpart	HFO	HEAT PUMP
HFO-Base	HFO	NONE

3.2.6 Heat pump

Heat pump systems offer an efficient alternative to recovering heat from different sources for use in various industrial, commercial, and residential applications. A heat pump extracts heat from a source (Streams #1-#2 in Figure 3.3), such as the atmospheric air or waste heat from a process. It then amplifies the energy through the compression of the working fluid and processes this to increase the temperature of the latter (#2-#3). Then the heat is transferred where it is needed through the condensation of the refrigerant (#3-#4). The cycle is finally closed through the lamination of the working fluid (#4-#5) (Figure 3.3).

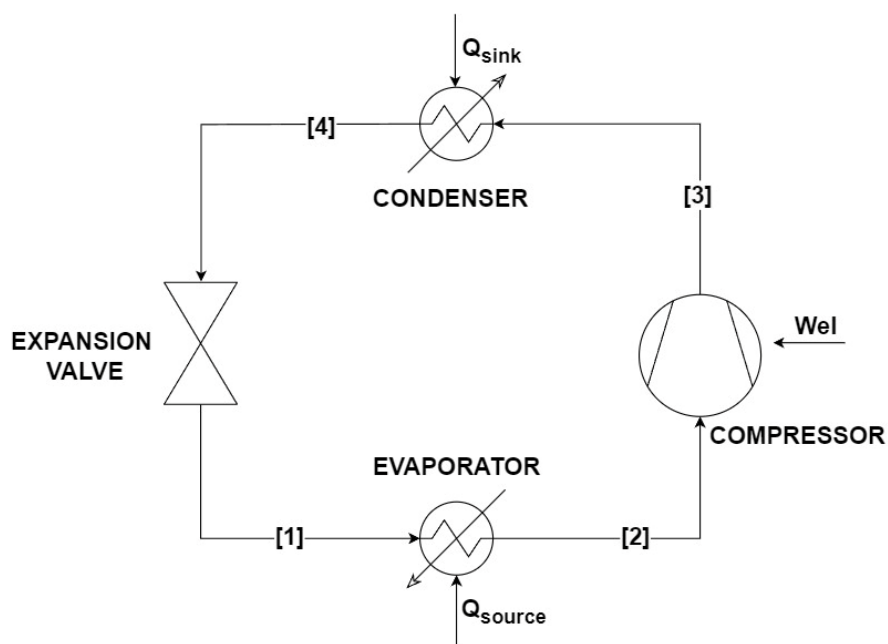


Figure 3.3. Generic heat pump scheme

The coefficient of performance (COP), is the ratio of useful heating provided by the heat pump to the work (energy) required. The COP is an index of the efficiency of the heat pump, higher COPs equate to higher efficiency, lower energy (electric power) consumption and thus lower operating costs. The COP for the system under exam can be computed from eq. 3.8.

$$COP = \frac{\dot{Q}_{sink}}{W_{el}} \quad (3.8)$$

The most common configurations are:

- Single-stage layout, are the classical heat pump systems characterized by a single compression stage, suitable for moderate temperature lift in order to limit decrease in efficiencies (Sun et al., 2021).
- Multi-stage system employs more than one compression stage to achieve a higher output temperature at the expense of mechanical energy consumption. A cascade heat pump system couples the circulation of two or more working fluids to achieve a larger temperature lift.
- Hybrid heat pump system integrates a vapor compression heat pump with other thermal systems like absorption, adsorption, solar energy, or chemical heat pump systems. (Jiang et al., 2022).

In this work, a single-stage layout is chosen due to the temperature lift being lower than 60°C and the compression ratio being limited to 4. The refrigerant employed is R1233ZD; the choice was based on the set of temperatures involved in order to have the best COP and for its low environmental impact (Hassan et al., 2022). In particular the heat exploited is provided by the flue gas stream coming from the reboiler at 150°C. The stream passes through a heat exchanger, where it is cooled to 85 °C (#2-#2a in Figure 3.4) thanks to the evaporation of the refrigerant, which is then compressed from 6 to 24 bar (#17-#18), with the temperature increasing from 139°C to 196°C. The heated refrigerant is then condensed to produce low-pressure steam at 3 bar (#18-#19).

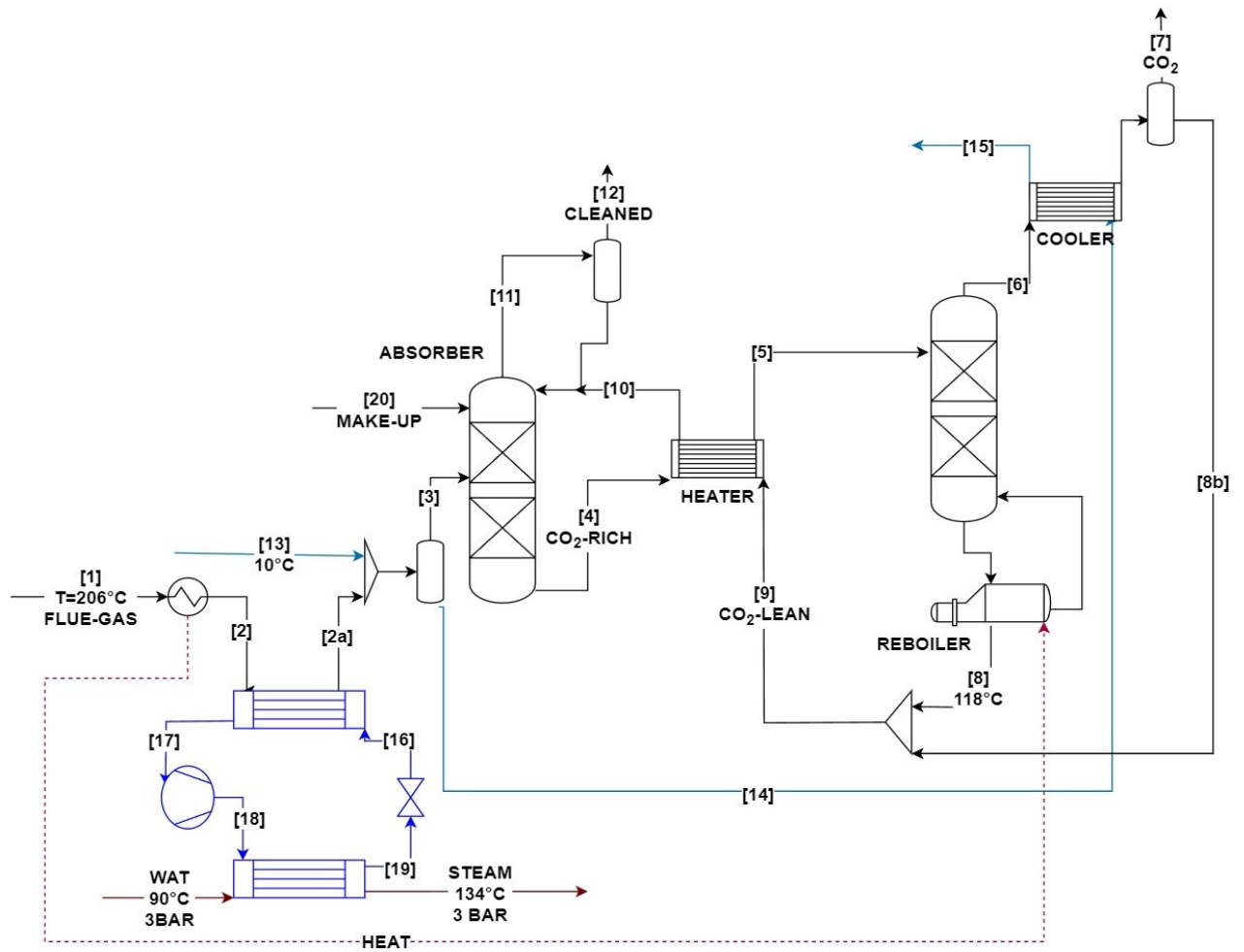


Figure 3.4. Heat pump cycle integration (dark blue). The steam produced, and directed to the reboiler, is recirculated in a closed cycle not showed for graphic reasons.

In the HP_{tot} case a second heat pump cycle is implemented. In addition to the HP_{part} plant, a fraction of the steam produced is conveyed to a second heater with the aim of further preheat the stripper charge (Stream #26 in Figure 3.5).

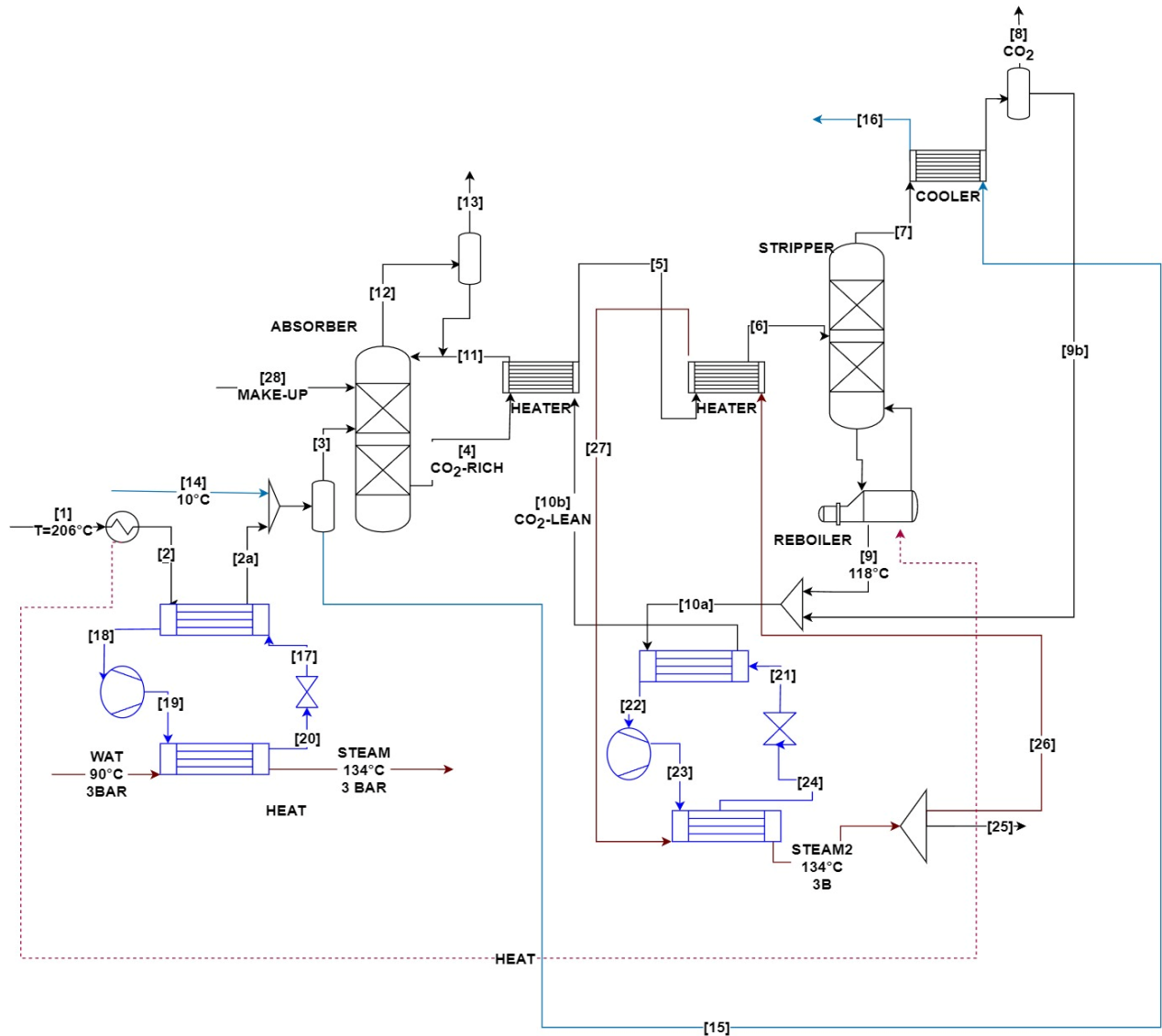


Figure 3.5. H₂tot plant. All steam cycles are closed, not showed for graphic reasons.

To evaluate the performance of the heat pump compared to conventional steam boiler the excess fuel needed to achieve the CCR is computed with eq. 3.9 and 3.10.

$$\text{excess fuel, no HP} = \frac{\dot{Q}_{reb} - \dot{Q}_{disp}}{LHV_{fuel} \cdot \eta_{boiler} \cdot \dot{m}} \cdot 100 \quad (3.9)$$

$$\text{excess fuel, HP} = \frac{W_{comp}}{\eta_{engine} \cdot \dot{m}} \cdot 100 \quad (3.10)$$

Where η_{boiler} is 95%, and η_{engine} 27.78 MJ/kg (LNG)-22.19 (HFO) are retrieved from the engine datasheet at the operating load factor. The fuels lower heating values (LHV) are considered and is 42.7 MJ/kg for HFO while for LNG it has been considered equal to the methane LHV or 50 MJ/kg.

3.3 Purification, liquefaction and storage

Carbon dioxide arrives from the capture with a concentration higher than 83%^m which varies depending on the fuel and case studied. It becomes imperative to undertake a purification process aimed at diminishing the presence of non-condensable gases and water. This necessity arises from the influence highlighted by Bui et al. (2018) on the phase envelope and, consequently, on the energy prerequisites due to impurities. Subsequently, the purified carbon dioxide is liquefied for storage, with the additional requirement of water removal to prevent freezing during the liquefaction process. Due to the absence of MEA, present only in traces, the thermodynamic model is changed to the Peng-Robinson in accordance with Deng et al. (2019). The gaseous stream is treated in different manners depending on the fuel; the one referring to the LNG ship is compressed to 15 bar with a multistage compressor with an isentropic efficiency of 85% (Streams #1-#5 in Figure 3.6). The multistage compressor is divided into two stages with intercooling in between, leading to the condensing of part of the water and purifying the gas to a resulting concentration of 99.3%. This level of purity is regarded as suitable for injection and storage, and thus no attempt was made to increase this value, Brownsort (2019). It is assumed that, if higher concentrations are required, this upgrade could be done once discharged onshore to better make use of the scale economy.

The purified carbon dioxide is then liquefied by using the evaporating LNG as a cooling medium (#5-#6). In fact, as reported by Awoyomi et al., (2020) and Fenstraa et al., (2019) the purified carbon dioxide stream of the LNG process can be liquefied using the LNG cooling capacity.

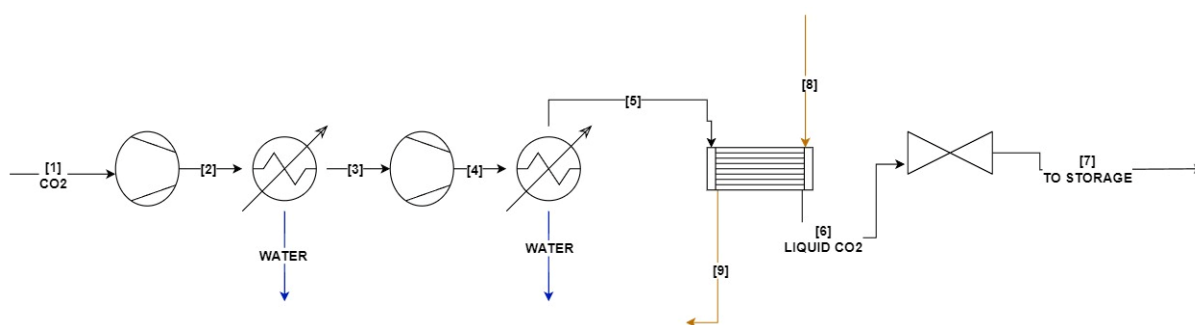


Figure 3.6 Purification and liquefaction section for LNG case

The stream resulting from the HFO ship, is compressed to 15 bar under the same process for the LNG case (Streams #1-#5 in Figure 3.7). After the purification the cooling requirement, in this case, is met by implementing a refrigeration cycle utilizing ammonia (6-11) as shown in

Figure 2.7. The liquefied CO₂ is subsequently laminated and stored at a pressure of 9 bar while maintaining a temperature of -45°C. This approach aligns with the findings of Roussanaly et al. (2021) and aims to reduce storage expenses.

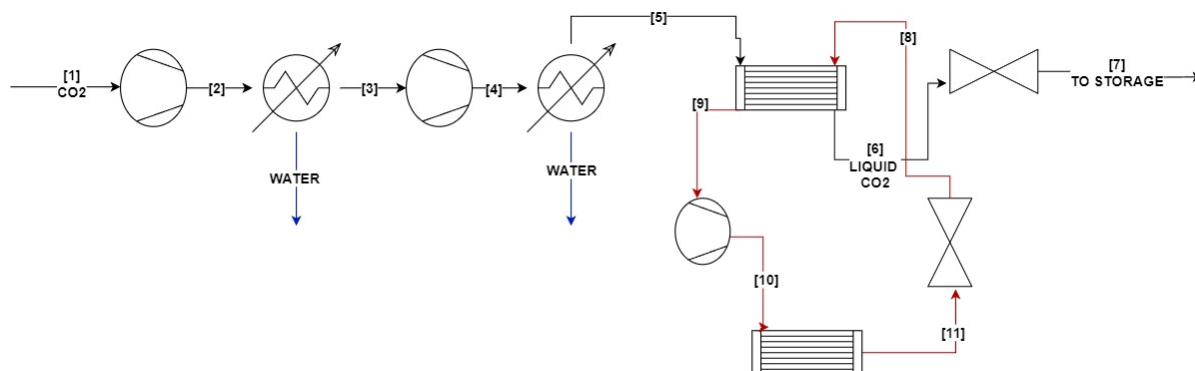


Figure 3.7 Purification and liquefaction section for HFO case with additional ammonia cycle

3.4 Economic analysis

For the economic evaluation the cost of CO₂ captured was computed taking into consideration capital expenditures (CAPEX), the fixed operational expenditure (FOPEX), the variable operational expenditure (VOPEX), and the total amount of carbon dioxide captured annually. These measures were combined in giving the total annual cost (TAC) which divided by the annualized captured carbon dioxide gave the cost of captured carbon or (CCC), a measure of the economic efficiency of the process.

$$TAC = \text{Annualized CAPEX} + FOPEX + VOPEX \quad (3.11)$$

$$CCC = \frac{TAC}{CO_2 \text{ captured annually}} \quad (3.12)$$

3.4.2 CAPEX

Capital expenditures were estimated for all equipment involved. First, the equipment purchase price was calculated using Eq. (3.13) found in Towler e Sinnott (2008) due to the non-availability of the aspen economic process evaluator (APEA) used by Awoyomi et al., (2020) and Feenstra et al., (2019).

$$C = a + b \cdot S^n \quad (3.13)$$

Where a and b are two equipment dependent parameters, S is the relevant equipment size measure and n is a scale coefficient. To evaluate the ISBL cost, to the purchase price was

applied an installation factor different for every equipment as suggested by Hand (1958). The ISBL cost were thus computed as in Eq. (3.14).

$$ISBL = \sum_i^n C_i \cdot f_{hand} \quad (3.14)$$

With f_{hand} being the hand installation factor and n being the total number of equipment.

The Fixed capital investments were then computed following the approach of Kvamsdal et al., (2015). Considering a 14% increment to the ISBL due to indirect construction costs and finally the CAPEX was computed using Eq. (3.16), which account for start-up cost, contingency, capital fee, and working capital (Kvamsdal et al., 2016).

$$FCI = ISBL \cdot (1 + 0.14) \quad (3.15)$$

$$CAPEX = \frac{FCI}{0.8} \quad (3.16)$$

Given the capital expenditure, considering a lifetime for this project of 25 years and 8% interest rates, it was decided in order to maximize comparability with other works that it was possible to calculate the annualized capital charge as in Eq. (3.17).

$$ACCR = CAPEX \cdot \frac{i \cdot (i+1)^n}{(i+1)^n - 1} \quad (3.17)$$

Where i stands for interest rate and n for the number of years

3.4.3 FOPEX

These refer to the operating costs that are fixed for the plant irrespective of usage of the ship and the other operating variables and they include long-term service arrangement costs, overhead costs, maintenance and labor cost (Kvamsdal et al., 2015). This can be calculated from Eq. (3.18) considering a 3 % fixed charge referred to the annualized capex. Labor is not included in this study.

$$FOPEX = 0.03 \cdot Annualized CAPEX \quad (3.18)$$

2.4.4 VOPEX

Secondly the variable operating expenses have been evaluated. The most important variable operating expenses are:

- Fuel cost (comprised of auxiliary estimated fuel cost)
- MEA cost
- Carbon underground storage
- Carbon transportation

- Revenue loss due to reduced transport capacity

3.4.5 Transport and storage cost

In this work it was tried to include in the computation major costs such as the container loss and also the carbon dioxide discharge cost which can be assumed to be the sum of the transportation and ground injection of the latter. This cost is taken into account based on the fact that the shipowner must sustain an unload fee in port to compensate the company that will handle the CO₂ transportation and subsequent underground storage. The unload cost is computed through Eq. (3.19).

$$\text{Unload cost} = \text{transport cost} + \text{storage cost} \quad (3.19)$$

The cost of CO₂ storage can vary greatly on a case-by-case basis, depending on the rate of CO₂ injection and the characteristics of the storage reservoirs, as well as their location.

As instance the cost of onshore carbon storage in the United States exhibits a significant variation. Nonetheless, it's estimated that more than half of the onshore storage capacity is accessible for less than 9.3 € per ton of CO₂. In some instances, storage costs can even be negative, particularly when CO₂ storage is linked to enhanced oil recovery, leading to increased revenue from oil sales (IEA 2021). On the other hand, offshore storage costs, as outlined by IEA (2020), tend to be higher, with approximately 80% of cases exceeding €18.5 per ton, and reaching a maximum slightly lower than 56 €/ton.

Given this wide range of reported prices, for the purposes of this study, a constant storage cost of €9.3 per ton was assumed. This assumption is supported by several factors, including the predominance of onshore carbon capture and storage in the analyzed voyage and the expectation of declining storage costs as the network develops.

For what concern the transportation an estimation was provided using a qualitative “density” of carbon injection projects in the world based on the same map used to define the three discharge location scenarios. Following this simple approach it was assumed that in all the ports excluded those part of the third scenario, the underground storage location is available at 100 km while for the ports included in the third scenario, Tangier, Suez the distance is assumed to be 1500 while for Singapore is 900 km. The transport method and cost were selected as described in table 3.5 according to (IPCC, 2005).

Table 3.5 Distance from injection storage facility, transportation method chosen and relative cost according to IPCC. All values are converted in Euro considering EUR/USD exchange rate of 1.08 (2023). Values are retrieved considering 6 mln tons of stored CO₂ per year.

distance km	method	cost €/ton
100	pipeline	4.6
900	pipeline	12
1500	ship	14.8

3.4.6 Container loss

To determine the container loss, the first computation needed is to evaluate the capacity of the baseline ship (no carbon capture) along the voyage.

During the entire voyage, the capacity of the ship tends to change between legs. In fact, assuming that the ship departs from the first port at full weight (where full weight is intended fuel and containers), when it arrives at the next port, the weight of the ship has diminished due to the fuel consumption, and thus the liner has the choice to either refuel or load more containers, based on the fuel price and container rates (Wang et al., 2019). A possible and simplified example of a capacity profile is shown in Figure 3.8.

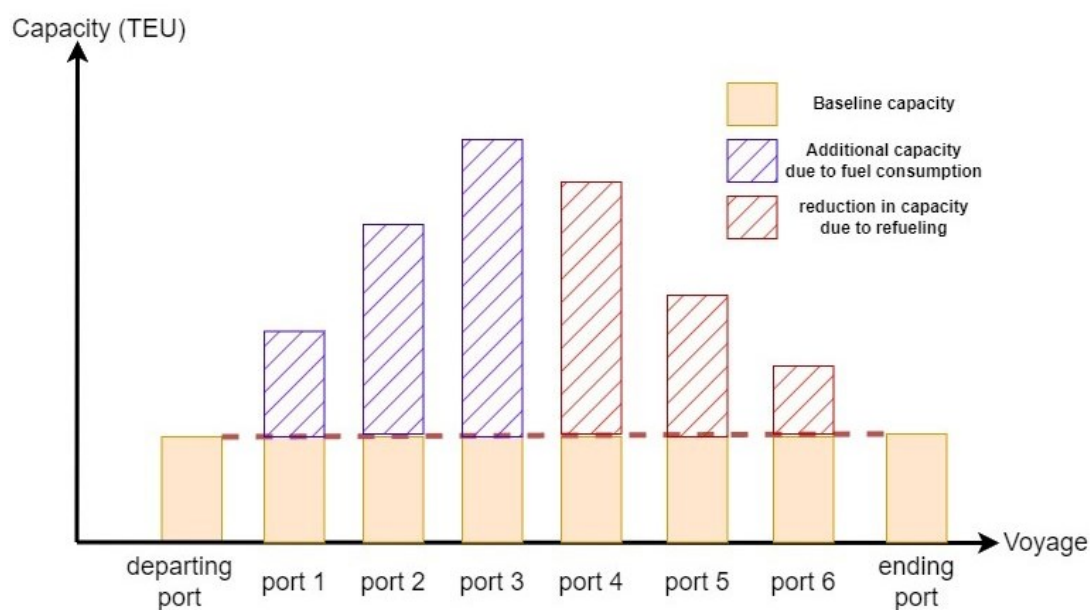


Figure 3.8. example of possible capacity profile along a voyage

Considering the total weight of the baseline ship as constant Eq. (3.20), assuming that the ship must refuel once the fuel tank is empty by 50% and applying Eqs. (3.20-3.23) for every leg of the voyage it was possible to compute the cargo load profile along the entire trip.

$$DWT_k = m_{fuel,k} + m_{cargo,k} = const \quad (3.20)$$

$$m_{fuel,k} = m_0 - \begin{cases} \sum_1^k (\dot{m}_{fuel,burned}) \cdot d_k, & m_{fuel,k-1} > 50\% \\ m_0, & m_{fuel,k-1} \leq 50\% \end{cases} \quad (3.21)$$

Where m_0 stands for the initial fuel mass, assumed to be 10000 tons for the LNG ship and 20000 tons for the HFO one, $\dot{m}_{fuel,burned}$ is instead the rate of fuel consumption at 80% load considering both the propulsion consumption and the excess fuel for running the capture plant while k is the leg number.

$$m_{cargo,k} = DWT_k - m_{fuel,k} \quad (3.22)$$

The capacity of the ship was thus computed following two methods:

In the first only the containers carried to destination are considered Eq. (3.23) in order to provide an estimation of the containers that the ship can handle from the begin of the trip to the final destination.

$$capacity = capacity \text{ end port} \quad (3.23)$$

The drawback if this method is that it does not take into consideration the number of containers that are unloaded and discharged during the voyage thus providing only a marginal picture of revenue associated with the voyage.

In the second method also the container handled during the voyage are computed in order to give an estimation of the total number of TEU carried in a route. The total number of containers carried (TCR) is thus computed as Eqs. (3.24-3.25) considering all the positive increments in capacity.

$$\Delta C_k = \frac{(m_{cargo,k} - m_{cargo,k-1})}{m_{container}} \quad (3.24)$$

$$TCR = C_0 + \sum_i^n \begin{cases} \Delta C_k & \text{if } \Delta C_k > 0 \\ 0 & \text{if } \Delta C_k \leq 0 \end{cases} \quad (3.25)$$

Where C_0 stands for the container capacity expressed in TEU at the departure port.

When carbon capture is implemented on the ship, the concept of cargo loss also arises. The container loss is due to the difference in weight between the carbon dioxide captured and stored on board and the fuel mass burned during the leg. In fact considering LNG, for every kg of burned fuel nearly 2.83 kg of CO_2 are produced; aiming for a CCR higher than 35% lead thus to an increase in weight effects this, even more important in the HFO ship where for every kg of fuel 3.11 kg of CO_2 are generated.

The methodology is the same as the baseline ship, with the addition of Eq. (3.27) for the calculation of the carbon dioxide stored on board and the modification of Eq. (3.26) with the incorporation of the CO₂ stored on-board.

$$DWT, k = m_{fuel, k} + m_{cargo, k} + m_{co2\ captured, k} = const \quad (3.26)$$

$$m_{co2, k} = m_{co2, k-1} + \begin{cases} (\dot{m}_{CO_2}) \cdot d_k, & \text{if no unload in port} \\ (\dot{m}_{CO_2}) \cdot d_k - m_{co2, k-1}, & \text{if unload is possible} \end{cases} \quad (3.27)$$

To determine the capacity loss is required to subtract the capacity value of the carbon capture ship from the baseline one, as done in Eqs. (3.28–3.29).

$$Capacity\ loss = capacity_{baseline} - capacity_{carbon\ capture} \quad (3.28)$$

$$TCR\ loss = TCR_{baseline} - TCR_{carbon\ capture} \quad (3.29)$$

To give a better representation of the loss, instead of the capacity, which presents more ambiguity, having different definitions as explained above, the total loss was reported as revenue loss, accounting in this way for all the containers that during the leg provided at least 1 euro of revenue. The revenue loss was thus computed following this procedure:

To the container effectively discharged in the ending port, the entire freight rate was given as revenue. After this, all the loadings and unloading during the voyage were computed. When a container was unloaded in an intermediate port, the associated revenue was computed considering the fraction of the entire trip sailed from the starting port. Instead, if a container was loaded, the fraction of revenue associated with this container was computed considering the trip duration from the loading port to the ending port of the trip.

$$REV = CO * fr + \sum_{k=1}^n fr * \Delta C_k * \left(\frac{d_{tot} - \sum_1^k d_{k,k}}{d_{tot}} \right) \quad (3.30)$$

Where fr is the freight rate per FEU associated with the voyage, d_{tot} is the entire duration of the voyage expressed in days and d_k is the time required for the leg in days. With these definitions the revenue loss can be computed through Eq. (3.31).

$$REV_{loss} = REV_{cc} - REV_{nocc} \quad (3.31)$$

3.4.7 Fuel cost and freight rates

The fuel price is based on the 20 port average provided by Ship&Bunker and the last value available was taken. In particular the price for LNG is 535 €/ton and HFO is 448 €/ton.

Regarding the freight rates, they were retrieved from the Drewry World Container Index (WCI). This index measures the bi-weekly ocean freight rate movements of 40-foot containers in seven

major maritime lanes. The index is composed by subindexes representing major trading routes. In particular for the route Shanghai-Rotterdam the freight rate is 1128 €/FEU, while for the route back is 528 €/FEU, where FEU stands for forty foot equivalent unit.

3.4.8 Carbon tax and freight rates increase

To complete the economic analysis, a carbon tax was implemented to understand the policy level required to make it convenient for the liner to switch to a system of ships with a high rate of carbon capture. This is done through a sensitivity analysis based on a global carbon tax. Once the key carbon tax level has been identified, the increase in freight rates necessary to sustain costs is computed.

From the revenue of the baseline ship without carbon capture computed with Eq. (3.23), the operative profit was identified considering a profit margin of 5%. The operative costs were thus estimated, and to this value, the total annual TAC for the carbon capture plant was added. Then, considering the same profit margin and the same transported capacity, the revenue and the freight costs were identified.

3.4.9 Other assumptions

Most of the prices are available in dollars and to make results more appreciable all values have been converted into euro. This was done considering $\text{EUR/USD} = 1.08$, which is the average for the six month of 2023.

Chapter 4

Case study

4.1 Voyage and scenario definition

The ship sails the voyage between Shanghai and Rotterdam, which are taken as a reference trip being these major container hubs. The total voyage, comprised of the major legs and ports called, was retrieved from the Maersk schedule website and shown in Figure 4.1 and summarized in Table 4.1.

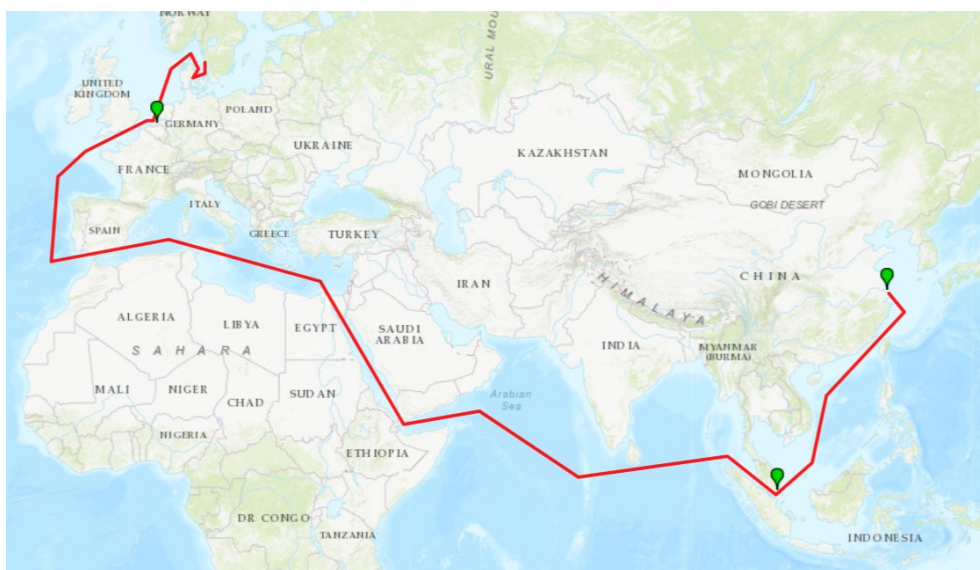



Figure 4.1. Route from Shanghai to Rotterdam and back

The study divided the total voyage into two main parts. The first one comprises the route traveling from Shanghai to Rotterdam, namely leg (2-11), and the second one comprises the route back (12-1). This is done to be as much as possible coherent with the freight rate pricing, which is based on the Shanghai-Rotterdam route and the Rotterdam-Shanghai route as two independent benchmarks, with the specifics being discussed in Section 3.4.7. Results per trip (Shanghai-Rotterdam and back) were then reconciled into a unique value summing the two giving thus a results for the entire voyage, reported on an annual basis assuming four voyages

per year.

Table 4.1. Port calls and details on leg duration

Port	leg number	duration [days]	leg number	Duration [days]
			Bremerhaven	2
Shanghai			Wilhelmshaven	6
Dalian		1	Port Tangier	11
Xingang	2	1	Suez Canal	5
Busan	3	2	Suez Canal	1
Ulsan	4	1	Singapore	13
Ningbo	5	2		
Shanghai	6	1		
Tanjung Pelepas	7	5		
Suez Canal	8	11		
Suez Canal	9	1		
Rotterdam	10	8		
Bremerhaven	11	3		
Gothenburg	12	3		
Aarhus	13	1		

After the voyages were defined, another important aspect to take into consideration was where the ship could effectively unload the carbon dioxide captured and liquefied on board. This led to the creation of three different scenarios.

- First scenario (S1): the ship is supposed to unload carbon dioxide at every port stop; this is an optimistic scenario which assumes a mature CCS network development.

- Second scenario (S2): the ship is allowed to unload CO₂ one at every two ports. This scenario is built to evaluate the impact on the flexibility of the ship; in fact, ships are known to make choices when in ports based on freight rates and fuel prices, whether to refuel or load more containers, leading to a problem of net income optimization (Wang et al., 2019).
- Third scenario (S3): this scenario is instead built in order to verify the impact of a insufficient future development of storage sites for CO₂ injection and also the regional distribution of these sites. In fact, as shown in figure 4.2, there is a wide distribution of projects at various stages of development in Europe and China, while there is a substantial lack of projects in north Africa and southeast Asia. So, the third scenario aims to respond to the question: what if the ship cannot unload in ports where a lack of regional storage hubs is present?
In particular, based on the data available to the CCS ongoing projects, S3 assumes that the ship cannot unload the CO₂ in Singapore, Suez, or Tangier ports.

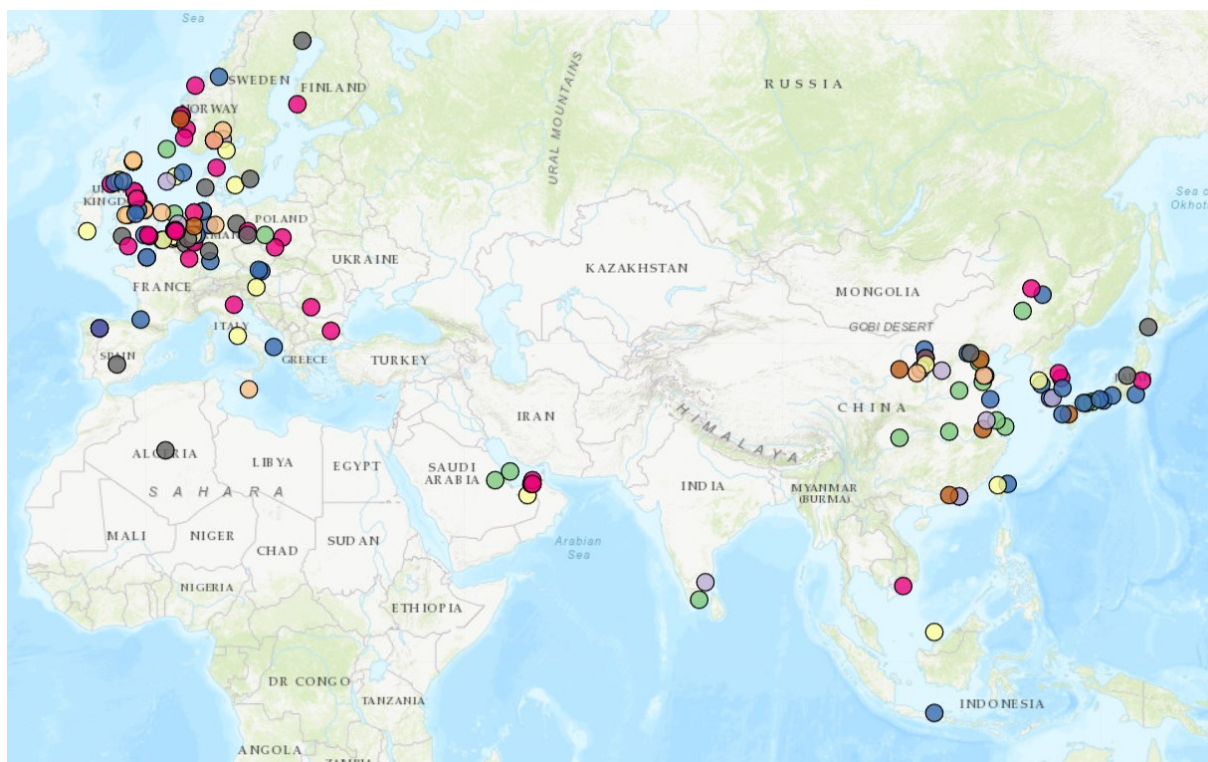


Figure 4.2. CCS project along there route sailed (SCCS org). Different colors represents stage of development of the site. Grey for finished site, green for operational site, brown for in building site, orange for in design site, yellow for in planning site, red for cancelled site, blue for pilot site

4.2 Scenario effect

The three scenarios described above are built to appreciate the impact of a voyage complexity on the economic outcomes. In particular the chosen scenarios aim to compute how costs change depending on geographic assumptions on CO₂ unloading possibilities, in particular:

- Effect on transport and storage costs: the first aspect to consider is the impact on storage volume requirements aboard the ship. These costs are closely tied to capital expenditures (capex). Additionally, changing the unloading port could affect transportation costs, thus influencing the total expenses incurred by the liner during the unloading process.
- Effect on container loss calculations: eq. 3.27 indicates that if the ship cannot unload CO₂ at a particular port, it results in an accumulation of CO₂ mass on board, which leads to the necessity of unloading some containers at that port. The implications of this scenario will be further elucidated in the results section.
- Effect on revenues: these scenarios are being studied to understand their impact on revenues. The different distribution of ports capable of handling CO₂ unloading could affect the ability of ships to generate revenues. In particular, the ship could be subject to more frequent container loading and unloading between legs and force to sail with at a low cargo rate for certain fraction of the voyage

Chapter 5

Results

5.1 Technical discussion

Table 5.1 Summary of plants main performance parameters

	LNG Self	LNG FB	LNG HPtot	LNG HPpart	HFO Self	HFO FB	HFO HPpart
Fuel	LNG	LNG	LNG	LNG	HFO	HFO	HFO
Engine load factor	80%	80%	80%	80%	80%	80%	80%
Fuel flow [kg/s]	1.9	1.9	1.9	1.9	2.4	2.4	2.4
CCR	36%	90%	90%	90%	33%	90%	72%
Effective CCR	36%	81%	84%	86%	33%	77%	69%
CO ₂ captured [kg/s]	1.97	4.84	4.84	4.84	2.47	6.67	5.31
Absorber Diameter [m]	5	5.5	5.5	5.5	5.5	5.5	5.5
Stripper Diameter [m]	1.8	2.5	2.5	2.5	2	3	2.5
Disposable heat [MWth]	6.8	6.8	6.8	6.8	8.2	8.2	8.2
Reboiler duty [MWth]	6.8	17.1	17.0	17.6	8.2	23.6	17.9
HP (heat pump)	no	no	yes	yes	no	no	yes
HP compressor electricity [MWe]	0	0	4.0	2.5	0	0	2.3
Specific duty [MJ/kg]	3.43	3.54	3.50	3.62	3.31	3.57	3.38
Fuel excess [kg/s]	0	0.21	0.15	0.09	0	0.40	0.10
Excess fuel [%]	0%	11.0%	7.6%	4.7%	0%	17.0%	4.4%

5.1.1 LNG and HFO: Fuel boiler plants

For the LNG-fueled engine, the results of the simulations show that to achieve a 90% Carbon Capture Rate (CCR), equivalent to capturing 418 tons/day of CO₂, 17.1 MWth are needed to cover the reboiler thermal duty of the carbon capture section. However, as the flue gas can only provide 6.8 MWth, the remaining thermal duty is covered by burning steam in a steam boiler, which requires an additional 0.2 kg/s of LNG, resulting in 52 tons/day of additional CO₂ emissions, bringing the total to 98 tons/day or a net CCR (or CO₂ avoidance) of 81%. The situation for the HFO-based variation is similar, with the main difference lying in the total CO₂ captured flow rate, which amounts to 576 tons/day, with a net CCR of 77% and an excess fuel consumption of 0.4 kg/s of HFO, which corresponds to an increase of 17% with respect to the baseline fuel consumption without carbon capture. The required reboiler duty for the HFO-fed engine is 23.8 MWth, with only 8.2 MWth being provided by thermal integration with the ship exhaust gas.

The HFO-FBLNG

case specific reboiler duty is 3.57 MJ/kg; hence, it is higher than that obtained in the LNG one (3.53 MJ/kg). This slightly higher specific reboiler duty suggests that the higher CO₂ concentration in the HFO case is not sufficient to positively impact in a substantial way the efficiency of the carbon capture process, because it is compensated by the higher flow rate of solvent required to achieve the 90% CCR target and the height of the stripper which, given the higher flowrate, should be higher to have the process optimized. The desorbing rate is in fact dependent on the contact between the vapor and the liquid phase, and a higher stripper height ensures enhanced contact and thus a higher desorbing rate. The decision to design both the column for HFO and LNG cases with the same height of 9 meters was made to isolate the impact of feedstock and highlight the influence of other variables, such as space limitation on process performance and in this regards the results show that despite similar performance in term of efficiency the LNG case is preferable due to lower flowrates and space requirements. The stripping column diameter shows a substantial variation between LNG and HFO cases and also between different capture rates (Table 5.1). In fact, the diameter ranges from 1.8 m to 2.5 m in the LNG cases, while it increases up to 3 meters for the HFO case. This could challenge the dual fuel engine mode and limit the operability of the plant to the design load factor flue gas flowrate. The absorber on the other hand does not pose any particular concern from a hydraulic standpoint between different cases, having a diameter nearly constant for every case

considered between 5 and 5.5 meters.

Another option would be to obtain a net CCR efficiency (or CO₂ avoidance) of 90%, which means capturing also the CO₂ generated by the additional combustion of fuel to cover the heat reboiler duty of the carbon capture section. As such, a test was performed on the LNG fueled ship and result was an increase in fuel consumption for CO₂ capture and in an excess fuel of up to 0.3 kg/s (the steam was provided by the boiler), equivalent to a 16% excess in propulsion fuel consumption.

5.1.2 Heat pump integration

The integration of a heat pump, (HPpart case) produces a decrease in the inlet temperature to the absorber compared to the base case. For the LNG case this leads to a slight increase in the reboiler duty, which reaches 17.6 MWth, and consequently to an increase in the specific reboiler duty for the HPpart case with respect to the base one. However, the heat pump effectively supplies the necessary thermal energy with a compressor work of 2.5 MWe, achieving a coefficient of Performance (COP) of 4.3. This, in turn, translates into a slight excess of 0.09 kg/s of LNG consumption, equivalent to a 4.7% increase in fuel consumption, notably below (-56.9%) the one for the LNG-FB due to the higher thermal heat recovered from the flue gas.

In the HPtot case, the addition of the second heat pump, placed between the reboiler and the cross heat exchanger, has the effect of generating surplus steam, which is deployed to preheat the stripper charge and enhance the carbon capture efficiency, thereby reducing the specific reboiler duty to levels below the base case. As shown in Table 4.1, the specific reboiler duty decreases to 3.50 MJ/kg, compared to 3.62 MJ/kg in the HPpart case (-3.3%) and 3.54 MJ/kg in the base one (-1.1%). However, it is worth noting that despite the improved capture efficiency, the excess LNG fuel consumption increases to 7.6%. This supports the argument that in on-board applications, the specific reboiler duty may not be the most critical performance metric since it does not account for how thermal energy is provided. In fact, the most critical metric is the excess fuel consumption which is related to how the steam to the reboiler is provided; implementing a heat pump can reduce the excess fuel to be burned even with an increase in the specific reboiler duty.

In the HFO case, it is important to mention that only the HFO-HPpart was developed, with the CCR target being lowered to 77% from 90% of the LNG cases. This is due to the lower available heat compared to the higher carbon dioxide mass to be separated; in fact, to achieve a 90% CCR

in the HFO case, a 38% reboiler duty increase is necessary with respect to the LNG case, with only a 21% increase in the available heat in flue gas. This difference prevents the HFO-HPpart case from achieving the same CCR as the respective LNG case. Is it thus possible to conclude that the chosen fuel has a notable influence on the applicability of the heat pumps and, more generally, on the technical impact of the carbon capture plant on ship operations. The integration of a heat pump system clearly plays a pivotal role in reducing fuel consumption within the process. As seen in Table 4.1, the excess fuel consumption for the LNG-based system, which employs a conventional steam boiler, stands at 10.8%. In contrast, for the LNG-HPpart case, where heat pumps are employed, it reduces to 4.4%. This represents a significant 59% reduction in excess fuel consumption, presenting a substantial operational advantage that allows liners to significantly cut costs associated with carbon capture.

Another important aspect to consider is that the specific reboiler duty is not the primary parameter for evaluating this process. If it were, the plant would be designed to maximize excess steam production in order to preheat the feed to the stripper column and reduce the reboiler duty (as in the LNG-Hptot case). However, this approach leads to an increase in excess fuel consumption (additional fuel needed to meet the thermal energy demand), resulting in higher operating costs and increased carbon dioxide emissions. If the goal is to achieve a 90% carbon capture rate while minimizing the cost of capture, the key parameter to focus on is excess fuel, which should be minimized. The minimization of this parameter is clearly related, as emphasized in Eqs. (2.9–2.10), to the steam production route. Using a heat pump can allow the plant to recover a greater amount of heat, thus lowering the external heat supply.

Furthermore, the engine's role in energy recovery is significant. The higher the flue gas temperature, the less steam is required and the greater the impact of the heat pumps. In the HFO case, where the temperature is relatively low compared to other diesel engines (Feenstra et al., 2019), the heat pumps are unable to produce sufficient steam to meet the duty required for a 90% carbon capture rate. Specifically, the disposable heat percentage of the base case reboiler duty is 39.4% for the LNG case, whereas it is 34.4% for the HFO case. Looking instead at the disposable heat content compared to the carbon dioxide content of the stream, the difference appears more evident, with the LNG case presenting 1.26 MW/kg while the HFO is limited to 1.10 MW/kg. Thus, for implementation on board, carbon capture requires a suitable engine system with a high energy content to minimize excessive fuel consumption, or alternatively, if low-flue gas-temperature engines are to be chosen, preference must be given to LNG-based engines, which present a lower carbon content at parity of power output.

5.1.3 Base case

The LNG-base (and HFO-Base) is built to understand the implications and the possibility of making the plant operate with a lower CCR while, in the meantime, trying to minimize costs for liners in order to favor investment at the start phase. The feasibility of this option is strictly dependent on the flue gas characteristics and thus on type of fuel deployed for the engine. In Figure 5.1 is showed the reboiler duty under variations in the CCR and the disposable heat in the flue gas rate both for LNG and HFO. As is possible to appreciate The reboiler duty increases almost linearly up to 90%. After this value, the steepness of the curve increases, highlighting a decrease in efficiency at higher capture rates.

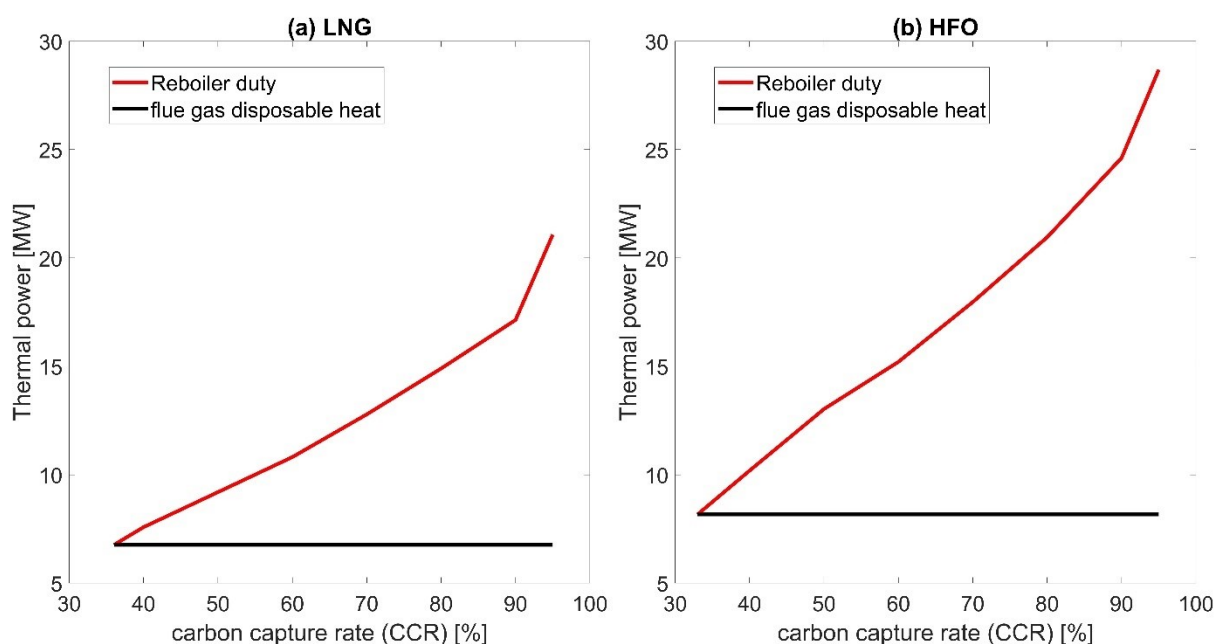


Figure 5.1. Reboiler duty profile varying the carbon capture rate and heat disposable in the flue gas for (a) LNG case and (b) HFO case

By looking for the intersection of the reboiler heat curve with the disposable heat, it was possible to retrieve the maximum CCR rate possible without any additional thermal energy requirement in the system. As a result, the CCR is limited to 36% for the LNG and 33% for the HFO case.

One consideration in analyzing this case is that with a more than 50% reduction in CCR rate, the absorber diameter is almost just 10% lower in comparison to the LNG-FB absorber diameter (5 meters vs. 5.5). On the other hand, the stripper diameter decreases by a greater extent both for the HFO and the LNG case. The fact that just a portion of the plant sees a decrease in size with a decrease in the CCR will have economic implications to be further discussed in the capex

analysis.

5.1.4 Purification and liquefaction

With respect to the liquefaction, all the plants are able to achieve the a purification above 99%, with the main difference being in the energy required. As is possible to observe from Table 5.2, the energy required by 90% CCR of the LNG case is 30% less than the HFO case thanks to the avoiding of the ammonia cycle. Also, this has important implications in term of capex as described a subsequent section.

Table 5.2. key operating parameters for purification and liquefaction

	LNG Base	LNG FB	LNG HPtot	LNG HPpart	HFO Base	HFO FB	HFO HPpart
CO ₂ purity %m	98.8	99.3	99.3	99.3	99.3	99.3	99.3
Compressor electricity [MWe]	0.377	1.2	1.2	1.2	0.589	1.59	1.269
Compressor ammonia [MWe]	0	0	0	0	0.392	1.11	0.872
P storage [Bara]	9	9	9	9	9	9	9
P purification [Bara]	15	15	15	15	15	15	15

The electricity needed to purify the carbon dioxide and to run the refrigeration cycle is provided by the auxiliary engines, resulting in auxiliary fuel consumption of 0.04 kg/s for the LNG base and 0.12 kg/s for the HFO ship which are respectively 19% and 30% of the excess fuel consumption for the capture process. The captured carbon dioxide was then stored at 9 bar and -45°C in liquid state as explained in Chapter 2.

5.2 Economic results

5.2.1 Baseline capacity

In Figures 5.2–5.3, the capacity profiles of the baseline LNG and HFO are presented. It is important to note that both for the HFO and the LNG-fueled ship, the number of TEUs that the

reference ship is able to carry is much below the 20658 nominal value. This is confirmed by the definition of the latter; in fact, the nominal capacity is calculated by considering all the containers as empty, which overstates the real capacity.

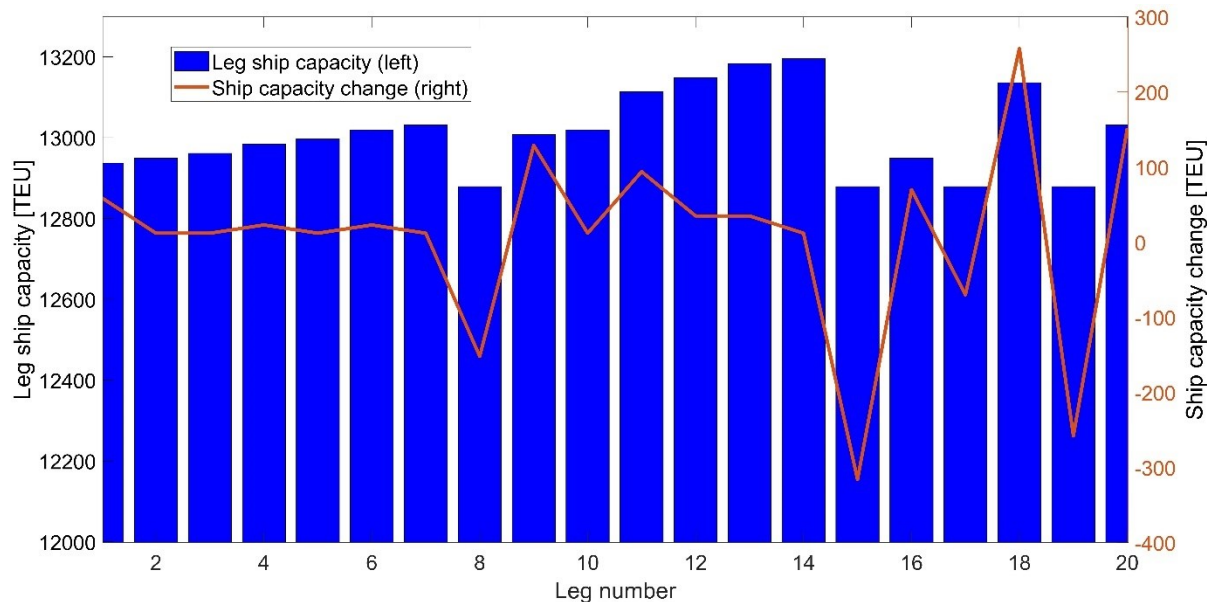


Figure 5.2 Capacity profile for baseline LNG ship.

From Figure 5.3, it is possible to appreciate that the LNG ship need to refuel more often, as expected by the lower starting fuel storage on-board. In particular, the LNG ship needs refueling in legs 8, 15, and 19 based on figure 4.3, while the HFO needs just one refueling in leg 15. It would be possible to argue that the HFO ship could handle the entire voyage without any refueling. While this is true, the ship would still be compelled to refuel in subsequent legs, so the 50% empty refueling constraint is decided arbitrarily to force the simulation of the refueling effect.

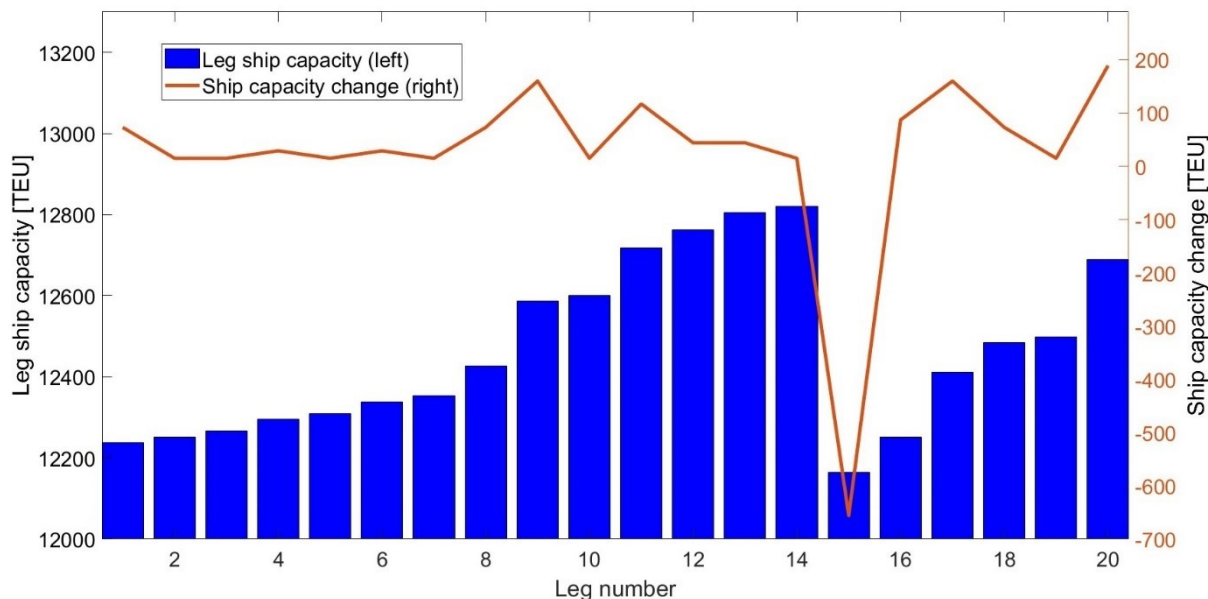


Figure 5.3 Capacity profile for baseline HFO ship.

5.2.2 Carbon dioxide volume requirements

Using the methodology explained in Chapter 3, it was possible to determine the mass stored on board, and, considering the CO₂ density of 1127 kg/m³ (9 bar and -45°C) also the volume requirements. In Figures 5.4–5.5, the volume requirement for CO₂ storage on board per leg is reported both for LNG and HFO cases.

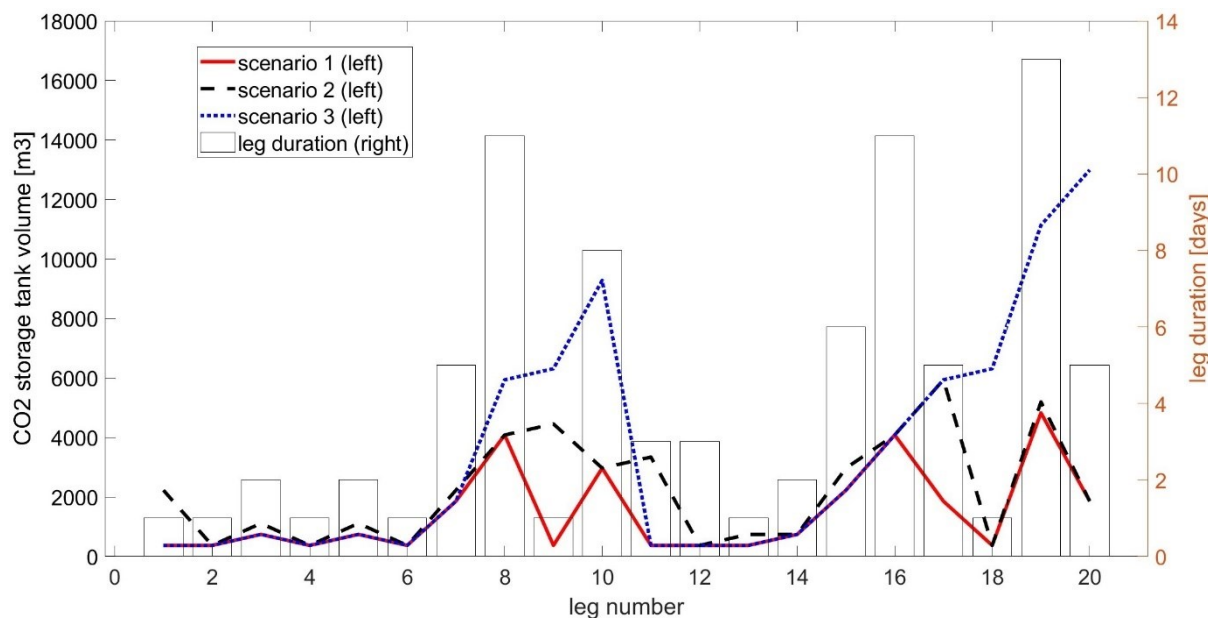


Figure 5.4. LNG-FB carbon dioxide volume requirement on a leg basis

The scenario effect holds significant importance because if carbon dioxide remains on-board the vessel due to either a deliberate operational decision (scenario 2) or a compelled situation

(scenario 3), it results in the accumulation of carbon dioxide within the ship, necessitating larger storage tanks. The necessary storage volume can be estimated by extrapolating the maximum value for each scenario from the route analysis, as summarized in Table 5.3 for each examined plant.

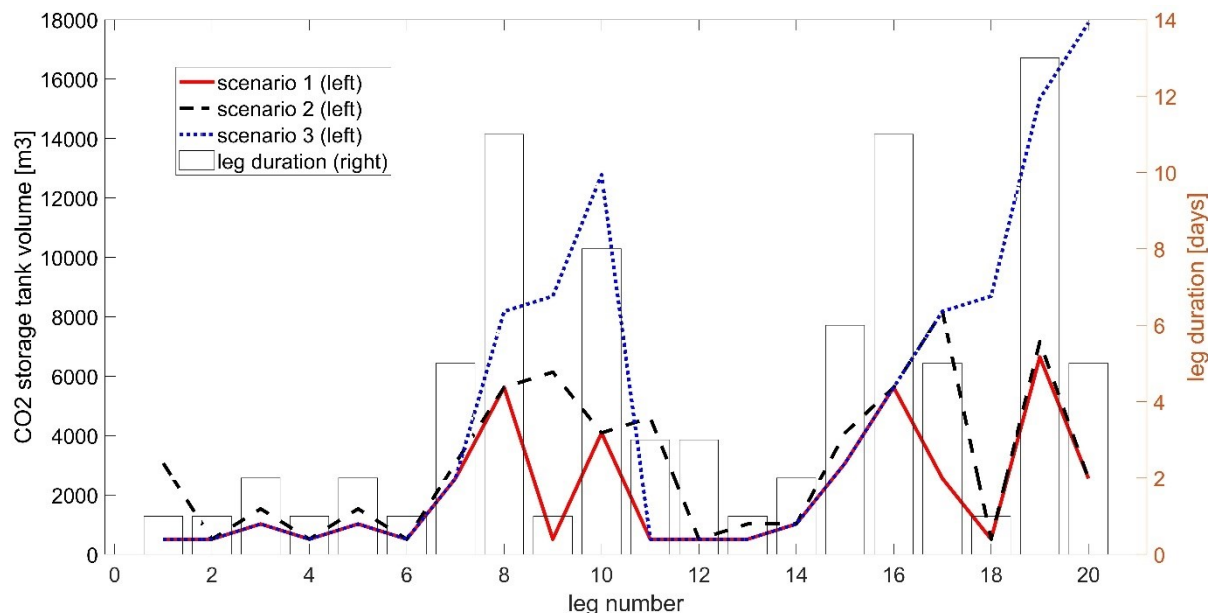


Figure 5.5. HFO-FB carbon dioxide volume requirement on a leg basis

Generally, from Table 5.3, it is possible to observe that in the third scenario, volume requirements are nearly three times or more the first scenario tank for every plant considered, while in the second scenario, the increase in storage requirements is more modest, between 20 and 30% of the scenario one requirements. In the first scenario the only thing which influences the storage requirements instead, considering that CO₂ is unloaded at every port, is the length of the leg itself.

Furthermore, it is possible to observe that the HFO ship needs bigger storage tanks than the LNG one due to the higher CO₂ production.

Table 5.3. max volume requirement for every proposed plant

Proposed plant		Scenario	Storage volume requirements [m³]
HFO	HFO-FB	Scenario 1	6647
		Scenario 2	8181
		Scenario 3	17895
	HFO-HPpart	Scenario 1	5317
		Scenario 2	6544
		Scenario 3	14315
	HFO-Base	Scenario 1	2437
		Scenario 2	2999
		Scenario 3	6560
LNG	LNG-FB	Scenario 1	4825
		Scenario 2	5938
		Scenario 3	12990
	LNG-HPpart	Scenario 1	4825
		Scenario 2	5938
		Scenario 3	12990
	LNG-HPtot	Scenario 1	4825
		Scenario 2	5938
		Scenario 3	12990
LNG-Base	Scenario 1	2437	
	Scenario 2	2999	
	Scenario 3	6560	

However, it is important to note that volume remains a relatively minor issue when evaluating operational and economic factors. Specifically, in the context of container ships, the storage volume required primarily influences the space needed for the tank, affecting capital expenditures, but it does not substantially affect the risk of container loss.

As we have previously illustrated using the baseline ship, the actual cargo capacity is significantly less than the nominal capacity. This indicates that container ships operate at full volume, and the crucial limitation is more related to the weight of the cargo than its volume.

5.2.2 Container loss

As discussed in Chapter 2, container loss is a result of the disparity between the weight of the on-board stored CO₂ and the fuel consumption rate. In scenarios 2 and 3, where the ship cannot offload carbon dioxide at every port, the cumulative effect of container loss places a more

significant economic burden on the shipping operation.

As figures from 5.6 to 5.8 illustrate, when carbon dioxide cannot be unloaded during a port stop, the ship must unload cargo to accommodate the additional carbon mass for the next leg of the journey. Furthermore, if the ship is compelled to refuel without the opportunity to offload carbon dioxide, the cargo loss escalates dramatically because cargo is the only variable the ship can adjust (e.g., legs 9 and 18 in Figure 5.7). This situation limits the flexibility of the ship, forcing it to refuel at a port with favorable bunker fuel prices in favor of one where it can also offload carbon dioxide. Another option is for the ship to carry less fuel to minimize cargo loss. However, this possibility also reduces flexibility, considering that ships typically carry excess fuel volume to enable extended voyages without refueling, maximizing the spread between fuel and freight rates by deciding where to refuel or add cargo.

It's important to note that if the ship is obliged to refuel in a situation where it cannot unload CO₂, container loss increases significantly compared to the baseline scenario.

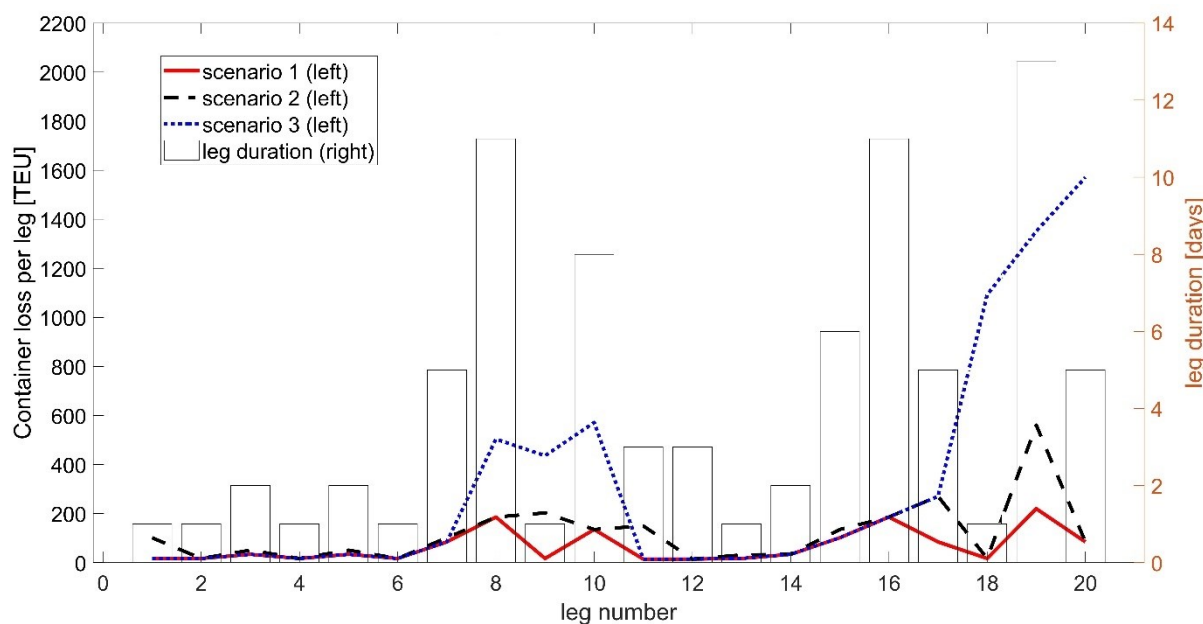


Figure 5.6. LNG-FB container loss expressed in TEU along the voyage

Same consideration applicable to the volume requirements are also applicable in terms of the container loss with the HFO being more unfavorable with a higher container loss than LNG.

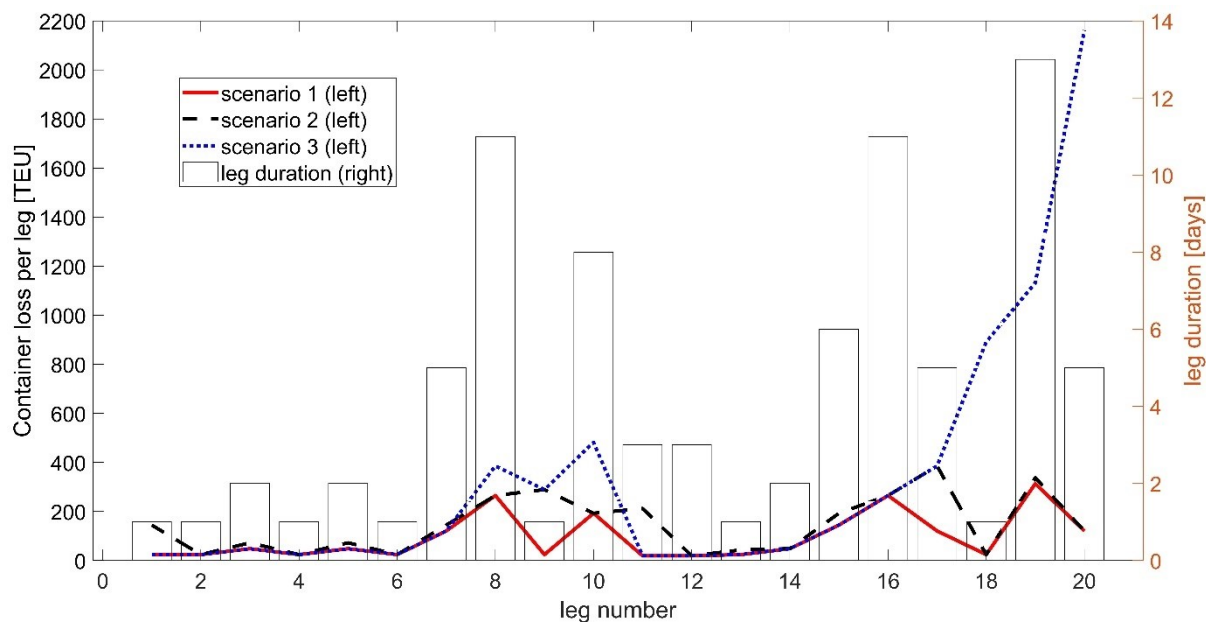


Figure 5.7. HFO-FB container loss expressed in TEU along the voyage

The effect of the refueling is much more appreciable in the Self case, in fact, as is possible to observe from Figure 5.8, scenarios 1 and 3 are characterized by a near-zero container loss due to the low carbon capture rate. Nevertheless, when scenario 3 is applied, two cargo loss spikes occurs. Both appear because of the ship refueling occurring in a port where unloading is not possible, leading to a 1400 TEU loss in capacity in the last leg.

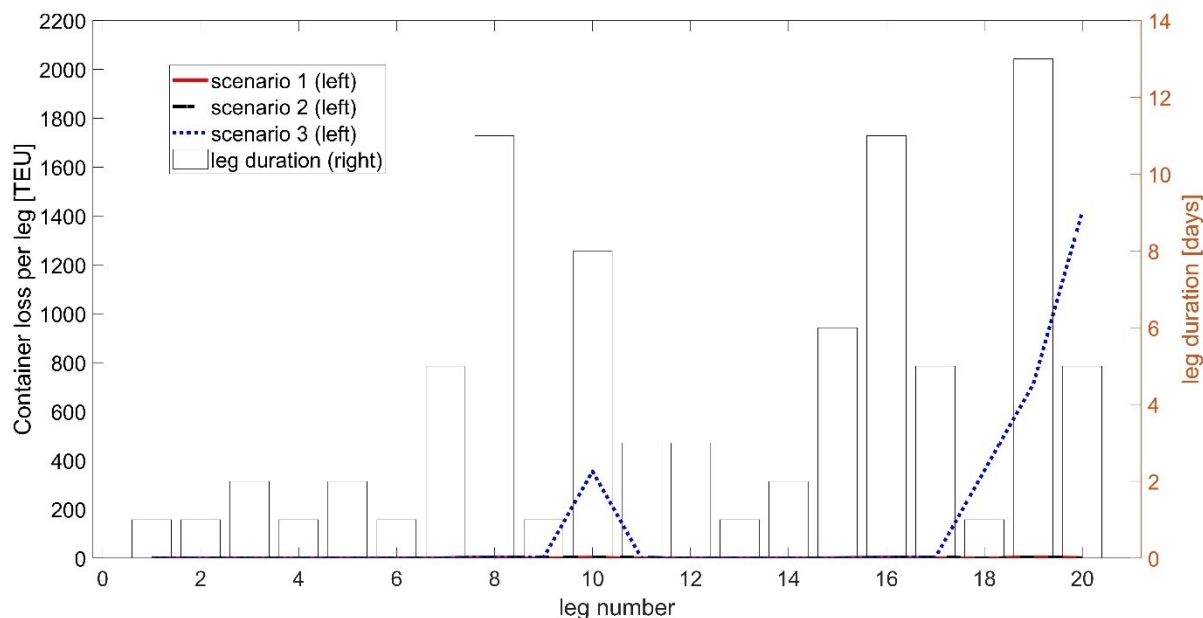


Figure 5.8. LNG-Base container loss expressed in TEU along the voyage

With the leg to leg container loss data it was possible to compute the capacity of the ship with the definitions provided in chapter 3. As is possible to appreciate from Figures 5.9 and 5.10

there is a significant difference in the change in capacity between the two possible definitions provided.

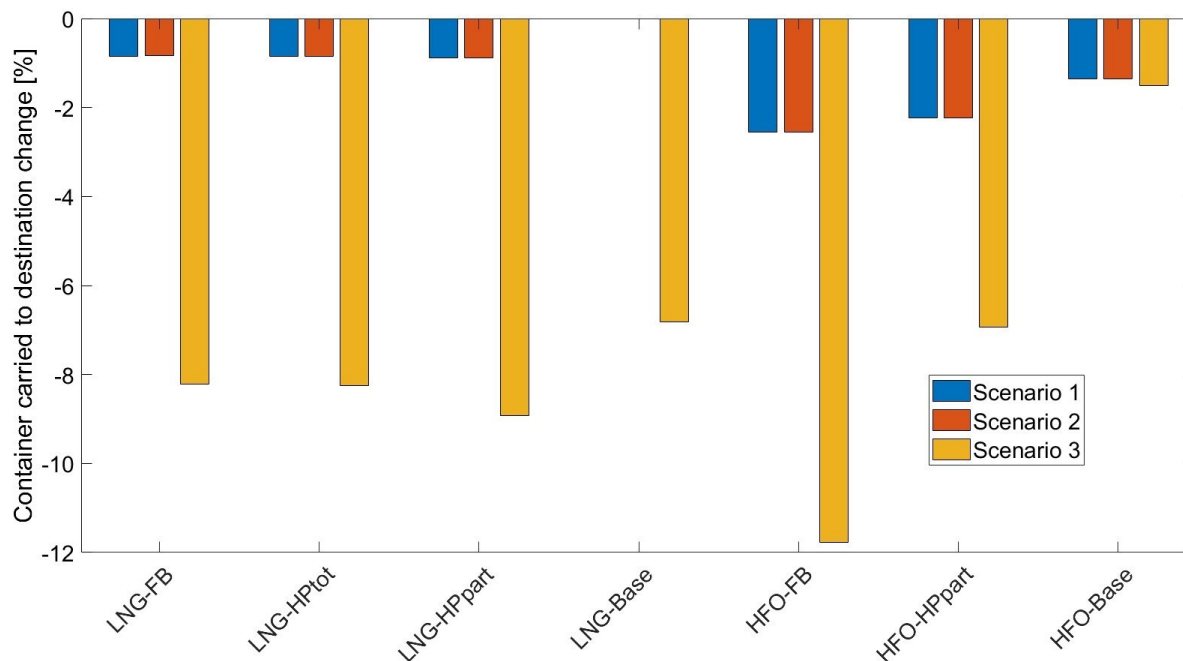


Figure 5.9. Total container to destination percentage change respect to baseline

This is due to the fact that the third scenario affects ports which are close to the final destination forcing the ship to unload more containers. This could affect logistics in a significant way, leading in fact to either more ships in the fleet or to higher shipping times due to other means of transport.

Regarding the total container carried, this measure highlights the extent of container turnover along a voyage. From Figure 5.10 is possible to observe that the LNG- Self and HFO Self are the one with higher TCR loss, this is due to the low carbon capture along the route which makes the necessity to unload cargo lower.

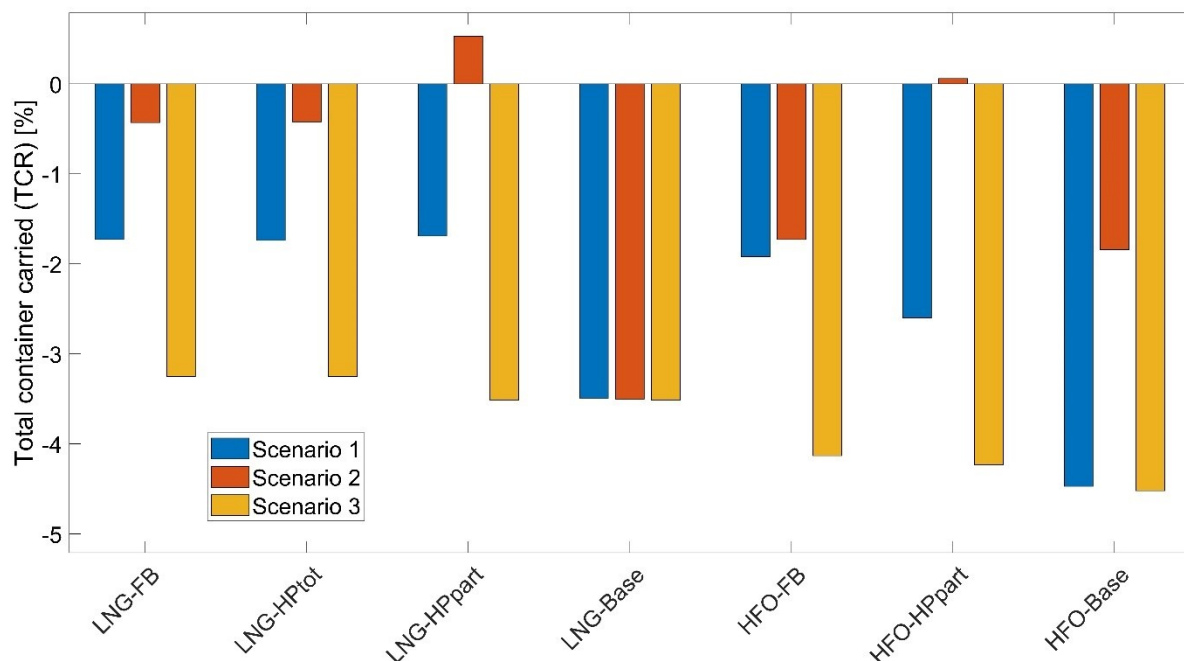


Figure 5.10. Total container carried percentage change respect to baseline

In figure 5.11 the revenue loss is reported. The values are quite different compared to the capacities above discussed but provide a more clear impact assessment. The difference in percentage is due to the fact that the revenue takes into consideration the number of length that a ship can carry the container on-board. Thus the ship which can sail for longer routes with less need of discharging and unloading at every port see a less pronounced impact in revenue, while on the opposite ships that are forced to discharge more containers in longest routes are more penalized from an economic standpoint. LNG-FB and HFO-FB are in fact the options that see the higher revenue loss which in the third scenario are 3.6% and 11.2% respectively. Higher TCR changes (decrease in total container carried) are thus a positive factor in terms of revenue because it implies a lower container turnover.

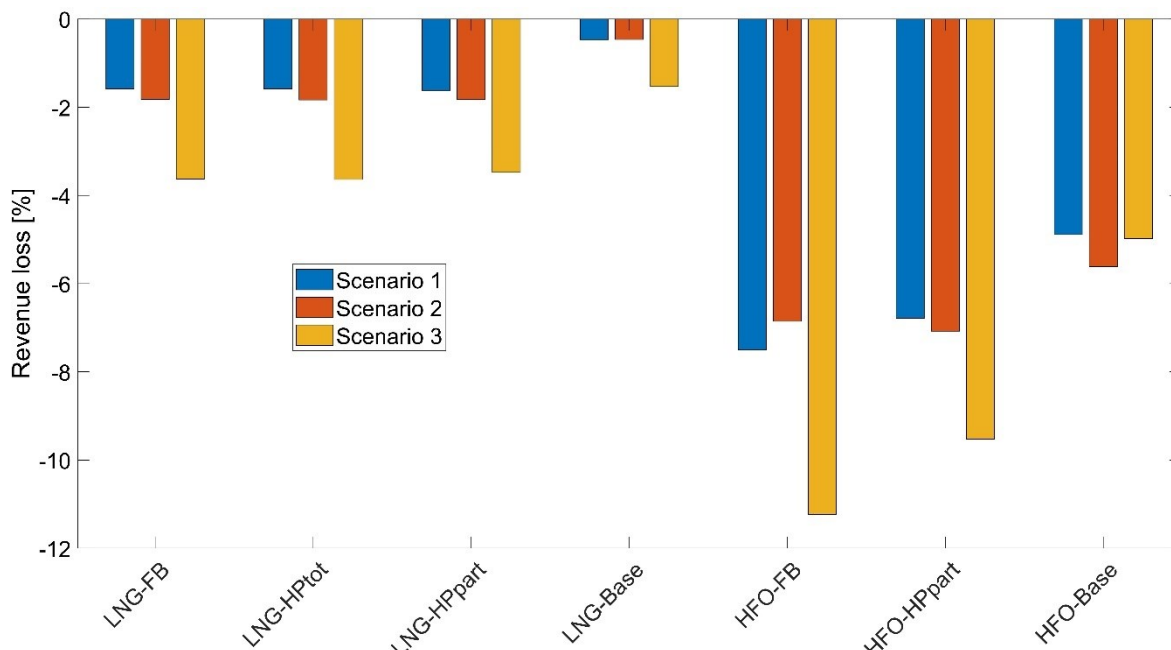


Figure 5.11. Container revenue percentage loss

In Figure 5.12 the absolute revenue loss in euro per voyage is reported.

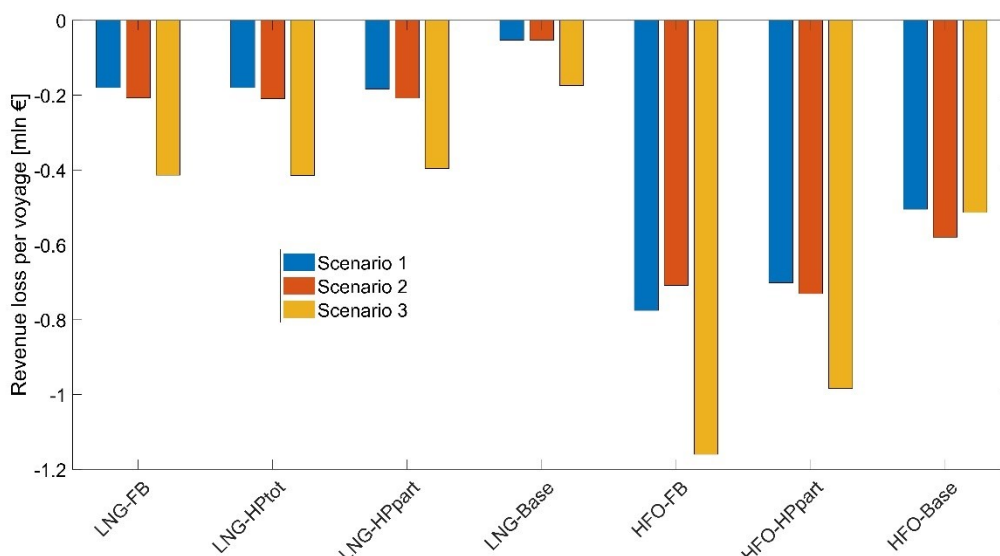


Figure 5.12. Container revenue loss expressed in euro

5.2.3 Transport ad storage

As can be observed in Figures 5.13-5.15, taking as reference the LNG-FB and HFO-FB plant, there are significant differences between the distribution of cost and the overall results. In scenario 1 the cost are incurred in every ports. This results in a total higher cost of transportation because also the ports with higher distances from final storage locations are reputed suitable for

unloading.

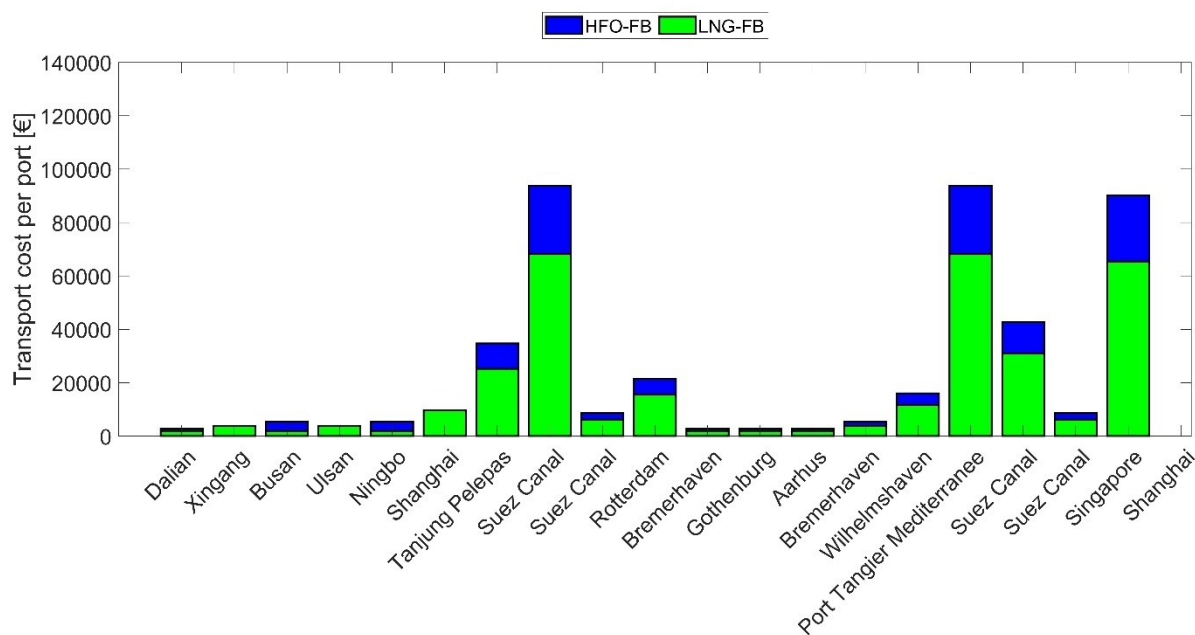


Figure 5.13. Transport cost for scenario 1, (unload every port)

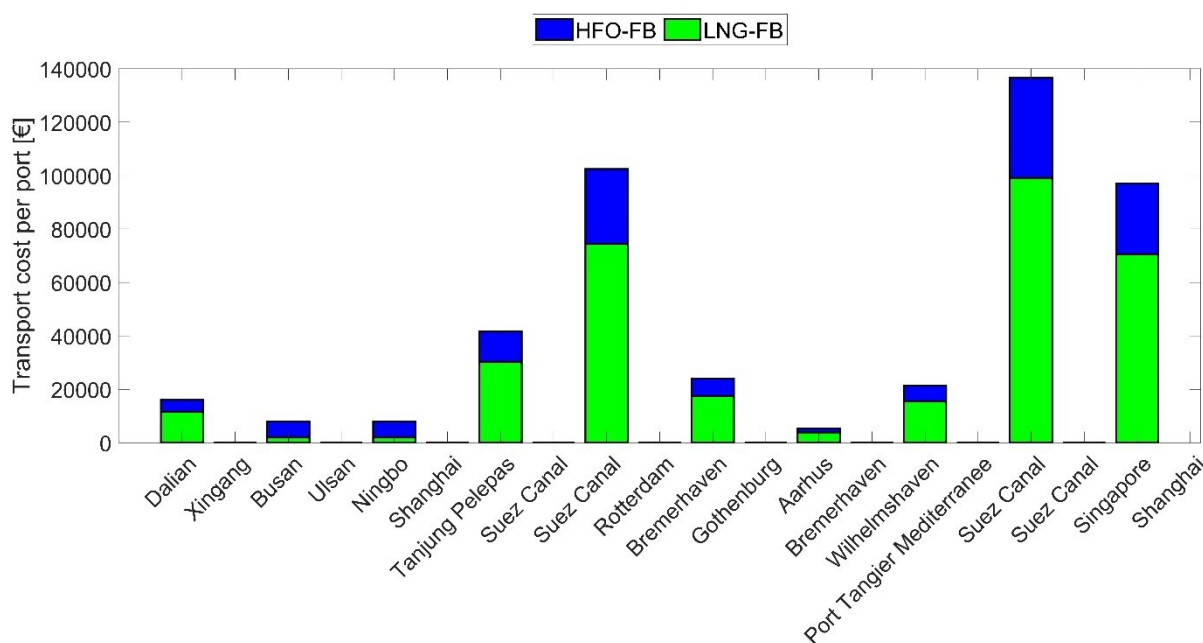


Figure 5.14. transport cost for scenario 2, (unload one every two ports)

On the opposite, scenario three presents the lower transportation cost because the ports which require longer pipelines or ship transport are skipped and carbon dioxide is discharged instead where a greater distribution of onshore storage sites is presents with lower costs.

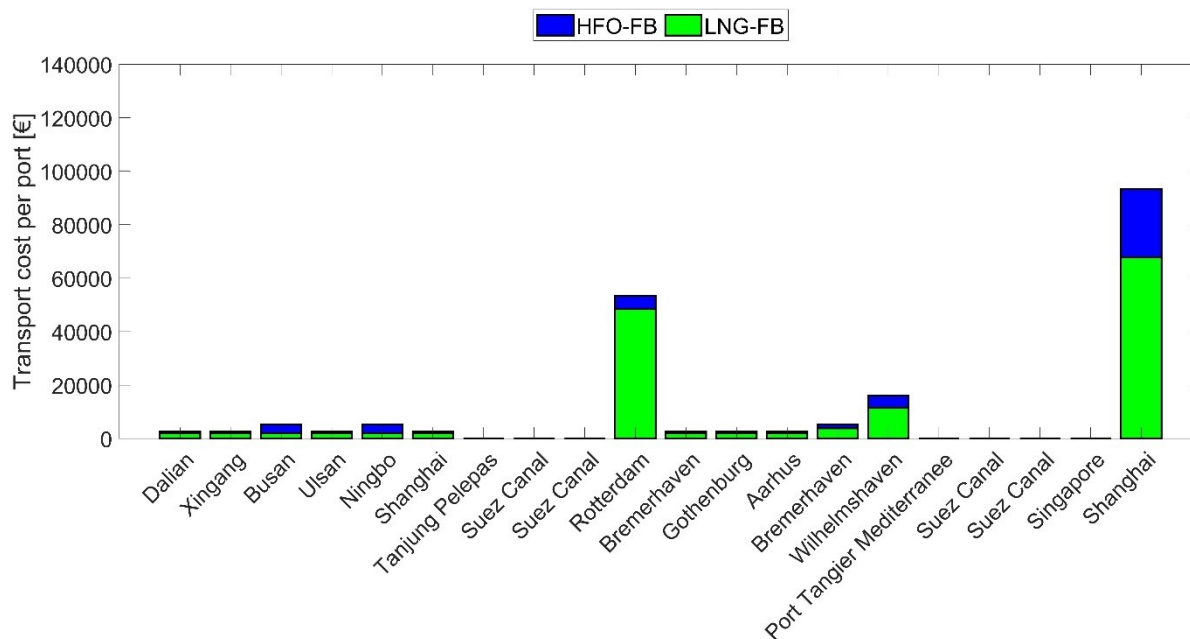


Figure 5.15. transport cost for scenario 3, (unload only when possible)

5.2.4 CAPEX

As it is possible to observe from Figure 5.16 In general LNG capital expenditure are lower compared to HFO due to the lower flue gas to be treated. LNG-Base and HFO-Base are the cheapest option as expected in in their fuel categories due to the lower size in machinery, even if the lower percentage CCR is not compensated equally by a decrease in cost, this due to the fact that some high cost equipment like the absorber present a similar diameter compared to 90% CCR thus preventing a lower capital cost.

Looking at 90% CCR cases is possible to observe that the heat pump integration increases capital costs by 20% if the partial case is implemented or by 37% if the total case is chosen.

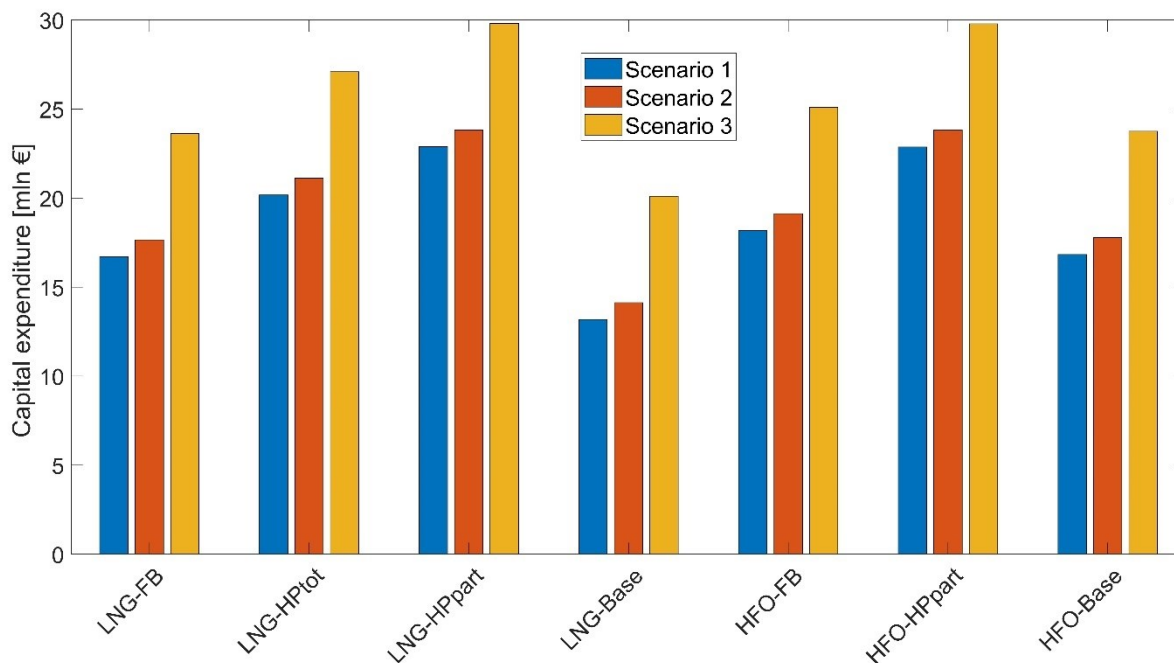


Figure 5.16. Capital expenditure in 2019 euro

Looking into the different cases, it is possible to observe that there is a noticeable difference in absolute capex costs depending on the scenario, this due to the difference in CO₂ storage volume requirements on board. It is in fact noteworthy as is appreciable from Figure 5.17. That the storage costs take more than 20% of the overall expenditure.

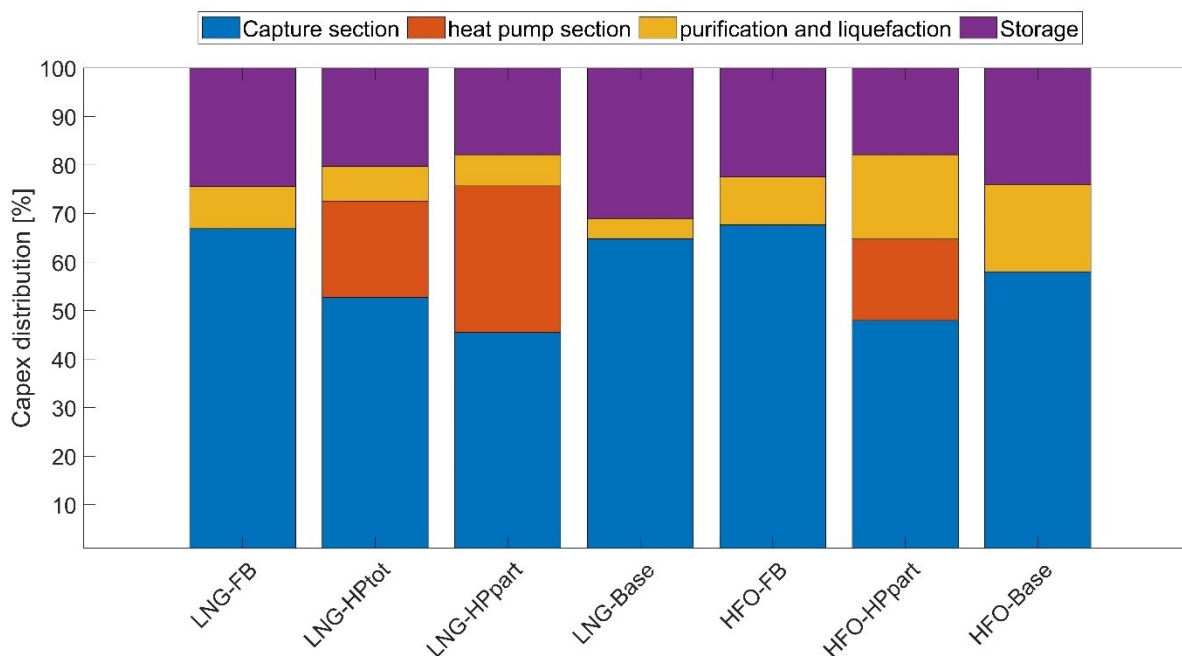


Figure 4.17. Capital expenditure distribution between different sections of the plant, scenario 1

5.2.5 Total annual costs

Regarding the total annual costs it is possible to observe from Figure 5.18 that in general operating a carbon capture plant in a LNG fueled ship is less expensive than operating in a HFO one. This is primarily due to the lower carbon dioxide produced which impacts several costs such as the capex (lower equipment volume), and the operative expenses such as the carbon storage, transportation and revenue loss due to additional mass on-board.

It is also possible to observe that without accounting for a carbon tax, the two options, LNG-Base and HFO-Base which operate with a 36-33% CCR rate are the less expensive options.

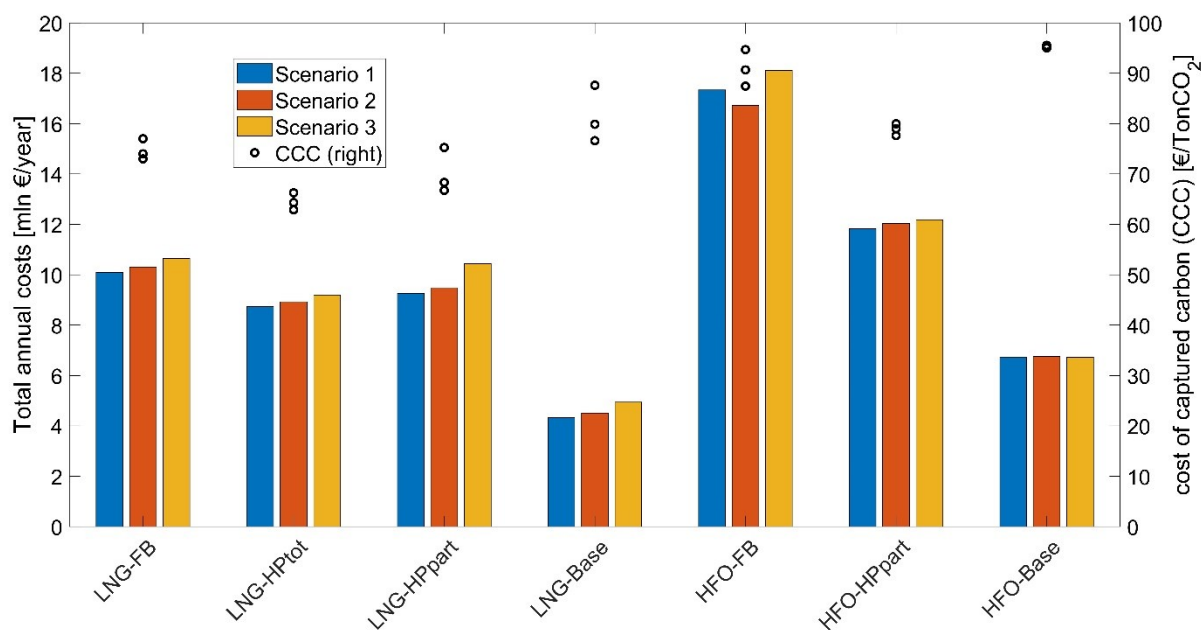


Figure 5.18. Total annual costs (left) and carbon capture cost expressed as €/ton (right)

Also it is possible to appreciate as the heat pump system studied to provide the steam required to the reboiler decreases the cost both for LNG and the HFO fueled ships.

It is important to notice however that the plants LNG-HPpart and HFO-HPpart are not directly comparable because of the different CCR. Looking at the LNG fueled ship in fact the single heat pump case can save nearly 1 million € per year with respect to the base one.

Regarding the cost of captured CO₂ (CCC), it ranges between 64 €/ton and 75 €/ton for the 90% CCR LNG fueled ships, is between 77 and 88 for the LNG-Base case while it increases notably for the HFO cases, in fact for the 90% CCR values of CCC stand in a range between 87 and 95 €/ton, decreasing to 80 €/ton for the HFO-HPpart case.

Also to notice that the different scenarios do not impact in a significant way on the overall result, this is due to the fact that just a number of operating expenditures are affected by the scenario changing, in particular, the transport and storage costs, the loss in revenue and the

capital annual charge. Instead, fuel price, which account for 33-36% of the operating costs and the MEA costs are independent of the scenario considered.

Looking at the distribution of the costs in Figure 5.19 we can see that the container loss and discharge cost represents quite a large percentage of the cost associated with operating the plant and neglecting them lead to a large error in the estimation. It is quite clear thus that one of the main cost to be abated in the future to make this plant feasible are the cost associated with the in port handling of the captured carbon dioxide in fact storage and transportation cost account a significant share of the overall costs, between 27 and 44% depending on the plant and fuel. In general as is possible to observe from for the HFO case the container loss is the most important cost, this coherent with the discussion above.

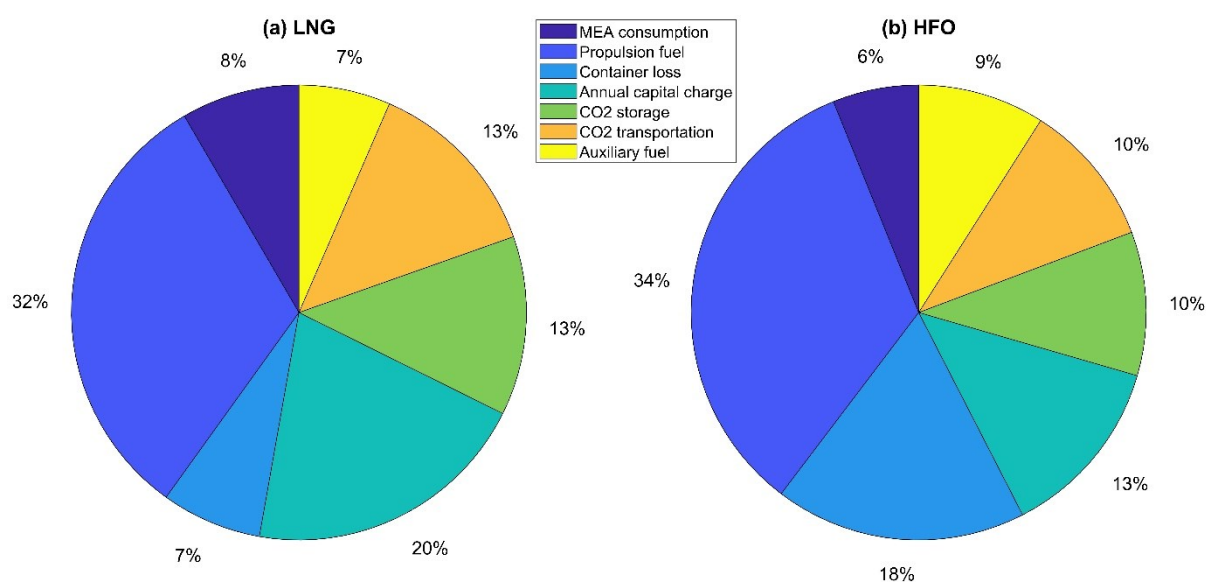


Figure 5.19. Total annual cost distribution for (a) LNG-FB and (b) HFO-FB

In Figure 5.20 the operating costs distribution for the LNG-Base case is reported. Here is possible to appreciate as in the case of no excess fuel consumption for capture, the operating costs are main related to capital expenditure and MEA and carbon dioxide storage with the remaining playing a minor role in the economic burden of the plant.

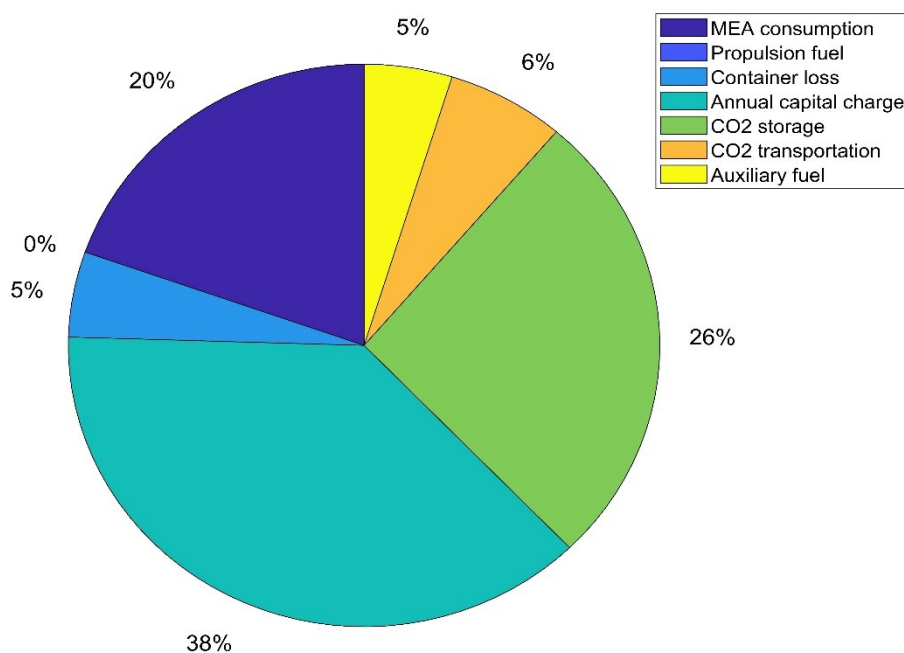


Figure 5.20. Total annual cost distribution for LNG-Base plant

5.2.6 Freight rates increase

By considering a 5% operating margin and the revenue associated with the baseline ship was possible to retrieve the operating costs per year of the ship with no carbon capture plant. To this value the operating expenses for the plants were summed giving the total cost per year associated with the ship. Taking a reference the LNG ship the implementation of carbon capture would increase with these assumption the annual costs for the liner by 21% for the Base case and 20% for the HPpart case and 9% for the Self one.

Considering the same operating margin the revenue has been calculated and finally considering the actual cargo profile of the ships along the voyage the freight revenue increase has been calculated. The increase in freight rates stand between 25% and 40% for the LNG fueled ships while it was found to be between 28% and 53% for the HFO fueled ships.

5.2.7 Carbon tax

The effect of a global carbon tax is to price the emissions of a ship. As is possible to appreciate in Figure 5.23, The case with no carbon capture is always more convenient until the carbon tax reaches 70 €/ton where the LNG-HPpart case becomes the less expensive followed by LNG-HPtot and finally the LNG-Base case at 79 €/ton.

Is interesting to note that the LNG-Base case while it was reported above as the lowest cost option, when a carbon tax is applied becomes the second least profitable plant with the breakeven reached at 85 €/ton due to the low CCR rate. Second only to the LNG-FB case with a 90€/ton breakeven carbon tax.

The LNG-FB case is the most costly option because of the amount of excess fuel consumed which increase the carbon emission not captured leading to the effective capture of CO₂ to 77% as discussed previously.

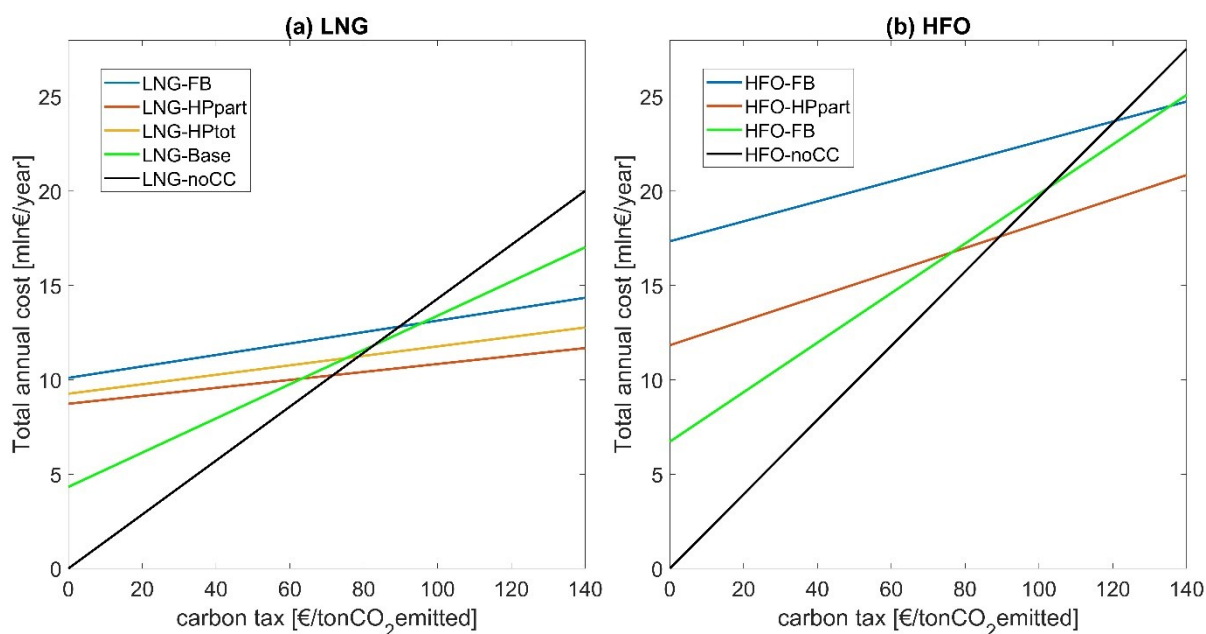


Figure 5.21. Carbon tax sensitivity and effect on annual expenses for (a) LNG case and (b) HFO case

Analogous results are reported in Figure 5.21 for the HFO case, with the only difference standing on the breakeven carbon tax level that for the cheapest option stands at 89 €/ton. It must be notice however that for HFO fuel the Self case is more convenient with respect to the Base case up to a carbon tax over 130 €/ton

A clear finding from this analysis is that the baseline plant with no carbon capture is always the most convenient cost but once a carbon tax is implemented the heat pump integration leads the 90% CCR to be the most convenient option. On the opposite if the heat pumps are not implemented the low CCR option will be the more convenient option up to higher value of taxes being applied.

The sensitivity analysis was further applied to the cost of capture carbon (CCC), Figure 4.22. The results show as these value increase substantially respect to the operating expenditures seen

previously. As expected the lower CCR cases like LNG/HFO-Base and HFO-HPpart are characterized by higher CCC.

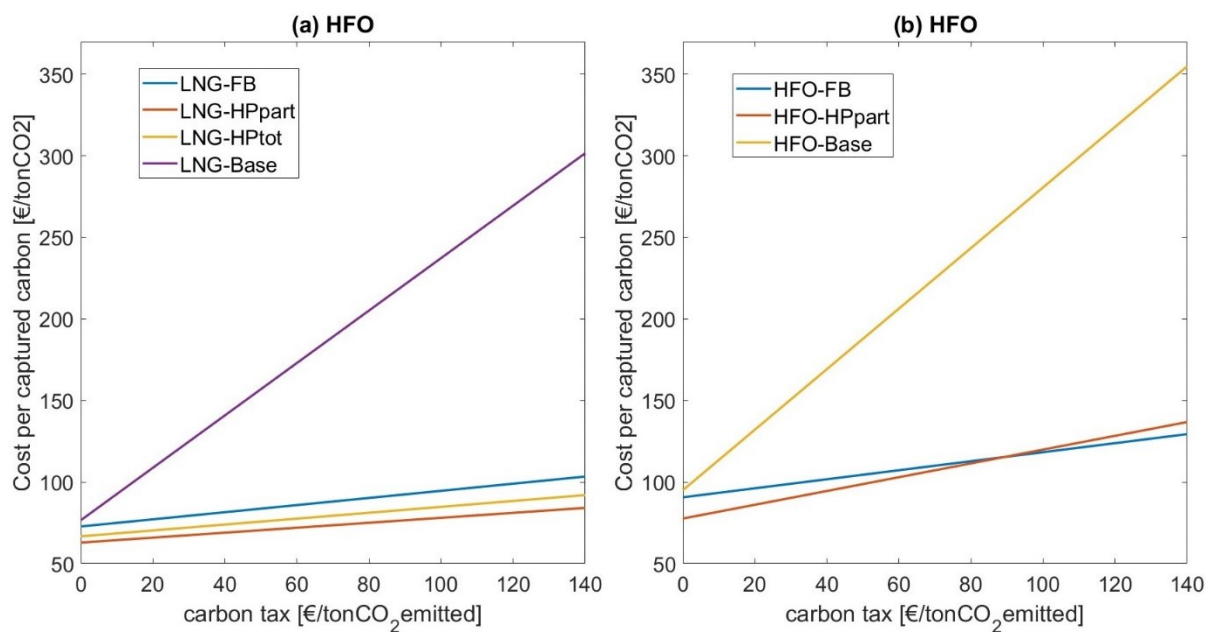


Figure 5.22. Carbon tax impact on cost of captured carbon (CCC) for (a) LNG case and (b) HFO case

Conclusion

The pursuit of diminishing carbon dioxide emissions in shipping operations presents a multifaceted challenge, requiring a comprehensive assessment of technical, economic, and operational aspects. The analysis discussed in this work focused on evaluating the feasibility of introducing the carbon capture technology on-board a large container ship.

The analysis considered several plant configurations under various scenarios, primarily distinguished by Carbon Capture Rates (CCR) and the energy implementation strategies, using either liquefied natural gas (LNG) or heavy fuel oil (HFO) as fuel sources.

For LNG-based propulsion systems, achieving a 90% CCR necessitates a substantial heat to cover the capture plant reboiler duty, which can only partially be provided by the hot engine flue gas. This leads to increased fuel consumption for steam generation, with a consequent increase in operating costs and consequent CO₂ emissions. The integration of a heat pump system proved to be instrumental in reducing fuel consumption, especially in the LNG-based system. It achieves a significant 59% reduction in fuel consumption, offering a valuable cost-saving opportunity for liners. The role of the engine is crucial in influencing the feasibility of heat pump integration. The heat pump effectiveness depends on the flue gas temperature, with relatively lower temperatures in HFO-based systems comparing to CO₂ flowrate posing challenges.

Furthermore the engine performance and characteristics have been proven to be crucial to minimize the energy consumption of the plant with a focus thus that must be at least partially moved from the burning efficiency to the exit flue gas temperature which will lead to important trade-off considerations.

This work evaluated the plant performance under a real voyage scenario in order to appreciate the complexity of such an option on the operation costs associated to the ship. The results showed a great variation in annual costs ranging from 4 mln €/year to 18 with the LNG-Base case being the lowest costs option but with a 36% CCR. It must be notice that for high CCR (90%), the increase in costs is almost 20% compared to the benchmark ship. A sensitivity analysis on carbon tax was found to be crucial if high level of CCR (90%) are aimed to be reached, with minimum level to balance the costs of 70 €/ton for the LNG ship and 89 €/ton for the HFO one. The study revealed that the application of a carbon tax to the case in which the carbon capture rate is limited by the maximum amount of heat that can be recovered from the

engine flue gas leads this configuration being the less advantageous due to its high level of not abated emissions.

In conclusion, the implementation of on-board carbon capture systems in maritime shipping is a complex task that is influenced by several technical, economic, and operational factors. Achieving the right balance between carbon capture rate, fuel consumption and associated costs is crucial. The integration of heat pump systems offers potentially promising fuel savings but requires careful consideration of engine compatibility. Moreover, the economics of carbon capture depends on exogenous factors like the carbon dioxide transport and storage infrastructure development and finally on an international agreement over a global carbon tax implementation, fundamental to allow a fast pace development of this technology

Nomenclature

K_{eq} = equilibrium constant

ΔG^0 = Gibbs free energy (J)

R = Gas constant

T^l = liquid temperature (°C)

k = kinetic constant

A = pre-exponential factor

E_a = Activation energy (cal/mol)

\dot{Q}_{disp} = Heat duty recovered from flue-gas (MW)

\dot{W}_{el} = Heat pump compression work (MW)

\dot{Q}_{reb} = Reboiler heat duty (MW)

LHV_{fuel} = Lower heating value fuel MJ/kg

η_{boiler} = boiler efficiency

\dot{m} = Fuel flow rate (kg/s)

η_{engine} = engine efficiency (MJ/kg)

C_i = equipment purchase cost (€)

i = interest rate

DWT, k = deadweight in leg k (tons)

$m_{fuel, k}$ = mass of fuel stored on board in leg k (tons)

$m_{cargo, k}$ = mass of container stored on board in leg k (tons)

$\Delta C, k$ = change of container on-board from leg k-1 to leg k (TEU)

$m_{container}$ = average container mass (tons)

$m_{co2, k}$ = carbon dioxide mass stored on board (tons)

$C0$ = container capacity at start port (TEU)

d_{tot} = total trip duration (days)

d, k = leg duration (days)

fr = freight rate (€)

ACRONIMS

GHG = greenhouse gases

IMO = international maritime organization

EEDI= Energy Efficiency Design Index (EEDI).

EU ETS = EU's Emissions Trading System

MEPC= Marine Environment Protection Committee

MARPOL= International Convention for the Prevention of Pollution from Ships

HFO=heavy fuel oil

LNG= liquefied natural gas

ICE= internal combustion engine

PEMFC= proton exchange membrane fuel cells

SMR= steam reforming of methane

CCUS=carbon capture & utilization or storage

CCS= carbon capture and storage

ULCV= ultra large container vessel

TEU= twenty-foot equivalent unit

FEU= forty-foot equivalent unit

DWT=deadweight

CCR=carbon capture rate

TCO= total cost of ownership

CCC= carbon capture cost

ASU=Air separation unit

MCFC = Molten carbonate fuel cell

CCR= carbon capture rate

WHR= waste heat recovery

EGR= exhaust gas recirculation

CAPEX= Capital expenditure

VOPEX=Variable operating expenditure

FOPEX=Fixed operating expenditure

OPEX= operating expenditure

MEA= Monoethanolamine

DEA= Diethanolamine

MDEA= Methyldiethanolamine

AMP=2-Amino-2-methyl-1-propanol

PZ= Piperazine

e-NRTL= electrolyte non-random two-liquid

COP=coefficient of performance

LHV=lower heating value

Bibliography

- Agbonghae, E.O., Hughes, K.J., Ingham, D.B., Ma, L., Pourkashanian, M., (2014). "Optimal Process Design of Commercial-Scale Amine-Based CO₂ Capture Plants," *Ind. Eng. Chem. Res.*, 53, 14815-14829. <https://doi.org/10.1021/ie5023767>
- Aspen Technology, Inc. (2008). "Aspen Plus: Rate-Based Model of the CO₂ capture process by MEA using Aspen Plus."
- Barreiro, J., Zaragoza, S., Diaz-Casas, V. (2022). Review of ship energy efficiency, *Ocean Engineering*, 257, 111594. <https://doi.org/10.1016/j.oceaneng.2022.111594>.
- Brownsort, P.A. (2019). "Briefing on carbon dioxide specifications for transport 1st Report of the Thematic Working Group on: CO₂ transport, storage and networks," EU CCUS PROJECTS NETWORK.
- Campanari, S., Chiesa, P., & Manzolini, G. (2010). CO₂ capture from combined cycles integrated with Molten Carbonate Fuel Cells. *Int. J. Greenhouse Gas Control*, 4, 441-451. <https://doi.org/10.1016/j.ijggc.2009.11.007>.
- Campanari, S., Chiesa, P., Manzolini, G. (2014). Economic analysis of CO₂ capture from natural gas combined cycles using Molten Carbonate Fuel Cells. *Appl. Energy*, 130, 562-573. <https://doi.org/10.1016/j.apenergy.2014.04.011>.
- Cao, C., Liu, H., Hou, Z., Mehmood, F., Liao, J., & Feng, W. (2020). A Review of CO₂ Storage in View of Safety and Cost-Effectiveness. *Energies*, 13, 600. <https://doi.org/10.3390/en13030600>
- Cebrucean, D., & Ionel, I. (2022). Biomass Co-Firing With Carbon Capture. In *Comp. Renew. Energy*, Elsevier, 330-347. <https://doi.org/10.1016/B978-0-12-819727-1.00044-3>.
- Chao, Y., Deng, Y., Dewil, R., Baeyens, J., & Fan, X. (2021). Post-combustion carbon capture. *Renew. Sustain. Energy Rev.*, 138. <https://doi.org/10.1016/j.rser.2020.110490>
- Chen, H., Yu, H., Zhou, B., Wang, R., Dai, Q., Qi, X., La, A., Abro, Z. (2023). Storage Mechanism and Dynamic Characteristics of CO₂ Dissolution in Saline Aquifers. *Energy Fuels*, 37, 3875–3885. <https://doi.org/10.1021/acs.energyfuels.2c03987>

- d'Amore, F., Pereira, L. M.C., Campanari, S., Gazzani, M., Romano, M. C. (2023). A novel process for CO₂ capture from steam methane reformer with molten carbonate fuel cell. *Int. J. Hydrogen Energy*, Article in press.
<https://dx.doi.org/10.1016/j.ijhydene.2023.06.137>
- Du, Z., Cao, Y., Fu, J. (2018). Simulation of Ship Maneuvering in Wind and Current Considering Time Effect. *Ocean Engineering*, 160, 264-273.
- Dubey, A., & Arora, A. (2022). Advancements in carbon capture technologies: A review. *J. Clean. Prod.*, 373, 133932. <https://doi.org/10.1016/j.jclepro.2022.133932>.
- Duijm, N. J., Markert, F., Paulsen, J. L. (2005). Safety assessment of ammonia as a transport fuel, Risø National Laboratory Roskilde Denmark.
- Farkas, A., Degiuli, N., Martić, I., Grlj, C. G. (2022). Is slow steaming a viable option to meet the novel energy efficiency requirements for containerships? *Journal of Cleaner Production*, 374. <https://doi.org/10.1016/j.jclepro.2022.133915> .
- Feenstra, M., Monteiro, J., van den Akker, J. T., Abu-Zahra, M. R. M., Gilling, E., & Goetheer, E. (2019). Ship-based carbon capture onboard of diesel or LNG-fuelled ships. *Int. J. Greenhouse Gas Control*, 85, 1-10. <https://doi.org/10.1016/j.ijggc.2019.03.008>
- Godin, J., Liu, W., Ren, S., & Xu, C. C. (2021). Advances in recovery and utilization of carbon dioxide: A brief review. *J. Environ. Chem. Eng.*, 9. <https://doi.org/10.1016/j.jece.2021.105644>
- H. Deng, S. Roussanaly, G. Skaugen (2019). "Techno-economic analyses of CO₂ liquefaction: Impact of product pressure and impurities," *Int. J. Refrig.*, 103, 301-315. <https://doi.org/10.1016/j.ijrefrig.2019.04.011>
- H. Hikita, S. Asai, H. Ishikawa, M. Honda (1977). "The kinetics of reactions of carbon dioxide with monoethanolamine, diethanolamine, and triethanolamine by a rapid mixing method," *Chem. Eng. J.*, 13, 7-12. [https://doi.org/10.1016/0300-9467\(77\)80002-6](https://doi.org/10.1016/0300-9467(77)80002-6)
- Hilliard, M.D. (2008). "A Predictive Thermodynamic Model for an Aqueous Blend of Potassium Carbonate, Piperazine, and Monoethanolamine for Carbon Dioxide Capture from Flue Gas." Ph.D. Dissertation, The University of Texas at Austin, Austin, Texas.
- <https://www.sccs.org.uk/resources/global-ccs-map>

- Hwang, H. T., Varma, A. (2014). Hydrogen storage for fuel cell vehicles. Current Opinion in Chemical Engineering, 5, 42-48. <https://doi.org/10.1016/j.coche.2014.04.004>
- IEA (2019). The Future of Hydrogen. IEA, Paris. <https://www.iea.org/reports/the-future-of-hydrogen>, License: CC BY 4.0.
- IEA (2020). CCUS in Clean Energy Transitions. IEA, Paris. <https://www.iea.org/reports/ccus-in-clean-energy-transitions>.
- IEA (2021), Ammonia Technology Roadmap, IEA, Paris <https://www.iea.org/reports/ammonia-technology-roadmap>, License: CC BY 4.0
- IEA (2021). "The world has vast capacity to store CO₂: Net zero means we'll need it," IEA, Paris. <https://www.iea.org/commentaries/the-world-has-vast-capacity-to-store-co2-net-zero-means-we-ll-need-it>
- IEA (2022). "The Future of Heat Pumps," IEA, Paris. <https://www.iea.org/reports/the-future-of-heat-pumps>, License: CC BY 4.0
- IEA (2023). Towards hydrogen definitions based on their emissions intensity. IEA, Paris. <https://www.iea.org/reports/towards-hydrogen-definitions-based-on-their-emissions-intensity>, License: CC BY 4.0
- IEA, "Indicative CO₂ storage cost curve for the United States, offshore," IEA, Paris. <https://www.iea.org/data-and-statistics/charts/indicative-co2-storage-cost-curve-for-the-united-states-offshore>, IEA. Licence: CC BY 4.0
- IMO (2018). Initial IMO Strategy on Reduction of GHG Emissions from Ships. https://unfccc.int/sites/default/files/resource/250_IMO%20submission_Talanoa%20Dialogue_April%202018.pdf
- IMO(2020).Fourth IMO GHG Study 2020. <https://www.imo.org/en/ourwork/Environment/Pages/Fourth-IMO-Greenhouse-Gas-Study-2020.aspx>
- IPCC (2005). Special Report on Carbon dioxide Capture and Storage . https://www.ipcc.ch/site/assets/uploads/2018/03/srccs_wholereport-1.pdf
- IPCC (2014): Climate Change 2014: Synthesis Report. Contribution of Working Groups I, II and III to the Fifth Assessment Report of the Intergovernmental Panel on Climate

Change [Core Writing Team, R.K. Pachauri and L.A. Meyer (eds.)]. IPCC, Geneva, Switzerland, 151 pp. <https://www.ipcc.ch/report/ar5/syr/>

- J. Jiang, B. Hu, R.Z. Wang, N. Deng, F. Cao, C.-C. Wang (2022). "A review and perspective on industry high-temperature heat pumps," *Renew. Sustain. Energy Rev.*, 161. <https://doi.org/10.1016/j.rser.2022.112106>
- J. Sun, Y. Wang, Y. Qin, G. Wang, R. Liu, Y. Yang (2023). "A Review of Super-High-Temperature Heat Pumps over 100 °C," *Energies*, 16, 12. <https://doi.org/10.3390/en16124591>
- Jansen, D., Gazzani, M., Manzolini, G., van Dijk, E., & Carbo, M. (2015). Pre-combustion CO₂ capture. *Int. J. Greenhouse Gas Control*, 40, 167-187. <https://doi.org/10.1016/j.ijggc.2015.05.028>
- Korberg, A.D., Brynolf, S., Grahn, M., Skov, I.R., (2021). Techno-economic assessment of advanced fuels and propulsion systems in future fossil-free ships, *Renewable and Sustainable Energy Reviews*, 142. <https://doi.org/10.1016/j.rser.2021.110861>
- Krevor, S., Blunt, M. J., Benson, S. M., Pentland, C. H., Reynolds, C., Al-Menhali, A., Niu, B. (2015). Capillary trapping for geologic carbon dioxide storage – From pore scale physics to field scale implications. *Int. J. Greenhouse Gas Control*, 40, 221-237. <https://doi.org/10.1016/j.ijggc.2015.04.006>
- Kvamsdal, H.M., Ehlers, S., Kather, A., Khakharia, P., Nienoord, M., Fosbøl, P.L. (2016). "Optimizing integrated reference cases in the OCTAVIUS project." *Int. J. Greenhouse Gas Control*, 50, 23-36. <https://doi.org/10.1016/j.ijggc.2016.04.012>
- Kvamsdal, H.M., Ehlers, S., Khakharia, P., Nienoord, M., Briot, P., Broutin, P., Fosbøl, P.L., Al-Azki, A. (2015). "OCTAVIUS- Deliverable No. D13.2 Report on methodology for benchmarking of large scale capture plants." Sintef.
- L. Øi, (2007). "Aspen HYSYS simulation of CO₂ removal by amine absorption from a gas-based power plant," SIMS2007 Conference.
- L.S. Tan, A.M. Shariff, K.K. Lau, M.A. Bustam (2012). "Factors affecting CO₂ absorption efficiency in packed columns: A review," *J. Ind. Eng. Chem.*, Volume 18, Issue 6, Pages 1874-1883. <https://doi.org/10.1016/j.jiec.2012.05.013>

- Lindstad, E., Bø, T. I. (2018). Potential power setups, fuels and hull designs capable of satisfying future EEDI requirements. *Transportation Research Part D: Transport and Environment*, 63, 276-290. <https://doi.org/10.1016/j.trd.2018.06.001>
- Liu, L., Xiao, Y., & Jiang, H. (2019). Research on CO₂ Pipeline Steel and Its Application Prospects. *IOP Conf. Ser. Earth Environ. Sci.*, 381.
- Lloyd's Register & UMAS (2020). Techno-economic assessment of zero-carbon fuels. March 2020. <https://www.lr.org/en/knowledge/research-reports/techno-economic-assessment-of-zero-carbon-fuels/>
- Lu, H., Ma, X., Huang, K., Fu, L., & Azimi, M. (2020). Carbon dioxide transport via pipelines: A systematic review. *J. Clean. Prod.*, 266, 121994. <https://doi.org/10.1016/j.jclepro.2020.121994>
- Luo, X., Wang, M. (2017). "Study of solvent-based carbon capture for cargo ships through process modelling and simulation," *Appl. Energy*, 195, 402-413. <https://doi.org/10.1016/j.apenergy.2017.03.027>
- Luo, Y., Shi, Y., Cai, N. (2021). Bridging a bi-directional connection between electricity and fuels in hybrid multi-energy systems. In *Hybrid Systems and Multi-energy Networks for the Future Energy Internet*, Academic Press, 41-84. <https://doi.org/10.1016/B978-0-12-819184-2.00003-1>
- M. Issa, H. Ibrahim, A. Ilinca, M.Y. Hayyani, (2019). "A Review and Economic Analysis of Different Emission Reduction Techniques for Marine Diesel Engines," *Open J. Mar. Sci.*, 9. <https://doi.org/10.4236/ojms.2019.93012>
- M.T. Mota-Martinez, J.P. Hallett, N. MacDowell (2017). "Solvent selection and design for CO₂ capture how we might have been missing the point," *Sustain. Energy Fuels*, 1, 2078. <https://doi.org/10.1039/C7SE00404D>
- Ma, X., & Wang, M. (2017). Study of solvent-based carbon capture for cargo ships through process modelling and simulation. *Appl. Energy*, 195, 402-413. <https://doi.org/10.1016/j.apenergy.2017.03.027>
- Madeddu, C., Errico, C., Baratti, R. (2017). "Rigorous modeling of a CO₂-MEA stripping system," *Chem. Eng. Trans.*, 57. <https://www.aidic.it/cet/17/57/076.pdf>

- Madeddu, C., Errico, C., Baratti, R. (2019). "CO₂ Capture by Reactive Absorption-Stripping: Modeling, Analysis and Design," SpringerBriefs in Energy, Springer Int. Pub., Cham. <https://doi.org/10.1007/978-3-030-04579-1>
- Mao, X., Rutherford, D., Osipova, L., Comer, B. (2020). Refueling assessment of a zero-emission container corridor between China and the United States: Could hydrogen replace fossil fuels? ICCT working paper 2020-05.
- Martin, S., Kraaij, G., Ascher, T., Baltzopoulou, P., Karagiannakis, G., Wails, D., Wörner, A. (2015). Direct steam reforming of diesel and diesel–biodiesel blends for distributed hydrogen generation. *Int. J. Hydrogen Energy*, 40, 75-84. <https://doi.org/10.1016/j.ijhydene.2014.10.062>.
- Martin-Roberts, E., Scott, V., Flude, S., Johnson, G., Haszeldine, R. S., Gilfillan, S. (2021). Carbon capture and storage at the end of a lost decade. *One Earth*, 4, 1569-1584. <https://doi.org/10.1016/j.oneear.2021.10.002>.
- McKinlay, C. J., Turnock, S. R., Hudson, D. A. (2021). Route to zero emission shipping: Hydrogen, ammonia or methanol? *International Journal of Hydrogen Energy*, 46, 28282-28297. <https://doi.org/10.1016/j.ijhydene.2021.06.066>
- Negri, V., Charalambous, M. A., Medrano-García, J. D., & Guillén-Gosálbez, G. (2022). Navigating within the Safe Operating Space with Carbon Capture On-Board. *ACS Sustain. Chem. Eng.*, 10, 17134-17142. <https://doi.org/10.1021/acssuschemeng.2c04627>
- Pinsent, B.R.W., Pearson, L., Roughton, F.J.W. (1956). "The kinetics of combination of carbon dioxide with ammonia." *Transactions of the Faraday Society*, 52, 1594-1598. <https://doi.org/10.1039/TF9565201594>
- Pires, J.C.M., Martins, F.G., Alvim-Ferraz, M.C.M., Simões, M. (2011). "Recent developments on carbon capture and storage: An overview." *Chem. Eng. Res. Des.*, 89, 1446-1460. <https://doi.org/10.1016/j.cherd.2011.01.028>
- Porrazzo, R., White, G., Ocone, R. (2016). "Fuel reactor modelling for chemical looping combustion: From micro-scale to macro scale." *Fuel*, 175, 87-98. <https://doi.org/10.1016/j.fuel.2016.01.041>
- Rackley, Steve A. *Carbon capture and storage*. Butterworth-Heinemann, 2017.

- Rahmanian, N., Rehan, M., A. Sumani, A., Nizami, A.S. (2018). "Effect of Packing Structure on CO₂ Capturing Process," Chem. Eng. Trans., 70 <https://www.aidic.it/cet/18/70/316.pdf>
- Stec, M., Tatarczuk, A., Iluk, T., Szul, M. (2021). Reducing the energy efficiency design index for ships through a post-combustion carbon capture process. International Journal of Greenhouse Gas Control, 108. <https://doi.org/10.1016/j.ijggc.2021.103333>
- Sun, S., Guo, H., Lu, D., Bai, Y., Gong, M. (2021). "Performance of a single-stage recuperative high-temperature air source heat pump." Applied Thermal Engineering, 193. <https://doi.org/10.1016/j.applthermaleng.2021.116969>
- Tesch, S., Morosuk, T., Tsatsaronis, G. (2020). "Comparative Evaluation of Cryogenic Air Separation Units from the Exergetic and Economic Points of View," Low-temp. Technol., IntechOpen. <http://dx.doi.org/10.5772/intechopen.85765>.
- Towler, G. P., & Sinnott, R. K. (2008). Chemical engineering design: Principles, practice and economics of plant and process design, second edition (2nd ed.). Butterworth-Heinemann.
- UNCTAD (2022). Review of Maritime Transport 2022, Navigating Stormy Waters. <https://unctad.org/rmt2022>
- Vakkilainen, E.K. (2017). "Boiler Processes, Steam Generation from Biomass," Butterworth-Heinemann, 57-86. <https://doi.org/10.1016/B978-0-12-804389-9.00003-4>
- Vasudevan, S., Farooq, S., Karimi, I. A., Saeys, M., Quah, M. C. G., Agrawal, R. (2016). Energy penalty estimates for CO₂ capture: Comparison between fuel types and capture-combustion modes. *Energy*, 103, 709-714. <https://doi.org/10.1016/j.energy.2016.02.154>
- Verbeek, R., Verbeek, M. (2015). LNG for trucks and ships: fact analysis Review of pollutant and GHG emissions Final, TNO Innovation For Life (Report No.: TNO 2014 R11668), The Netherlands. https://www.nationaalngplatform.nl/wp-content/uploads/2016/04/TNO-report_LNG_fact_analysis.pdf
- Wang, S., Gao, S., Tan, T., Yang, W. (2019). "Bunker fuel cost and freight revenue optimization for a single liner shipping service," Comput. & Oper. Res., 111, Pages 67-83. <https://doi.org/10.1016/j.cor.2019.06.003>
- Ye, M., Sharp, P., Brandon, N., Kucernak, A. (2022). System-level comparison of ammonia, compressed and liquid hydrogen as fuels for polymer electrolyte fuel cell

powered shipping. *International Journal of Hydrogen Energy*, 47, 8565-8584. <https://doi.org/10.1016/j.ijhydene.2021.12.164>

- Yokoyama, T. (2012). "Analysis of reboiler heat duty in MEA process for CO₂ capture using equilibrium-staged model," *Sep. Purif. Technol.*, 94, 97-103. <https://doi.org/10.1016/j.seppur.2011.12.029>
- Zaman, M., Lee, J.H. (2013). "Carbon capture from stationary power generation sources: A review of the current status of the technologies." **Korean J. Chem. Eng.**, 30, 1497–1526. <https://doi.org/10.1007/s11814-013-0127-3>
- Zhang, Y., Chen, H., Chen, C.-C., Plaza, J., Dugas, R., Rochelle, G. (2009). "Rate-Based Process Modeling Study of CO₂ Capture with Aqueous Monoethanolamine Solution," *Ind. Eng. Chem. Res.*, 48, 9233-9246. <https://doi.org/10.1021/ie900068k>

